

# Modeling the Greenland Ice Sheet response to climate change in the past and future

KUMULATIVE DISSERTATION

zur Erlangung des akademischen Grades  
Doktor der Naturwissenschaften (Dr. rer. nat.)  
in der Wissenschaftsdisziplin Geophysik

eingereicht an der  
Mathematisch-Naturwissenschaftlichen Fakultät  
der Universität Potsdam

vorgelegt von  
**Alexander Robinson**  
geboren am 25.07.1982 in Hayward, Kalifornien

Potsdam, im Februar 2011

Published online at the  
Institutional Repository of the University of Potsdam:  
URL <http://opus.kobv.de/ubp/volltexte/2011/5043/>  
URN [urn:nbn:de:kobv:517-opus-50430](http://nbn-resolving.org/urn:nbn:de:kobv:517-opus-50430)  
<http://nbn-resolving.org/urn:nbn:de:kobv:517-opus-50430>

Referent: Prof. Dr. Stefan Rahmstorf  
Koreferent: Prof. Dr. Marisa Montoya  
Koreferent: Prof. Dr. Philippe Huybrechts

Datum der Einreichung: 24. November 2010  
Tag der mündlichen Prüfung: 01. Februar 2011

Diese Arbeit ist bisher an keiner anderen Hochschule eingereicht worden, sowie wurde selbständig und ausschließlich mit den angegebenen Mitteln angefertigt.

Alexander Robinson  
Potsdam, Februar 2011





# ABSTRACT

The Greenland Ice Sheet (GIS) contains enough water volume to raise global sea level by over 7 meters. It is a relic of past glacial climates that could be strongly affected by a warming world. Several studies have been performed to investigate the sensitivity of the ice sheet to changes in climate, but large uncertainties in its long-term response still exist. In this thesis, a new approach has been developed and applied to modeling the GIS response to climate change. The advantages compared to previous approaches are (i) that it can be applied over a wide range of climatic scenarios (both in the deep past and the future), (ii) that it includes the relevant feedback processes between the climate and the ice sheet and (iii) that it is highly computationally efficient, allowing simulations over very long timescales.

The new regional energy-moisture balance model (REMBO) has been developed to model the climate and surface mass balance over Greenland and it represents an improvement compared to conventional approaches in modeling present-day conditions. Furthermore, the evolution of the GIS has been simulated over the last glacial cycle using an ensemble of model versions. The model performance has been validated against field observations of the present-day climate and surface mass balance, as well as paleo information from ice cores. The GIS contribution to sea level rise during the last interglacial is estimated to be between 0.5-4.1 m, consistent with previous estimates. The ensemble of model versions has been constrained to those that are consistent with the data, and a range of valid parameter values has been defined, allowing quantification of the uncertainty and sensitivity of the modeling approach.

Using the constrained model ensemble, the sensitivity of the GIS to long-term climate change was investigated. It was found that the GIS exhibits hysteresis behavior (i.e., it is multi-stable under certain conditions), and that a temperature threshold exists above which the ice sheet transitions to an essentially ice-free state. The threshold in the global temperature is estimated to be in the range of 1.3-2.3 °C above preindustrial conditions, significantly lower than previously believed. The timescale of total melt scales non-linearly with the overshoot above the temperature threshold, such that a 2 °C anomaly causes the ice sheet to melt in ca. 50,000 years, but an anomaly of 6 °C will melt the ice sheet in less than 4,000 years. The meltback of the ice sheet was found to become irreversible after a fraction of the ice sheet is already lost – but this level of irreversibility also depends on the temperature anomaly.



## ZUSAMMENFASSUNG

Das grönländische Inlandeis (GIS) besteht aus einem Wasservolumen das ausreicht, um den globalen Meeresspiegel um 7 Meter ansteigen zu lassen. Es ist ein Relikt der vergangenen Eiszeit, das in einer zunehmend wärmer werdenden Welt stark in Mitleidenschaft gezogen werden könnte. In der vorliegenden Dissertation ist ein neues Verfahren zur Modellierung des Antwortverhaltens des Inlandeises auf Klimaänderungen entwickelt und angewendet worden. Die Vorteile des neuen Verfahrens im Vergleich zu den bisherigen Verfahren sind, (i) dass es über einen groen Bereich von Klimaszenarien (sowohl für die ferne Vergangenheit als auch für die Zukunft) anwendbar ist, (ii) dass es die wesentlichen Rückkopplungsprozesse zwischen Klima und Inlandeis enthält und (iii) dass es wegen seiner guten Rechenzeiteffizienz Simulationen über sehr lange Zeitskalen erlaubt.

Das neue Modell (REMBO) ist für die Modellierung des Klimas und der Massenbilanz an der grönländischen Oberfläche entwickelt worden und stellt ein verbessertes Verfahren im Vergleich zu den bisherigen dar. Die Entwicklung von GIS über den letzten glazialen Zyklus ist mittels eines Ensembles von verschiedenen Modellversionen simuliert worden. Anschließend ist die Tauglichkeit der Modellversionen durch Vergleich mit Beobachtungsdaten des gegenwärtigen Klimas und der Oberflächenmassenbilanz, sowie mit paleoklimatischen Rekonstruktionen von Eisbohrkernen verifiziert worden. Der Anteil von GIS am Meeresspiegelanstieg während des letzten Interglazials ist im Bereich von 0.5 bis 4.1 m berechnet worden, was konsistent mit bisherigen Schätzungen ist. Von den Ensemblesimulationen sind diejenigen ausgewählt worden, deren Ergebnisse gut mit den Daten übereinstimmen. Durch die Auswahl von geeigneten Modellversionen sind gleichzeitig die Unsicherheiten der Parameterwerte begrenzt worden, so dass sich nun mit dem neuen Verfahren die Sensitivität von GIS auf Klimaänderungen bestimmen lässt.

Mit den ausgewählten Modellversionen ist die Sensitivität von GIS auf langfristige Klimaänderungen untersucht worden. Es zeigt sich, dass das GIS ein Hystereseverhalten besitzt (d.h., eine Multistabilität für gewisse Klimazustände) und dass ein Temperaturschwellwert existiert. Bei Überschreiten des Schwellwertes bleibt das GIS nicht erhalten und wird langsam eisfrei werden. Der Temperaturschwellwert der globalen Mitteltemperatur relativ zur vorindustriellen Mitteltemperatur ist im Bereich 1.3-2.3 °C ermittelt worden und liegt damit deutlich niedriger als bisher angenommen. Die Zeitdauer bis zum völligen Abschmelzen zeigt ein nichtlineares Verhalten hinsichtlich einer Erwärmung über den ermittelten Schwellwert. Eine Erwärmung von 2 °C relativ zur vorindustriellen Zeit führt zu einem Abschmelzen nach 50.000 Jahren, aber eine Erwärmung um 6 °C lässt das Inlandeis bereits nach 4.000 Jahren abschmelzen. Ein weiteres Ergebnis ist, dass der Abschmelzvorgang irreversibel werden kann, nachdem ein gewisser Anteil des Inlandeises abgeschmolzen ist – jedoch ist die Irreversibilität eines Abschmelzvorganges auch von der Temperaturanomalie abhängig.



## ACKNOWLEDGEMENTS

This work has been conducted during my stay as a researcher at the Potsdam Institute for Climate Impact Research. Generous funding was provided by the European Commission's Marie Curie 6<sup>th</sup> Framework Programme, as a part of the Research Training Network, Network for Ice and Climate Interactions (NICE). Several people deserve recognition for their contribution to the completion of this work.

Andrey, thank you for guiding me through this experience and helping me find my way. You were always willing and supportive, and your keen insight and patient guidance helped me exceed my own expectations. Reinhard, you were instrumental in helping me succeed. Our discussions were thought-provoking and enjoyable, and always led me to a deeper and more concrete understanding.

My transition to the University of Potsdam would not have been possible without the strong support of Stefan Rahmstorf, who believed in my potential and constantly aided my rather unorthodox journey through to the end. In addition, I would like to recognize the support and guidance of Klaus Keller, who introduced me to the field and encouraged me to pursue graduate studies in climate science.

Gilles Ramstein and Céline Moncoursis deserve special recognition for organizing the NICE network and expanding my horizons as a scientist. This was a beautiful experience that enriched my life and work here in Europe. A warm thank you goes to my many colleagues and friends that made this network such a success and so enjoyable.

A heartfelt thanks goes to all of my colleagues at the PIK – you made work particularly enjoyable! Dim, Thomas, Mahé, Christoph, thank you for lengthy discussions, both scientific and not, that helped me keep an even keel.

Fontina, none of this would have come to be without your inspiration. And to my family, even though you are far away, knowing that you support me gives me strength. Thank you for your patience with my 'European adventures' away from home and for your constant encouragement.

Alexander Robinson  
Potsdam, February 2011



# CONTENTS

<b>1. Introduction</b>	1
1.1 The Greenland Ice Sheet	1
1.2 Modeling the GIS	4
1.3 The GIS and future climate change	7
1.4 Motivation	10
1.5 Overview	11
<b>2. An efficient regional energy-moisture balance model for simulation of the Greenland Ice Sheet response to climate change<sup>1</sup></b>	15
2.1 Introduction	15
2.2 Model description	18
2.2.1 Regional energy-moisture balance model	19
2.2.2 Surface mass balance	23
2.3 Modeling results	25
2.3.1 Simulations of climatology and surface mass balance with fixed topography	25
2.3.2 Coupled simulations of equilibrium state	34
2.4 Conclusions	35
<b>3. Greenland Ice Sheet model parameters constrained using simulations of the Eemian Interglacial<sup>2</sup></b>	39
3.1 Introduction	39
3.2 Model setup and experimental design	42
3.3 Modern and paleo empirical constraints	44
3.3.1 Present-day surface mass balance partition	45
3.3.2 Present-day GRIP elevation	45
3.3.3 Eemian GRIP elevation	45
3.3.4 Additional possible paleoclimate constraints	46
3.4 Perturbed model parameters	46
3.4.1 Geothermal heat flux	47
3.4.2 Sliding coefficient	47
3.4.3 Melt model parameter, $c$	47
3.4.4 Atmospheric moisture diffusion coefficient	48
3.4.5 Paleo climate forcing	49
3.5 Transient simulations of the GIS	50
3.6 Constraining the model parameters	53
3.7 Discussion	55
3.8 Conclusions	57
3.9 Appendix A	59

---

3.9.1	Surface albedo parameterization . . . . .	59
<b>4.</b>	<b>Multistability and critical thresholds of the Greenland Ice Sheet<sup>3</sup></b> . . . . .	<b>61</b>
4.1	Methods . . . . .	67
4.2	Supplementary Information . . . . .	68
4.2.1	Insolation-temperature melt . . . . .	68
4.2.2	Simulations of the basins of attraction . . . . .	68
<b>5.</b>	<b>Discussion</b> . . . . .	<b>73</b>
<b>6.</b>	<b>Conclusions and outlook</b> . . . . .	<b>81</b>
<b>7.</b>	<b>Appendix</b> . . . . .	<b>85</b>
7.1	Ice sheet model field equations . . . . .	85
7.2	Boundary conditions . . . . .	87

---

<sup>1</sup> Robinson, A., Calov, R., and Ganopolski, A.: An efficient regional energy-moisture balance model for simulation of the Greenland Ice Sheet response to climate change, *The Cryosphere*, 4, 129–144, doi:10.5194/tc-4-129-2010, 2010.

<sup>2</sup> Robinson, A., Calov, R., and Ganopolski, A.: Greenland Ice Sheet model parameters constrained using simulations of the Eemian Interglacial, *Climate of the Past Discussions*, 6, 1551–1588, doi:10.5194/cpd-6-1551-2010, 2010, **in discussion**.

<sup>3</sup> Robinson, A., Calov, R., and Ganopolski, A.: Multistability and critical thresholds of the Greenland Ice Sheet, **submitted**.



# 1. INTRODUCTION

The overall aim of this thesis is to improve our current understanding of the sensitivity of the Greenland Ice Sheet to changes in climate. This task requires modeling work that extends both into the deep past and the potential future of the ice sheet under global warming. The central chapters of the thesis, comprised of articles that are either already published or in review, include the appropriate context of the work and the obtained results. This introduction provides a brief overview of the general understanding of the Greenland Ice Sheet, the state of the art in modeling efforts, motivation for the work and an overview of the publications.

## 1.1 The Greenland Ice Sheet

The Greenland Ice Sheet (GIS) is one of only two large-scale ice sheets that presently exist on Earth, containing enough ice mass to raise sea level by over 7 meters. The volume of the GIS is 2.91 million km<sup>3</sup> and it covers 80% of the land area of Greenland (1.71 million km<sup>2</sup>). It extends roughly 1000 km from West to East and over 2000 km from South to North (see Fig. 1.1). The underlying bedrock topography is relatively low-lying over central to northern Greenland, whereas a high elevation mountain range exists to the East and down the southeastern edge. The weight of the ice sheet has depressed the bedrock in the central regions significantly because it is over three kilometers thick at the summit (Fig. 1.2). This results in a relatively smooth “desert plain” at high elevations in the center and steep slopes towards the margins. Additionally, several deep and narrow fjords exist near the margins, through which outlet glaciers discharge ice into the ocean.

Greenland likely first experienced glacial inception during the Pliocene-Pleistocene transition (ca. 3-3.5 million years ago), which may have resulted from a drop in atmospheric CO<sub>2</sub> levels around this time leading to colder temperatures (Lunt et al., 2008). During the last several glacial cycles, the GIS was part of a group of ice sheets in the northern hemisphere that covered large areas of North America, Scandinavia and Asia. The size and coverage of these largely land-based ice sheets have changed in the past in response to changes in the magnitude and distribution of solar radiation as a result of a changing orbital configuration (orbital forcing). Over the past several hundred thousand years, the Earth has transitioned between glacial and inter-glacial conditions with a period of roughly 100,000 years (see Fig. 1.3).

Because of the deep ocean surrounding Greenland, the ice sheet has largely been con-

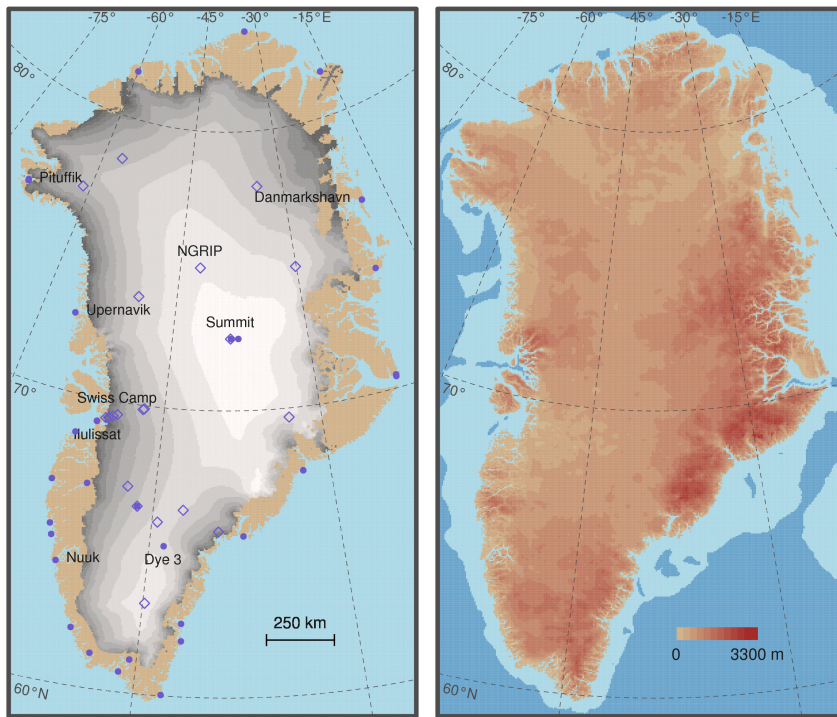


Figure 1.1: (**left panel**) Map of Greenland with the ice sheet relief shaded from grey to white (300 m contour intervals). Locations where surface observations have been recorded over the past several decades are shown for two data sets: DMI (filled circles) and GC-NET (open diamonds). (**right panel**) The uplifted, ice-free bedrock of Greenland. The dark blue regions in the ocean indicate where deep ocean begins (500 m below sea level and deeper). Topography and bathymetry data are from Bamber et al. (2001) and Smith and Sandwell (1997), respectively.

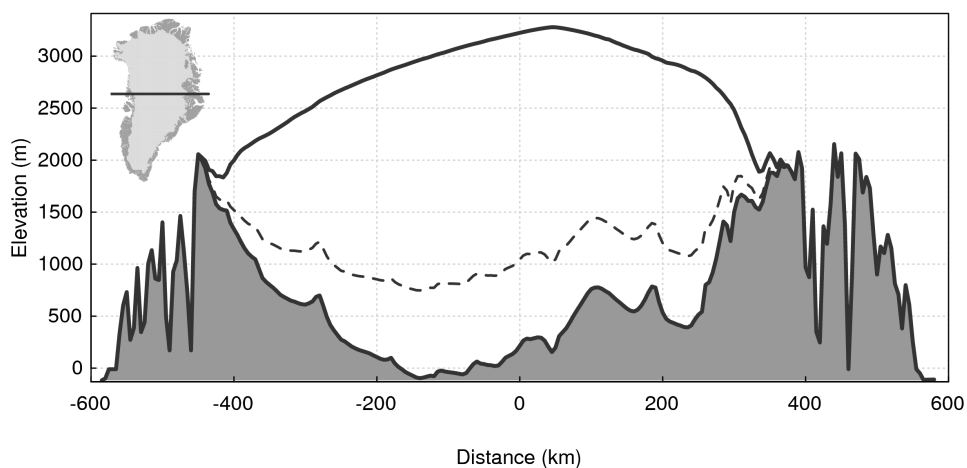
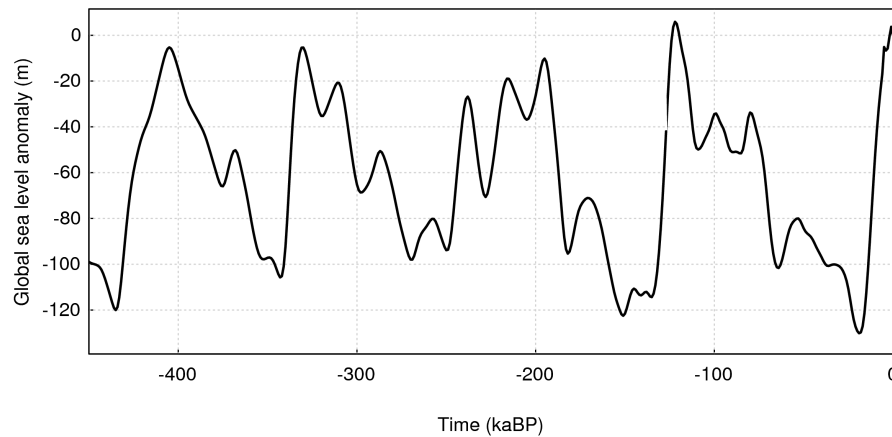


Figure 1.2: A cross section of the GIS approximately crossing through the summit (-73N, 38W). The depressed bedrock topography is represented by the lower grey shaded region. The surface elevation of the ice sheet (solid line) and the unweighted, bedrock elevation (dashed line) are also shown. Data are from Bamber et al. (2001).



*Figure 1.3:* The global sea level relative to present day for the past several glacial cycles, as inferred from  $\delta^{18}\text{O}$  proxy data from the SPECMAP project (Imbrie et al., 1984). The large changes in sea level reflect changes in the volume of the world’s ice sheets.

strained to the area on or above the continental shelf (see the right panel of Fig. 1.1). Thus, although during glacial times, the volume of the northern hemispheric ice sheets increased dramatically, the GIS could not grow much larger than the area of the island. Conversely, when the majority of ice coverage disappeared during the warmer interglacial periods, Greenland generally remained ice covered to some extent. Evidence from ice cores show that the ice sheet only partially deglaciated during the last interglacial period (Alley et al., 2010) and the last time that Greenland was completely ice free may have been over 400 ka before today (Willerslev et al., 2007). During this particularly long interglacial period, positive temperature anomalies of perhaps only a couple of degrees relative to today lasted for more than 20,000 years (Alley et al., 2010).

The GIS lies in the high latitude region of the North Atlantic, near the deep-water formation site of the Atlantic thermohaline circulation (THC). Freshwater from melting of ice and iceberg discharge from outlet glaciers can affect the strength of the THC, which transports heat northwards. Increasing freshwater generally reduces overturning, which in turn, leads to cooler temperatures over the North Atlantic and Europe (Rahmstorf, 1995). Unlike the Antarctic Ice Sheet, which experiences almost no melt at the surface, the GIS extends into lower latitudes and experiences warmer summer temperatures over large areas. In summertime, regions near the margin of the ice sheet are exposed to temperatures well above  $0\text{ }^{\circ}\text{C}$ , producing large amounts of surface runoff (Box et al., 2009; van den Broeke et al., 2009). Thus, this land-based ice sheet both interacts with the ocean and is also strongly affected by the regional climate.

The total mass balance of the ice sheet dictates its overall size. Best estimates from observations (Bales et al., 2009) and from modeling studies (e.g., Ettema et al., 2009) indicate that the incoming mass to the ice sheet from precipitation ranges between ca.

560-750 Gt/a. For perspective, this is equivalent to roughly 2 mm of sea level equivalent<sup>1</sup>. At present, approximately 50% of the incoming mass contributes to a positive surface mass balance (i.e., mass gain of the ice sheet), while the remaining 50% is converted into runoff via melting at the surface (Lemke et al., 2007). Additionally, ice discharge through calving into the ocean means that while the ice sheet gains mass in the interior due to accumulated precipitation, it loses mass at the margins. By monitoring these processes, the total mass balance of the ice sheet can be estimated. Ice loss by calving has been estimated to be about 300 Gt/a (Lemke et al., 2007), essentially balancing the positive surface mass balance. Therefore, over the past several decades, the total mass balance has been close to zero, meaning the GIS has been in a state fairly close to equilibrium.

## 1.2 Modeling the GIS

Three-dimensional, thermomechanical ice sheet models have only been developed and applied for studies of the GIS in the last few decades (e.g., Janssen, 1977). An ice sheet can be modeled using the principles of continuum mechanics, in particular, the laws of conservation of momentum, energy and mass. Development of the first comprehensive model of the GIS at high resolution was a major step forward in understanding the ice sheet's dynamics and the processes important to its evolution (Huybrechts et al., 1991). Today there are several models available for large-scale ice sheet modeling (e.g., Huybrechts et al., 1991; Ritz et al., 1997; Greve, 1997a; Tarasov and Peltier, 1999) based on approximations of the fundamental governing equations. In an attempt to refine the ice sheet's representation, higher order models (accounting for more stress terms in the momentum balance) have been developed in the last several years (e.g., Pattyn, 2003; Bueler and Brown, 2009; Hubbard et al., 2009; Pollard and Deconto, 2009). Such models are especially important for studying an ice sheet like Antarctica that has floating ice shelves and several large, fast-flowing ice streams. However, higher order models come with a higher computational cost, so when possible, it is advantageous to apply simplifying assumptions.

The most common approximation used for large-scale ice sheet modeling is the shallow ice approximation (SIA), which is a good approximation for ice sheets that are grounded and much broader than they are thick (Hutter, 1983). Using this approximation, the ice sheet is assumed to deform under simple shear stress in planes parallel to the surface. SIA is not valid directly under the ice dome or when the surface or basal slope is large (Greve and Blatter, 2009). For the most part, the GIS can be considered "shallow", in that it is several hundred kilometers wide, but only 3 km thick at the summit. Neglecting stress terms can become problematic when ice flow is fast (i.e., in ice streams) and in regions of variegated bedrock topography (i.e., in mountainous regions and fjords). It is clear from a longitudinal cross-section (Fig. 1.2) that the assumptions likely break down in some regions, especially near the margins. Thus, when modeling the large-scale ice sheet with

---

<sup>1</sup> 1 mm sea level equivalent = 362 Gt of ice

an SIA model, it generally makes sense to apply a relatively smooth topography and a grid spacing greater than 10 km. Since Greenland has relatively little area with fast ice flow or floating ice, SIA models are considered valid for the large-scale representation of the ice sheet and are especially useful for longer timescale simulations. For the current work, the SIA ice sheet model SICOPOLIS was used (Greve, 1997a,b). A detailed description of the relevant ice sheet model equations is presented in the Appendix.

To drive an ice sheet model, boundary conditions are needed at the base (bedrock elevation, basal temperature, basal velocity) and at the surface (surface mass balance, surface temperature) of the ice sheet. Very few observations exist for ice sheets that can aid in quantifying and modeling the boundary conditions. Thus, irrespective of the degree of complexity of the ice sheet model, contemporary modeling efforts include imperfect boundary information. This likely represents the largest source of uncertainty in the models.

For context, the equation for the time-dependent evolution of ice thickness is provided below:

$$\frac{\partial H}{\partial t} = -\nabla \cdot \mathbf{Q} + B - S, \quad (1.1)$$

where  $H$  is the ice thickness,  $m$  is the vertically-integrated mass flux of the ice,  $B$  is the surface mass balance (accumulation minus ablation) and  $S$  is the basal melt rate. Equation (1.1) generally holds for ice sheet modeling and is not specific to SIA models. It is obtained from integration of the continuity equation ( $\nabla \cdot \mathbf{v} = 0$ ) and kinematic boundary conditions. It is clear from Eq. (1.1) that the change in ice thickness at a given location depends only on the horizontal ice flux ( $Q_x, Q_y$ ), the addition or removal of mass at the surface and any melting that occurs at the base.

It is the term  $B$ , or the annual surface mass balance (SMB) that we are most concerned with in this work. The annual SMB is defined as the net accumulation of mass at the surface minus the net melt, summed over one year. This quantity modifies the driving stress of the ice sheet, which depends on ice thickness and surface slope (see Appendix). Greenland's harsh, isolated arctic environment makes it difficult to obtain detailed observations of surface conditions. Nonetheless, in ice-free coastal regions and several locations on the ice sheet itself, observational time-series over the last century are available from the Danish Meteorological Institute (Cappelen et al., 2001). In addition, the Greenland Climate Network (GC-NET) has been in operation since 1996, collecting data from automatic weather stations (AWS) from several additional locations on the ice sheet (Steffen et al., 1996). Together these datasets comprise an inhomogeneous temporal picture at over 50 locations on the ice sheet (shown in Fig. 1.1). Even with the limited temporal range and spatial resolution of these observations, the data are invaluable for validating and improving models of the surface of the GIS. Their sparseness, however, makes it difficult to perform comprehensive model validation.

To model the surface of the GIS, studies performed over the past two decades (e.g., Huybrechts et al., 1991; Calov and Hutter, 1996; Ritz et al., 1997; Greve, 2000) have generally employed some form of a semi-empirical surface mass balance method based

on observations of temperature, accumulation and melt rates (Braithwaite, 1980; Reeh, 1991). Typically, mean July and annual temperatures are obtained by making a bilinear fit of temperature observations to latitude and elevation:

$$\begin{aligned}\bar{T}_a &= c_a - \kappa_a \phi - \gamma_a z \\ \bar{T}_j &= c_j - \kappa_j \phi - \gamma_j z\end{aligned}\tag{1.2}$$

Here,  $\bar{T}_a$  and  $\bar{T}_j$  are the mean annual and mean July temperature, respectively,  $\phi$  is the latitude and  $z$  is the surface elevation.  $c_a$ ,  $c_j$ ,  $\kappa_a$ ,  $\kappa_j$ ,  $\gamma_a$  and  $\gamma_j$  are positive constants tuned to minimize the error with observations (Reeh, 1991). From the equations, it becomes apparent that temperatures decrease with increasing latitude – as would be expected given the lower levels of solar radiation at higher latitudes. Furthermore, temperatures also decrease with increasing elevation. From the July (maximum) and annual mean temperature at each point on the ice sheet, a sine curve can be used to generate a seasonal cycle between the winter and summer means.

Given a monthly mean temperature, a Gaussian distribution is used to mimic diurnal, intra- and inter-annual temperature variations, such that a sum of all days with temperatures above freezing (i.e., 0 °C) can be obtained (Reeh, 1991). Observations of melting on the ice sheet have shown that there is a strong correlation between this sum of “positive degree days” (PDDs) and the melt rate at a given location (Reeh, 1991). These PDDs can be converted into melt rates for snow and ice using empirically derived constants.

With this method, the SMB of the ice sheet can be estimated using inputs of only the monthly temperature and annual accumulation rate, which are often the only quantities available. Given that even these data are sparse, it provides at least a plausible way to force ice sheet models at the surface. In addition, the approach is simple and computationally efficient, thus allowing long integration times of ice sheet models. The disadvantages are that several important processes are ignored or poorly represented and that it is empirically based. This makes it difficult to justify using this approach under different climatic or topographic conditions.

More advanced coupled climate-ice sheet approaches have been applied in recent years. Calov et al. (2005) used an energy balance approach to produce SMB fields for the northern hemispheric ice sheets. The approach relied on various climatic variables including wind velocity and radiation fluxes, which were obtained from a global climate model. The simulations successfully reproduced fluctuations of ice sheet extent during glacial cycles (Calov et al., 2005; Ganopolski et al., 2010) and hysteresis behavior of the northern hemisphere ice sheets (Calov and Ganopolski, 2005). Still, the resolution of this approach is too coarse to apply to a smaller domain like that of the GIS. van den Berg et al. (2008) used a simplified equation for the surface energy balance to model the Eurasian ice sheet through the last glacial cycle. Melt on the ice sheet was considered to result from either incoming short-wave radiation or long-wave temperature-dependent radiation. Reducing complexity

in this way improves the model's computation time, while still solving for the most important terms in the energy balance. Both of the above coupled approaches improve the representation of surface boundary conditions for ice sheet models, although neither have yet been applied to investigate the evolution of the GIS at high resolution.

A separate line of development has been taking place more recently in the form of regional climate models (RCMs). These models have mainly been developed as diagnostic tools to provide more realistic and detailed climatic information above and around the ice sheet and, until now, none have been coupled directly with an ice sheet model. Because they include atmospheric dynamics and a full energy balance at the surface of the ice sheet, a much more realistic representation of the climate and surface conditions is possible. Indeed, these models capture seasonal and inter-annual variability substantially better than simplified approaches, providing climatic and surface variables that agree well with observations (Box et al., 2006; Fettweis, 2007; Ettema et al., 2009). However, these improvements come at a high computational cost. Generally, only simulations of less than 100 years are feasible, while most large-scale ice sheet modeling studies require simulations on the order of several thousand years.

### 1.3 The GIS and future climate change

Given large-scale changes to the GIS in the past, directly resulting from changing climatic conditions (Alley et al., 2010), it is likely that anthropogenic climate change will also have a strong impact on the ice sheet. Several sets of observations already confirm that conditions on the GIS are changing and that the ice sheet is shifting out of balance (Lemke et al., 2007). Most recent estimates put the rate of mass loss in the last decade near 200 Gt/a (or a rate of sea level rise of 0.5 mm/a, Wouters et al., 2008; van den Broeke et al., 2009). Over the 20<sup>th</sup> century, sea level rose at a rate of about 1.4 mm/a, whereas in the last two decades, this rate has doubled to about 3 mm/a (Lemke et al., 2007). Based on these estimates, mass loss from Greenland contributes 15% to the current rate of sea level rise. The satellite measurements of gravitational changes around Greenland, used to estimate its mass loss, show that the rate of loss has been accelerating in the last decade (Velicogna, 2009). Both melting at the surface and ice discharge into the ocean from outlet glaciers are increasing (Rignot et al., 2008; van den Broeke et al., 2009). The record of the latter only extends back for the last decade, so it is not yet known if this trend will continue. The outlet glaciers in direct contact with the ocean may increase discharge further as temperatures warm, leading to thinning and further retreat (Rignot and Kanagaratnam, 2006). If the ice sheet retreats from the margins and loses contact with the ocean, however, it is possible that the outlet glacier flux would also diminish. Even without large-scale retreat, modeling has shown that the currently observed acceleration in discharge could be a short-term response to boundary forcing and that it may only produce significant discharge on short timescales (Nick et al., 2009).

On longer timescales, melting at the surface will play the larger role in determining the overall mass balance of the GIS and its equilibrium size. Remote sensing from satellites has been used to quantify changes in the melt extent on the ice sheet since the 1970s (Abdalati and Steffen, 2001; Mote, 2007; Bhattacharya et al., 2009). A positive linear trend exists across various melt metrics (e.g., cumulative melt extent, average melt extent), which indicate that the area of the ice sheet experiencing melt is increasing. This can be attributed to the recent increase in summer temperatures around Greenland, which had shown minimal trends in the last century but have begun to catch up with global trends in the last two decades (Hanna et al., 2008; Box et al., 2009). As this trend has only been observed over a short period, it is still possible that the associated melt is due to natural variability. Nonetheless, there is no inherent negative feedback in the climate-ice sheet system that would counteract the warming and thus reduce the melt area. As long as temperatures continue to increase in the region, the melt extent is expected to increase as well.

It is possible that a temperature threshold exists for the GIS, above which the ice sheet cannot maintain its current size and would, therefore, eventually melt completely (Huybrechts et al., 1991). This follows from the mass balance argument. A positive surface mass balance is the only mechanism that contributes to mass gain of the ice sheet (i.e., snow and frozen rain accumulating at the surface). For an ice sheet in equilibrium, any mass gain of the ice sheet must be balanced by calving at the margins. Above a certain temperature threshold, the surface mass balance turns negative because the overall rate of melt becomes higher than the rate of accumulation. Although precipitation would increase in a warmer climate, this is likely not enough to counter the strong melt rates. Under such conditions, the ice sheet would be losing mass overall and it could eventually disappear (Gregory and Huybrechts, 2006).

Recently, the GIS was classified as a so-called *tipping element* in the Earth system (Lenton et al., 2008). When nearing the *tipping point*, tipping elements need only a rather small perturbation in forcing to shift them towards a new state. For the GIS, it is assumed that a warmer climate could trigger a shift in the GIS equilibrium towards an ice-free state, due to two important feedback processes: the *albedo* and *elevation feedbacks*. The albedo (reflectivity of the surface) feedback results from changes in the surface properties. Dry snow reflects close to 80% of the solar radiation it receives, much more than melted snow or ice (Paterson, 1994). As the temperature at the surface increases, the snow begins to melt, lowering the albedo and, thus, increasing the absorption of solar radiation, which in turn induces more melt. The elevation feedback is active on longer timescales, as the ice sheet topography evolves. As the ice sheet melts, the surface elevation decreases bringing the surface into contact with warmer air, which produces stronger melt rates. Both of these feedback processes can contribute to an irreversible decline of the ice sheet.

Several studies have investigated how the GIS would respond to a changing climate. The earliest comprehensive study used a three-dimensional ice sheet model coupled to a



semi-empirical surface mass balance approach (Huybrechts et al., 1991). The mass budget of the GIS as quantified by this classical study have largely been confirmed by later work (e.g., Box et al., 2006; Fettweis, 2007). The study also presented a threshold estimate of 2.7 °C above preindustrial, above which the surface mass balance would turn negative. In a complementary study, Letréguilly et al. (1991) investigated the GIS equilibrium response for various levels of warming. This study not only showed that the ice sheet would melt completely for a 6 °C temperature anomaly, it was the first to show that the GIS exhibits hysteresis behavior. Starting from ice-free conditions, colder temperatures were needed to regrow the ice sheet than those needed to melt it.

In later work, Huybrechts and de Wolde (1999) performed experiments using an ice sheet model coupled to a two-dimensional climate model to investigate the dynamic aspect of ice sheet decline. They found that surface melting played the largest role in volume reduction, and that ice dynamics could act to slow the process on the century timescale, by causing the ice to thicken near the margins and reduce melt. Over longer periods, however, ice dynamics and the overall reduction in elevation induced more melt, causing higher mass loss. The most advanced study to date was performed using an atmosphere-ocean general circulation model (AOGCM) coupled to an ice sheet model (Ridley et al., 2005). The present-day ice sheet was forced by a scenario of four times the preindustrial atmospheric CO<sub>2</sub> concentration. Under those conditions, the GIS melted completely in a period of just over 3,000 years. The reduction in elevation and change in the surface type induced local and regional climate changes as well. Ridley et al. (2009) used partially melted ice sheet configurations from the high CO<sub>2</sub> scenario to see if the GIS could regrow when temperatures were returned back to preindustrial levels. They found that in some cases a threshold was crossed, after which full or partial mass loss became inevitable.

The tipping point, or threshold in temperature, that would initially lead to such a decline has not yet been well determined for the GIS. The more advanced studies have focused on high CO<sub>2</sub> scenarios, while older studies were unable to incorporate the relevant feedback processes or climatic changes in a robust way. The accepted estimate for the threshold, as reported by the IPCC (Meehl et al., 2007), is rather uncertain and lies in the range of 1.9-4.6 °C above preindustrial temperatures. To make this estimate, the surface mass balance of the GIS was calculated, using the semi-empirical PDD model, for temperature anomalies determined by simulations of AOGCMs under various global warming scenarios (Gregory and Huybrechts, 2006). The GIS topography was kept fixed and the threshold leading to GIS deglaciation was defined as the temperature at which the SMB turned negative. They provided a probabilistic estimate of the threshold and the study represents a major advancement in the understanding of how the GIS and the climate may interact in the future. Further improvements could be made, however, given a model that accounts for the relevant feedbacks in the system (i.e., both albedo and elevation changes) coupled to a dynamically changing ice sheet model.

## 1.4 Motivation

The aim of this thesis is to improve the representation of the surface forcing of the GIS and to study the sensitivity of the ice sheet to long-term changes in climate. This entails coupled climate-ice sheet model simulations, in which the most important processes and feedbacks are explicitly represented. At the same time, the approach must be computationally efficient, to allow simulations over very long timescales. This novel approach is needed for two reasons.

First, though only limited observations of the boundary conditions for modeling the GIS exist, their accurate representation is critically important for modeling its evolution. This is especially true at the surface, because the GIS is particularly vulnerable to warmer climatic conditions through surface melt.

The second reason is that existing methods are either too simple or too complex for coupled simulations on long timescales. For almost two decades, the majority of ice sheet models used some form of the conventional PDD approach (Reeh, 1991) for surface boundary conditions. Indeed, this approach produces fairly accurate forcing of the ice sheet under present-day conditions with minimal computational cost. However, it is questionable whether a parameterization based solely on present-day observations holds under different climatic or topographic conditions. Meanwhile, the shortcomings of semi-empirical approaches are addressed by complex RCMs that include all of the relevant physical processes to a high degree of complexity (e.g., Fettweis, 2007; Ettema et al., 2009). However, the high computational demand of such models limits their applicability to short-term diagnostic studies, rather than long-term coupled simulations.

In this thesis, we developed a new approach to incorporate the advantages of both existing methods. The regional energy-moisture balance model (REMBO) developed here provides a simple, yet physically-based, representation of the surface boundary conditions of the ice sheet. The key advantage of this approach is that it is computationally efficient, while capturing the most important climate-ice sheet feedbacks in the system. This allows long timescale simulations of the past and future evolution of the GIS and, thus, to address several unresolved scientific questions:

**Can the surface conditions of the GIS and its regional climate be accurately captured by a simple, yet physically-based approach?**

This is the first fundamental question to be answered. As an approach of this type has not been applied to the GIS until now, it is not certain *a priori* that such an intermediate complexity model can be built successfully. Proving that such a model can reproduce physical variables accurately, and react to physical forcing in a realistic way is a prerequisite to further study. In addition, the success of such a model can give insight into the dominant physical processes that determine the climate and surface conditions of Greenland.

---

**Can model parameters be constrained and uncertainties reduced using available present-day and paleo data? What was the contribution of the Greenland Ice Sheet to the sea level high-stand during the Eemian Interglacial?**

The past evolution of the GIS, particularly during warm, interglacial periods, is not well known or constrained by data. It is important to investigate, both to help better understand the sensitivity of the GIS to future climate changes, but also to develop our understanding of the processes important to the ice sheet on glacial timescales. Several studies have estimated past changes to the GIS during the Eemian (the most recent interglacial period), but conclusions remain highly uncertain. The previous studies used modeling approaches fundamentally different from that applied in this thesis, so it may be possible to reduce or at least quantify the uncertainty of such estimates. Thus, the goal of this study is to reduce the uncertainty in model performance and, in doing so, improve our understanding of the past. By applying constraints different from those used so far, it may be possible to reduce uncertainty and improve our overall understanding of the processes and timescales important to the evolution of the GIS. In addition, this can also improve the predictive capability of the model by providing a constrained range of model parameters.

**What is the long-term sensitivity of the GIS to future climate change? What is the temperature threshold that would lead to complete melting of the GIS? At what point would such a disappearance become irreversible?**

These questions are highly relevant to our future as a whole and by addressing them, the impact of human behavior on the planet can be quantified more precisely. Until now, these questions have largely been addressed indirectly, by inferring long-term behavior from diagnostic estimates for short-term changes, or through studies unable to systematically map the long-term response because it is computationally prohibitive. Simulations through the glacial cycles are needed to prescribe the initial conditions of the ice sheet and a reliable method to produce surface forcing is essential. Here the prerequisites for such a long-term study are fulfilled, preparing ground for a systematic analysis of the stability and thresholds of the GIS.

## 1.5 Overview

This thesis is organized around three published (or in review) scientific articles based on this work. Each paper provides its specific motivation and background. Topics addressed in each of them are the model description, validation of its performance through simulations of the past and an application of the model to scenarios of future warming. Following the articles is a discussion of the work in a broader context and its relevance to climate change science and ice sheet modeling. Here a list of each article is given, with a brief description of its contents and the work contributed by each author.

**Article 1: An efficient regional energy-moisture balance model for simulation of the Greenland Ice Sheet response to climate change***Alexander Robinson, Reinhard Calov, Andrey Ganopolski*

The first published article (Chapter Two) describes the regional climate and surface mass balance model developed in this study. The theoretical fundamentals and governing equations of the energy-moisture balance and melt model are explained in detail. Furthermore, the new approach is compared to conventional methods, RCMs and observational data. This article thus provides a proof of concept by introducing and justifying the modeling approach.

Alexander Robinson wrote and developed the complete model code of REMBO, while Reinhard Calov and Andrey Ganopolski supervised this work, providing feedback and suggestions for improvement. All simulation and data processing tasks were performed by Alexander Robinson and all three authors contributed to the analysis of the results and the conclusions reached. Alexander Robinson wrote the first draft of the paper and several iterations of changes and improvements between all three authors produced the final version.

**Article 2: Greenland Ice Sheet model parameters constrained using simulations of the Eemian Interglacial***Alexander Robinson, Reinhard Calov, Andrey Ganopolski*

The second published article (Chapter Three) presents the model validation using observational data to constrain several model parameters. Here, both present-day observations and paleo data from the Eemian are used to constrain model performance for a broad range of climatic and topographic conditions. Parameter combinations that do not agree with the constraints are eliminated and model uncertainty is thus both quantified and reduced. The GIS contribution to the sea level high-stand during the Eemian Interglacial is also examined.

Alexander Robinson modified the REMBO code to work for glacial cycle simulations, including input and processing of boundary forcing data. Alexander Robinson performed the simulations and prepared the large data sets and designed the plots for this article. The large number of simulations and data output required automatic pre- and post-processing tools, which were developed by Alexander Robinson. Reinhard Calov and Andrey Ganopolski supervised the study and provided feedback and suggestions for improvement. All three authors contributed to the analysis of the results and the conclusions reached. Alexander Robinson wrote the first draft of the paper and several iterations of changes and improvements between all three authors produced the final version.

**Article 3: Multistability and critical thresholds of the Greenland ice sheet***Alexander Robinson, Reinhard Calov, Andrey Ganopolski*

The third article, submitted for publication (Chapter Four), presents results using the

---

validated modeling approach. In this article, the critical thresholds and possible multi-stable characteristics of the ice sheet are investigated. Models versions that were valid for glacial cycle simulations are used to perform simulations into the future under varying levels of global warming. The critical thresholds (or tipping points) of the GIS are quantified with more certainty and the irreversibility of large-scale ice sheet decline is explored.

Alexander Robinson performed the simulations, analyzed and prepared the large data sets and designed the plots for this article. Reinhard Calov and Andrey Ganopolski supervised the study and provided feedback and suggestions for improvement. All three authors contributed to the analysis of the results and the conclusions reached. Alexander Robinson wrote the first draft of the paper and several iterations of changes and improvements between all three authors produced the submitted version.



## 2. AN EFFICIENT REGIONAL ENERGY-MOISTURE BALANCE MODEL FOR SIMULATION OF THE GREENLAND ICE SHEET RESPONSE TO CLIMATE CHANGE<sup>1</sup>

### Abstract

In order to explore the response of the Greenland ice sheet (GIS) to climate change on long (centennial to multi-millennial) time scales, a regional energy-moisture balance model has been developed. This model simulates seasonal variations of temperature and precipitation over Greenland and explicitly accounts for elevation and albedo feedbacks. From these fields, the annual mean surface temperature and surface mass balance can be determined and used to force an ice sheet model. The melt component of the surface mass balance is computed here using both a positive degree day approach and a more physically-based alternative that includes insolation and albedo explicitly. As a validation of the climate model, we first simulated temperature and precipitation over Greenland for the prescribed, present-day topography. Our simulated climatology compares well to observations and does not differ significantly from that of a simple parameterization used in many previous simulations. Furthermore, the calculated surface mass balance using both melt schemes falls within the range of recent regional climate model results. For a prescribed, ice-free state, the differences in simulated climatology between the regional energy-moisture balance model and the simple parameterization become significant, with our model showing much stronger summer warming. When coupled to a three-dimensional ice sheet model and initialized with present-day conditions, the two melt schemes both allow realistic simulations of the present-day GIS.

### 2.1 Introduction

Modeling the future evolution of the Greenland Ice Sheet (GIS) has attracted considerable attention in recent years, due to a potentially significant contribution of the GIS to future sea level rise (Lemke et al., 2007). Over recent decades, significant GIS mass losses have been diagnosed by on-site measurements (Abdalati and Steffen, 2001), InSAR

---

<sup>1</sup> Robinson, A., Calov, R., and Ganopolski, A.: An efficient regional energy-moisture balance model for simulation of the Greenland Ice Sheet response to climate change, *The Cryosphere*, 4, 129–144, doi:10.5194/tc-4-129-2010, 2010.

velocity measurements (Rignot and Kanagaratnam, 2006; Rignot et al., 2008), GRACE satellite measurements of gravity changes (Velicogna and Wahr, 2005; Ramillien et al., 2006; Velicogna, 2009) and regional modeling (Box et al., 2006). While it is expected that only a rather small portion of the GIS can melt over the 21<sup>st</sup> century (Lemke et al., 2007), modeling studies (van de Wal and Oerlemans, 1994; Huybrechts and de Wolde, 1999; Ridley et al., 2005; Charbit et al., 2008) show that on the millennial time scale, the GIS can melt completely if temperatures stay above a certain threshold.

For the 21<sup>st</sup> century, a number of coupled general circulation model (GCM) runs for several emission scenarios are available and can be used to force ice sheet models. The use of high-resolution, regional models driven by GCMs could additionally improve the representation of climate change over Greenland (Box et al., 2006; Fettweis, 2007; Ettema et al., 2009). However, for longer time scales, coupled GCMs are not only computationally expensive, but gradual changes in the topography and ice sheet extent should also be taken into account. This requires bi-directional coupling between climate and ice sheet models, which makes these models even more computationally expensive. So far, only a few experiments of this sort have been performed, using rather coarse resolution GCMs (e.g., Ridley et al., 2005; Mikolajewicz et al., 2005, 2007; Vizcano et al., 2008).

Most studies of the short- and long-term response of the GIS to global warming use a rather simple approach, in which a simulated temperature anomaly field or a constant temperature offset is added to the modern climatological temperatures and a simple correction for elevation change is employed (e.g., Greve, 2000; Huybrechts et al., 2004; Parizek and Alley, 2004; Gregory and Huybrechts, 2006). While such an approach is justified for short-term predictions, it becomes less applicable on longer time scales, when the GIS can change dramatically. Changes in ice sheet extent and elevation will lead to pronounced changes in temperature and precipitation patterns. In particular, the reduction in surface albedo due to a retreat of the ice sheet would cause a large temperature change that would not be captured by a simple elevation correction. These changes would also affect the spatial and seasonal distribution of precipitation, as well as the relative amount of precipitation falling as snow.

The representation of accumulation over the ice sheet using the annual observational field suffers further limitations, in that (1) estimates of the present-day annual accumulation rate are derived from a rather sparse observational network (Bales et al., 2009), and (2) real precipitation over Greenland exhibits significant seasonality. Since most precipitation over the GIS currently occurs in the form of snow, the use of an annual accumulation field has been assumed to allow a reasonable approximation for modeling the surface mass balance (SMB). Depending on the time of year, however, new snow can have a strong effect on surface albedo. In addition, precipitation over the GIS is, to a large extent, topographically controlled. Changes in the elevation (let alone a complete disappearance of the GIS) would have a pronounced effect on the distribution of precipitation and snowfall over Greenland. To overcome some of the limitations of the conventional approach to



representing the climate over the GIS, particularly when used for long-term simulations of the GIS, we developed a new approach based on a regional energy and moisture balance model. Though relatively simple compared to regional climate models (RCMs), our approach accounts for most essential physical processes. It should therefore be considered as a physically-based downscaling technique, rather than a regional climate model on its own. This approach can be used to determine realistic temperature and precipitation fields over Greenland, given topographic and climatic conditions that are dramatically different from today. Importantly, it is also computationally efficient enough to permit long-term simulations of the response of the GIS to climate change. The model is evaluated here for both present-day and ice-free topographic conditions.

Furthermore, in most previous modeling studies, surface ablation has been simulated using the positive degree day (PDD) method. Besides several applications on a smaller scale (e.g., Braithwaite, 1980), the PDD method has also been utilized to calculate surface ablation in large-scale models of the GIS (e.g., Reeh, 1991; Huybrechts et al., 1991; Calov and Hutter, 1996; Ritz et al., 1997; Janssens and Huybrechts, 2000; Huybrechts et al., 2004; Ridley et al., 2005). In this method, surface melt is explicitly determined from surface air temperature alone. The effect of albedo on surface melt is accounted for implicitly, via different empirical coefficients for snow and ice. Although the method has been successfully tested against present-day empirical data, its applicability to future climate change may be compromised, since the relationship between temperature and albedo will be different under global warming induced by greenhouse gases. van de Wal (1996) performed a comparison between the PDD method and an energy balance model for Greenland, finding that the sensitivity of the two approaches to climate change varied considerably.

In contrast to the PDD method, another simplified method for computing surface ablation explicitly includes the effects of both temperature and insolation. It has recently been employed by van den Berg et al. (2008) to simulate ice sheet changes through glacial cycles. Such a parameterization, introduced early on by Pollard (1980), found its application to the simulation of the evolution of ice sheets during the ice ages (Esch and Herterich, 1990; Deblonde et al., 1992; Peltier and Marshall, 1995) and is nowadays becoming more prevalent in ice sheet modeling (e.g., Hebel et al., 2008). However, this method is still not as widely used or accepted as the PDD method. For convenience, we will call it the insolation-temperature melt (ITM) method. ITM requires essentially the same input as the PDD method, although an additional parameterization of surface albedo is needed. It is also computationally efficient, allowing its use for long-term simulations. As it is not known a priori which melt calculation method provides more realistic ice sheet forcing, a comparison of both methods to each other and to RCM results could help quantify uncertainties in future predictions related to the choice of the surface mass balance scheme.

## 2.2 Model description

The model used here to compute the surface boundary conditions over the GIS consists of two parts: (1) the regional energy-moisture balance orographic model (REMBO) that computes surface air temperature and precipitation; and (2) the surface interface, which provides surface ice temperature and surface mass balance to the ice sheet model. Both REMBO and the surface interface calculate daily fields, which allow seasonal variations in surface albedo to affect the climate and melt rate. This provides an important positive feedback, since changes in planetary albedo (via changes in surface albedo) affect the computed temperature and surface mass balance. In turn, changes in topography, simulated by the ice sheet model, affect the simulated climatology via elevation and slope effects (see section 2.1).

The REMBO model is coupled via the surface interface to the ice sheet model SICOPOLIS version 2.9 (Greve, 1997a). SICOPOLIS is a three-dimensional polythermal ice sheet model, which is based on the shallow-ice approximation (SIA). This type of model is the standard for modeling large ice sheets, as the SIA method neglects longitudinal stress gradients, providing significant computational advantages. Its main difference to other ice sheet models is the treatment of the temperate basal ice layers, in which the total heat flux and the diffusive water flux are calculated assuming a mixture of water and ice (Greve, 1997b). The cold ice regions are treated in a similar way to other thermomechanical ice sheet models via a temperature/energy balance equation including vertical diffusion, three-dimensional advection and dissipation terms.

While REMBO calculates climate fields on a low resolution grid (100 km), surface boundary conditions are computed via the surface interface on the grid of the ice sheet model, which has a spatial resolution of 20 km. This allows the surface interface to better resolve the rather narrow ablation zone on the margin of the ice sheet. We also performed equilibrium experiments with a spatial resolution of 10 km for the ice sheet model and surface interface and found minimal difference between the results obtained for the two grids. Therefore, all simulations presented hereafter were performed using the 20 km grid. The topography and albedo computed on the 20 km grid are aggregated to the 100 km grid of REMBO and are then used in the computations of surface temperature and precipitation. In turn, surface temperature and precipitation computed by REMBO are bilinearly interpolated onto the 20 km grid to provide input for computing the surface boundary conditions for the ice sheet model. To compute the daily surface mass balance, we used a simple snowpack model combined with one of the melt models mentioned in the introduction (PDD and ITM). In section 3, we will compare results obtained using these two approaches.

### 2.2.1 Regional energy-moisture balance model

The energy balance model follows a familiar form, first employed by Budyko (1969) and Sellers (1969), and reviewed by North et al. (1981), and still found in most simplified climate models. The equation for the atmospheric moisture budget, similar to that for temperature, was later added to energy balance models to simulate precipitation (e.g., Fanning and Weaver, 1996). Unlike most energy and moisture-balance models of the climate, which are global, the model employed in this study is regional and only applied over Greenland. Compared to conventional climate parameterizations used for forcing the long-term simulation of GIS evolution, the REMBO model provides a number of important advantages, because it explicitly accounts for the ice-albedo feedback, the effect of continentality (namely, enhanced seasonal temperature variations over the central part of Greenland as compared to the coastal areas) and the orographic effect on precipitation.

REMBO is based on two-dimensional, vertically integrated equations for energy (temperature) and water content in the atmosphere. The two prognostic variables are sea level temperature and specific humidity. The temperature and moisture balance equations are only solved over Greenland. Over the boundary ocean, surface air temperature and relative humidity are prescribed, either from climatology or GCM results. The governing equations are based on a number of assumptions. First, it is assumed that the lateral exchange of energy and moisture can be described in terms of macroturbulent diffusion, which implies the dominance of synoptic-scale processes over mean horizontal advection. Second, we assume that changes over Greenland do not affect the climate outside it, i.e., we consider only uni-directional interaction. Third, vertical temperature and humidity profiles are assumed to have a universal structure (e.g., Petoukhov et al., 2000). Finally, the heat capacity of the active soil or snow/ice layer is neglected, as well as changes in cloud cover.

The vertically-integrated energy balance for the total atmospheric column is written in terms of the sea-level temperature  $T_{SL}$  as

$$c_p \rho_a H_a \frac{\partial T_{SL}}{\partial t} = D_T \nabla^2 T_{SL} + (1 - \alpha_p) S - [A + BT] + L_w P_w + L_s P_s - L_s M_{s,net} + R(CO_2), \quad (2.1)$$

where the first term on the right side of the equation represents the horizontal diffusion of the temperature, second – absorbed solar radiation, third – outgoing long-wave radiation, fourth to sixth – latent heat related to condensation of liquid water, snow formation and surface melting of snow/ice, respectively, and the last term – radiative forcing of CO<sub>2</sub> relative to the preindustrial state (set to zero in this study),  $c_p$  is the air heat capacity,  $\rho_a$  is the air density,  $H_a$  is the atmospheric height scale,  $D_T$  is the coefficient of horizontal energy diffusion,  $S$  is the insolation at the top of the atmosphere,  $\alpha_p$  is the planetary albedo,  $A$  and  $B$  are empirical coefficients in Budyko's parameterization of outgoing long-wave radiation,  $P_w$  and  $P_s$  are precipitation in liquid and solid form,  $M_{s,net}$  is the net surface melt rate (including refreezing), and  $L_w$  and  $L_s$  are the latent heats of condensation and

snow formation, respectively. The surface temperature,  $T$ , is then related to the sea-level temperature by surface elevation  $z_s$ , multiplied by the free atmospheric lapse-rate,  $\gamma_a$ ,

$$T = T_{SL} + \gamma_a z_s. \quad (2.2)$$

Next, the moisture balance equation is written as

$$\rho_a H_e \frac{\partial Q}{\partial t} = D_Q \nabla^2 Q - P, \quad (2.3)$$

where  $Q$  is the surface air specific humidity,  $H_e$  is the water vapor scale height,  $D_Q$  is the coefficient of horizontal macroturbulent moisture diffusion and  $P$  is the total precipitation. To make the model applicable to the simulation of different climate states, outside of the modeling domain we prescribed relative humidity rather than specific humidity, since the former is less sensitive to temperature changes than the latter. Therefore, the boundary value for specific humidity is computed from the formula

$$Q = Q_{sat}(T) r, \quad (2.4)$$

where  $r$  is the relative humidity and  $Q_{sat}(T)$  is the saturation specific humidity, which is described by the Clausius-Clayperon function of air temperature. The total amount of precipitation is computed, following an approach similar to that of Petoukhov et al. (2000) and Calov et al. (2005), as

$$P = (1 + k |\nabla z_s|) \left( \frac{Q}{\tau} \right). \quad (2.5)$$

Here  $|\nabla z_s|$  is the module of the gradient of surface elevation,  $\tau$  is the water turnover time in the atmosphere (set to 5 days), and  $k$  is an empirical parameter. Note that Eq. (2.5) is also similar to that used by van den Berg et al. (2008), in that precipitation is strongly dependent on the surface gradient.

The amount of snowfall at each point is calculated as a fraction of the total precipitation,

$$P_s = P f(T), \quad (2.6)$$

where the fraction,  $f$ , depends on the surface temperature. Below a minimum temperature, this fraction is 1 (all precipitation falls as snow), and above a maximum temperature, this fraction is 0 (no snow). The fraction follows a sine function from 1 to 0 between the minimum and maximum temperatures, which were set to  $-7^\circ\text{C}$  and  $7^\circ\text{C}$ , respectively, as these were found to provide a reasonable ratio between total snowfall and precipitation, and follow estimates from empirical data over Greenland (Calanca et al., 2000; Bales et al., 2009).

The diffusion coefficients,  $D_Q$  and  $D_T$ , in Eqs. (2.1) and (2.3), both decrease linearly with latitude  $\phi$  (in degrees), and  $D_T$  also increases linearly with surface elevation  $z_s$  (in meters):

$$D_Q = (1 - 0.01\phi) \cdot \kappa_Q, \quad (2.7)$$

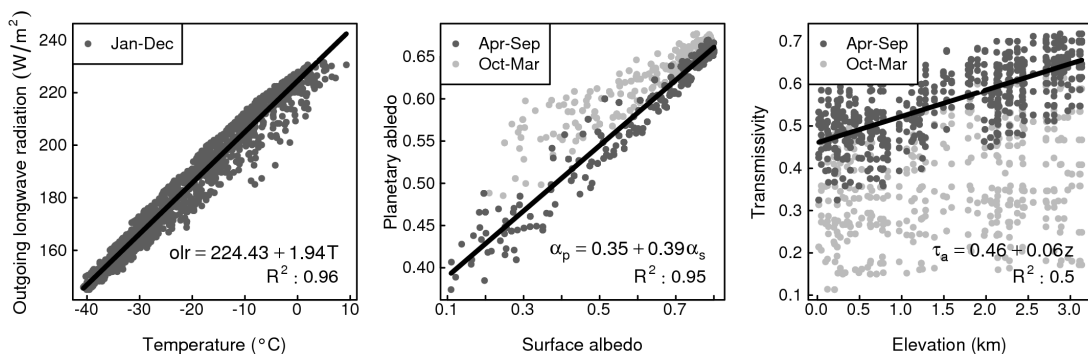


Figure 2.1: (a) Monthly ERA-40 data of outgoing long-wave radiative flux versus temperature, shown with a linear fit to all data. Monthly ISCCP data, Apr-Sep (dark points) and Oct-Mar (light points), of (b) planetary albedo versus surface albedo with a linear fit to the months Apr-Sep, and (c) transmissivity versus elevation with a linear fit to the months Apr-Sep. All points are from data over Greenland.

$$D_T = (1 + 0.00125z_s) (1 - 0.01\phi) \cdot \kappa_T, \quad (2.8)$$

where  $\kappa_Q$  and  $\kappa_T$  are the diffusion constants for moisture and temperature, respectively. The decrease of diffusion with latitude accounts for reduced synoptic activity from the middle to high latitudes, while the dependence on elevation assumes that wind increases with elevation. The latter dependence was necessary for the model to produce the seasonal cycle of temperature correctly over the central part of Greenland.

Outgoing long-wave radiation is parameterized as a linear function of surface air temperature. The values of parameters  $A$  and  $B$  were found using values for upward long-wave radiation and surface temperature over Greenland from the European Center for Medium Range Weather Forecasts (ECMWF) Reanalysis 40 (ERA-40) data set (Uppala et al., 2005), shown in Fig. 2.1a. Monthly climatological data over the entire year were used, and the best fit to these data gave parameter values close to those used by Budyko (1969). These and other important numerical parameters of the model are summarized in Table 2.1.

Planetary albedo is parameterized as a linear function of surface albedo (Fig. 2.1b). The fit was found from values of surface and planetary albedo, derived from monthly International Satellite Cloud Climatology Project (ISCCP) radiation data (Zhang et al., 2004), and is given by

$$\alpha_p = 0.35 + 0.39\alpha_s. \quad (2.9)$$

Only summer values (April-September) were used to obtain the fit, since at high latitudes, insolation in winter is insignificant, thus the winter albedo is not relevant. Surface albedo,  $\alpha_s$ , is calculated as a function of ground albedo (ice or bare soil) and the snow thickness, similar to that proposed by Oerlemans (1991), and more recently used by Bintanja et al.

Table 2.1: Selected parameters used in REMBO and the two melt models, PDD and ITM.

Parameter	Units	Best value	Description
REMBO parameters			
$\kappa_T$	W/K	2.8e12	Temperature diffusion constant
$c_P$	J/(K kg)	1000	Air heat capacity
$B$	W/(m <sup>2</sup> K)	1.97	Long-wave radiation parameter
$A$	W/m <sup>2</sup>	222.3	Long-wave radiation parameter
$\gamma_a$	K/m	0.0065	Free atmospheric lapse rate
$\kappa_Q$	kg/s	9.8e5	Moisture diffusion constant
$k$	- -	50	Precipitation parameter
$\tau$	days	5	Water turnover time
$H_a$	m	8600	Atmospheric scale height
$H_e$	m	2000	Water vapor scale height
PDD parameters			
$\sigma$	K	5	Standard deviation of temp. normal distribution
$b_s$	mwe/(day K)	0.003	Degree-day factor for snow
$b_i$	mwe/(day K)	0.008	Degree-day factor for ice
ITM parameters			
$c$	W/m <sup>2</sup>	-55	Short-wave radiation and sensible heat flux constant
$\lambda$	W/(m <sup>2</sup> K)	10	Long-wave radiation coefficient
$r_{max}$	- -	0.6	Refreezing fraction

(2002) and van den Berg et al. (2008),

$$\alpha_s = \min \left( \alpha_g + \frac{d}{d_{crit}} (\alpha_{s,max} - \alpha_g), \alpha_{s,max} \right). \quad (2.10)$$

The maximum snow albedo,  $\alpha_{s,max}$ , has a value of either 0.8 or 0.6, representing either a dry-snow or wet-snow covered surface, respectively. The value is chosen based on whether any melting has occurred at that location on that day. The ground albedo,  $\alpha_g$ , has a value of 0.4 for ice and 0.2 for ice-free land. If no snow is present, the surface albedo equals the ground albedo. Comparison with the ISCCP satellite data for radiation at the surface shows that this parameterization provides a quite realistic range of values of surface albedo for Greenland.

To prescribe boundary conditions for temperature and humidity, we used ERA-40 data (Uppala et al., 2005), since the ECMWF reanalysis data sets have been shown to be quite realistic in representing important climate variables for the Greenland region (Hanna and Valdes, 2001; Hanna et al., 2005). Monthly climatological fields (averaged from 1958 to 2001) of temperature and relative humidity from the 2.5° ERA-40 grid were bi-linearly interpolated to the Cartesian 100 km grid used in REMBO. In addition, temperature fields were corrected for elevation differences (Hanna et al., 2005) between ERA-40 and REMBO using, for simplicity, the free atmospheric lapse rate  $\gamma_a = 0.0065$  K/m.

The equations for temperature and moisture (Eqs. (2.1) and (2.2)) are solved using an alternating-direction implicit discretization scheme, which allows a larger time step than a standard explicit scheme. Still, for numerical stability reasons, the time step used to solve the energy balance equations is quite small, on the order of 1/10 of a day and, therefore, the REMBO model is more computationally demanding than the ice sheet model. This

does not present a problem for short-term (decadal to centennial time scale) simulations, but for millennial and longer simulations, asynchronous coupling between REMBO, the surface interface and the ice sheet model was used. In the equilibrium runs described below, the surface mass balance interface was only called for every ten ice sheet model years and REMBO was called for every one hundred ice sheet model years. This calling frequency would affect the transient behavior of the GIS somewhat, but not the simulated equilibrium state reached after several thousand years.

### 2.2.2 Surface mass balance

The annual surface mass balance is computed using a simple snowpack model through equations of snow ( $h_s$ ) and ice ( $h_i$ ) thickness in water equivalent, calculated daily over the year:

$$\frac{dh_s}{dt} = P_s - M_s, \quad h_s \in (0, h_{max}), \quad (2.11)$$

$$\frac{dh_i}{dt} = \begin{cases} M_s r_f, & h_s > 0 \\ \min(P_s - M_s, 0), & h_s = 0 \end{cases}, \quad (2.12)$$

where  $M_s$  is the potential surface melt rate and  $r_f$  is the refreezing fraction. Snow cover thickness is not allowed to exceed an arbitrary maximum height of 5 m (in water equivalent). At each time step, any excess of snow thickness above this limit is added to the ice thickness computed by Eq. (2.12), and snow thickness is reset to 5 m. The refreezing fraction is equal to zero in the absence of snow, while for  $0 < h_s < 1$  m, it is defined following Janssens and Huybrechts (2000) as

$$r_f = r_{max} f(T), \quad (2.13)$$

where  $f(T)$  is the fraction of snow of the total precipitation, and  $r_{max}$  is equivalent to the ‘‘PMAX’’ factor originally described by Reeh (1991), which indicates the maximum fraction of snow that is able to refreeze. For snow thickness  $h_s > 1$  m, refreezing is set to 1, i.e., for the thick firn layer, surface melt does not contribute to runoff, but converts into ice at the bottom of the firn layer. This difference in parameterization of the refreezing from the standard PDD model does not affect the surface mass balance of the ice sheet in equilibrium but plays an important role for the transient response of the GIS surface mass balance on decadal to centennial time scales. Finally, the annual mean surface mass balance of the ice sheet is computed at the end of each year as the difference between the final and initial thickness of the ice.

The surface ice temperature used as a boundary condition for the ice sheet model is determined as  $T_i = \min(T_a, 0) + 29.2h_{i,sup}$ , where  $T_a$  is the mean annual temperature and  $h_{i,sup}$  is the amount of superimposed ice (m.w.e.) resulting from refrozen snow and rain during the year (Reeh, 1991). To initialize the surface interface, the snow height is set to the maximum everywhere. Then REMBO and the surface interface are run interactively

for 200 years until the melt variables and the snow height reach approximate equilibrium values.

### Positive degree day (PDD) method

The PDD method is the conventional approach used to determine the melt potential of a given year, using calculated positive degree days from a seasonal cycle of temperature. It was initially introduced for the simulation of local glaciers by Braithwaite (1980) and was further developed by Reeh (1991). It has been described by several others and is consistently used for ice sheet model surface forcing (e.g., Ritz et al., 1997; Cuffey and Marshall, 2000; Huybrechts et al., 2004; Charbit et al., 2008). To account for inter- and intra-annual variability, an “effective” daily temperature,  $T_{eff}$ , is calculated from the daily temperature,  $T_m$ , as

$$T_{eff} = \frac{1}{\sigma\sqrt{2\pi}} \int_0^{\infty} T \exp\left(-\frac{(T - T_m)^2}{2\sigma^2}\right) dT \quad (2.14)$$

The value of the standard deviation,  $\sigma$ , was set to 5 °C, as in many previous studies, and  $T_{eff}$  was numerically calculated according to the method described by Calov and Greve (2005). Usually, the annual positive degree days (PDDs) are computed as the sum of the effective temperature over the year. In our case, since the model resolves the seasonal cycle, the effective temperature is used to compute daily potential melt rate in much the same way, as

$$M_s = bT_{eff}, \quad (2.15)$$

where the empirical coefficient  $b_s = 0.003$  mwe/(day K) for snow and  $b_i = 0.008$  mwe/(day K) for ice (and mwe = meters water equivalent).

### Insolation-temperature melt (ITM) method

The ITM method is based on the work of Pellicciotti et al. (2005) and van den Berg et al. (2008). In this method, the potential daily surface melt rate is determined from surface air temperature and absorbed insolation:

$$M_s = \frac{\Delta t}{\rho_w L_m} [\tau_a (1 - \alpha_s) S + c + \lambda T], \quad (2.16)$$

where  $\tau_a$  is the transmissivity of the atmosphere (i.e., the ratio between downward short-wave radiation at the land surface and at the top of the atmosphere),  $L_m$  is the latent heat of ice melting,  $\alpha_s$  is the surface albedo,  $S$  is the insolation at the top of the atmosphere,  $\Delta t$  is the day length in seconds and  $\lambda$  and  $c$  are empirical parameters. Unlike the PDD method, this method explicitly accounts for shortwave radiation, and the difference between snow and ice is expressed in Eq. (2.16) via different surface albedo values.



Based on the summer (April-September) ISCCP radiation data, transmissivity over Greenland was prescribed as a function of elevation, with values ranging from about 0.4 to 0.7 (Fig. 2.1c). The linear fit was provided by

$$\tau_a = 0.46 + 0.0006z_s, \quad (2.17)$$

where  $z_s$  is the surface elevation in meters. The winter data were again not used for the fit, because such low values of incoming radiation increase the data spread, making any trend indiscernible. While more complex radiation schemes exist (e.g., Konzelmann et al., 1994), this equation provides a reasonable range of transmissivity values without the need for additional inputs. It should be noted that, at lower elevations, where the short-wave radiation term in the melt equation is more significant, the value of transmissivity is similar to the value of 0.5 used by van den Berg et al. (2008).

The parameter  $\lambda$  was set to  $10 \text{ W}/(\text{m}^2 \text{ K})$ , equal to that used by van den Berg et al. (2008), while  $c$  was used as a free parameter. The latter can range from  $-40 \text{ W}/\text{m}^2$  to  $-60 \text{ W}/\text{m}^2$  and still produce acceptable melt values for the present-day GIS, indicating large uncertainty in the choice of this value. This is discussed further below.

## 2.3 Modeling results

In order to evaluate the performance of REMBO and the melt models, we first performed simulations with the fixed, present-day topography of Greenland and modern climatological lateral boundary conditions. These results were compared with observations and a conventional parameterization of climate forcing used in the European Ice Sheet Modeling Initiative intercomparison project (Huybrechts, 1998, EISMINT,) and many recent publications (e.g., Ritz et al., 1997; Janssens and Huybrechts, 2000; Greve, 2005), in which temperature is parameterized as a function of elevation and latitude. Ablation and the surface mass balance of the GIS were also diagnosed from these experiments and compared with existing empirical and modeling estimates. REMBO was then coupled with the ice sheet model SICOPOLIS to simulate the equilibrium ice sheet under present-day climate conditions. The equilibrium simulations were performed using both the PDD and ITM surface melt approaches.

### 2.3.1 Simulations of climatology and surface mass balance with fixed topography

For diagnostic simulations of the present-day climatology and surface mass balance of the GIS, we used the 5 km resolution gridded topography from Bamber et al. (2001), aggregated to the resolution of the ice sheet model (20 km). Temperature and accumulation fields obtained from REMBO for the present-day Greenland topography have been compared to best estimates from observational data sets (correcting for elevation differences via the free atmospheric lapse rate). Several coastal observations were obtained from Technical Report 00-18 of the Danish Meteorological Institute (Cappelen et al., 2001), which provides

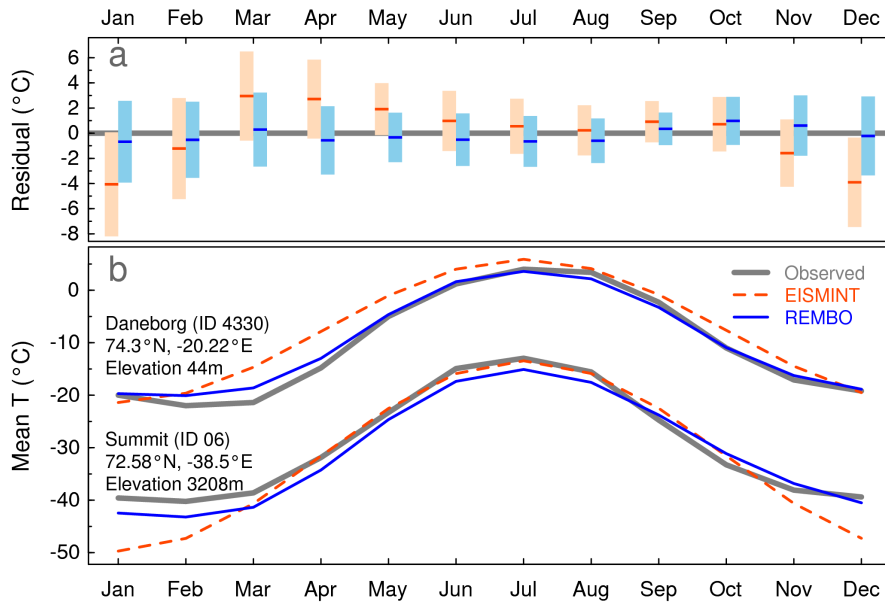


Figure 2.2: (a) Average and standard deviation of monthly residuals of REMBO (blue) and EISMINT (red) temperatures compared to station data at 52 locations. (b) Monthly temperatures from REMBO (solid blue line) and the EISMINT temperature parameterization (dashed red line), orographically-corrected and compared with DMI station data (thick grey line) for one high- and one low-elevation station on Greenland.

long-term means (1958-1999) of various climatic variables taken from automatic weather stations. Other observations were obtained from the GC-Net program for locations on the ice sheet itself (Steffen et al., 1996). Although the earliest GC-Net observations only began in 1995, they are the best resource available currently. The combination of these datasets provided mean monthly observations from 52 station locations, although due to their temporal inhomogeneity, we consider agreement with these observations only as a simple validation.

Temperatures from REMBO agree well with the observations, with an annual mean residual of  $-0.16 \pm 2.48$  °C. Temperatures obtained from the EISMINT parameterization (corrected for elevation differences via the parameterization’s lapse rates) also match observational data almost perfectly in the annual mean, with a residual of  $0.03 \pm 3.62$  °C. However, this agreement in annual mean masks some systematic seasonal biases, which are not present in REMBO simulations (Fig. 2.2a). REMBO temperatures around the Greenland coast are determined by the boundary ERA-40 reanalysis temperatures over the ocean, so the consistency of the REMBO temperatures with empirical data around the coast is not surprising. The EISMINT temperatures are directly based on coastal temperature data, but nonetheless show a slight warm bias at low elevations, as exemplified by the DMI station at Daneborg (id 4330), shown in Fig. 2.2b. At higher elevations on the ice sheet, where REMBO-simulated temperatures have more freedom to evolve away

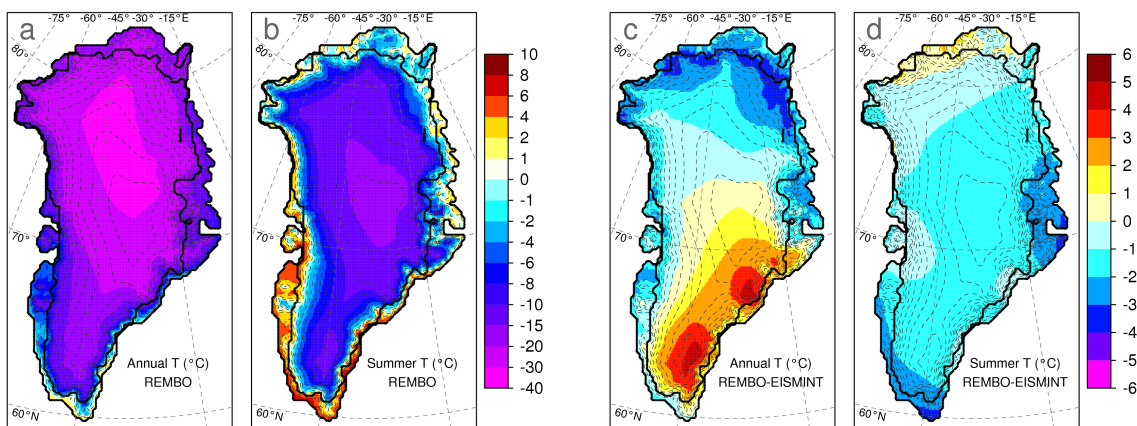


Figure 2.3: REMBO model output of (a) mean annual temperature and (b) mean summer (JJA) temperature. Difference between REMBO and EISMINT for (c) mean annual temperature and (d) mean summer (JJA) temperature. Elevation contours are shown at 300m intervals.

from the boundary conditions, the observed seasonal temperature variability is reproduced, except for a small cold bias. An example GC-NET high elevation station at Summit (id 06) is given in Fig. 2.2b. The EISMINT parameterization matches summer temperatures reasonably well, but winter temperatures are usually underestimated (a similar conclusion was reached by van der Veen, 2002).

The actual annual and summer temperatures predicted using REMBO can be seen in Figs. 2.3a and 2.3b, respectively. The differences between these temperatures and those obtained via the EISMINT parameterization are shown in Figs. 2.3c and 2.3d. Both the annual and summer temperatures are quite comparable, although there are notable differences in the annual mean temperature at high elevation in the South and for high latitudes. The biases in the annual EISMINT temperatures are due to the choice of latitudinal and elevation gradients optimized to improve the fit in warmer months. This results in a worse annual fit in the North and at high elevations in the South. This difference has little practical effect on ice sheet modeling for present day, given that temperatures in these regions remain well below freezing in the winter. The summer temperatures compare especially well around the coast and margin of the ice sheet, where temperature is most important for diagnosing melt. Figure 2.4 shows annual accumulation and total precipitation patterns simulated by REMBO, as well as the most recent estimates obtained from station data and several ice core samples, compiled by Bales et al. (2009). The simulated fields agree reasonably well with observations in large-scale patterns, despite local discrepancies. Particularly, low accumulation in the north and on the highly elevated central part of the GIS is reproduced well, and high accumulation values can be found along the Southeast coast. In REMBO, the gradient of elevation mainly determines how much precipitation will occur, implying that it is a result of orographic uplifting. Notably, however, REMBO

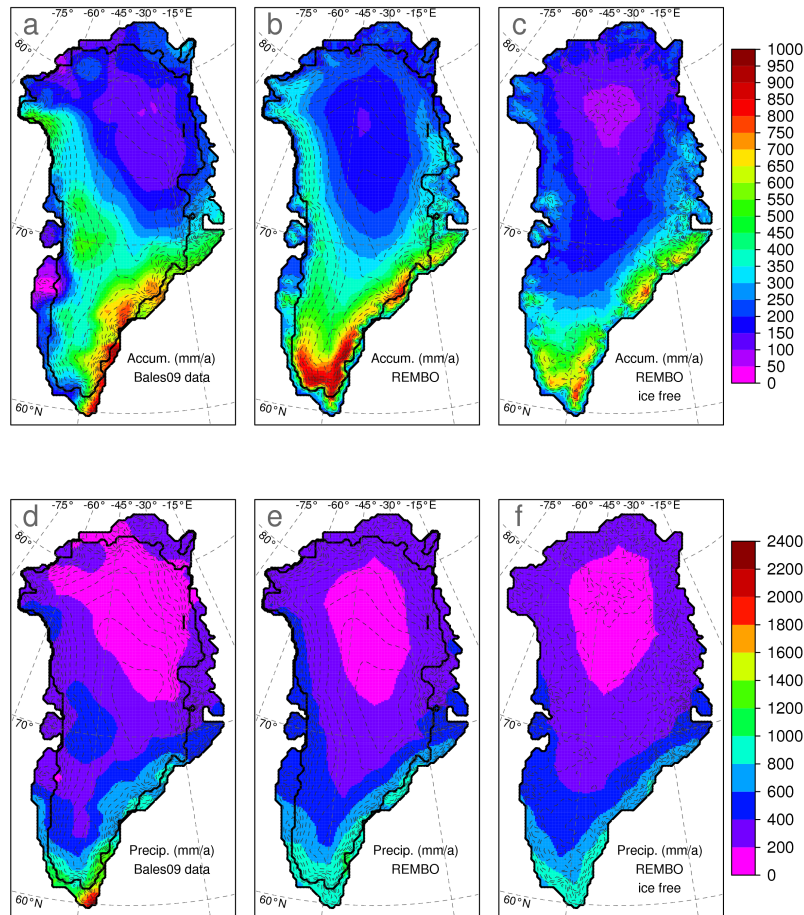


Figure 2.4: Greenland accumulation fields from (a) present-day data, (b) REMBO for present-day topography and (c) REMBO for ice-free, uplifted bedrock topography. Total precipitation fields for the same are shown in (d), (e) and (f), respectively. Elevation contours are shown at 300m intervals.

produces too much precipitation on the southwest coast and not enough on the southern tip of Greenland – an indication that local circulation may play a role that is not accounted for here. The annual accumulation total for the GIS simulated by REMBO is ca. 560 Gt/a, which matches the best estimate from Bales et al. (2009) and is within the range of several recent regional climate model studies (see Table 2.2).

Given the accumulation and temperature fields, it is then possible to diagnose the surface mass balance of the ice sheet (Figs. 2.5a and 2.5b). Using the fixed, present-day topography, REMBO was coupled with each melt model. Using both approaches, the overall area of melt predicted is fairly consistent; however, using the ITM approach, the area of melt is rather sensitive to the choice of the free parameter  $c$ . Here we chose  $c = -55 \text{ W/m}^2$  to simulate surface melt at similar levels to the PDD model. In Fig. 2.6, melt obtained from the ITM approach is plotted versus melt obtained from PDDs. For low levels of melt (at high elevation), the models tend to agree, with the ITM approach producing somewhat more intense values. At low elevation, the PDD approach produces

Table 2.2: REMBO diagnosed mass balance components for the present-day ice sheet compared to the range of RCMs, composed of results from PolarMM5 (Box et al., 2006), MAR (Fettweis, 2007) and RACMO2/GR (Ettema et al., 2009). All values are in Gt/a.

	Precip	Snow	Melt	Runoff	Refreezing	SMB
PDD	598	564	358	290	102	307
ITM	597	564	337	302	68	295
Range RCMs	600-743	578-697	249-580	232-307	35-295	287-469

considerably higher levels of melt compared to the ITM approach, indicating that the former has a stronger dependence on elevation. Both van de Wal (1996) and Bougamont et al. (2007) showed a similar relationship existed when comparing the PDD approach to an energy balance model. Furthermore, the ITM approach tends to show higher values of melt at high latitudes (difference shown in Fig. 2.5c), a tendency also shown by the energy balance model used by van de Wal (1996). This indicates that the ITM approach likely captures the first-order behavior of an energy balance model and produces a more realistic representation of melt.

In cumulative terms, any difference between the models is difficult to discern. A summary of surface mass balance components using REMBO with both melt models is compared to results from RCMs in Table 2.2. For individual components, our approach is generally able to perform well within the range of RCM results. Figure 2.7 shows the surface mass balance versus elevation for REMBO using PDD and ITM compared to output from two RCMs: the RACMO2/GR model for 1958-2008 (Ettema et al., 2009) and the PolarMM5 model for 1988-2004 (Box et al., 2006). The four panels show results for the GIS as divided into four quadrants, with the origin near Summit ( $-39^\circ\text{E}$ ,  $72^\circ\text{N}$ ). Results from the RCMs have been binned to reduce the number of points in the plot, with darker boxes indicating a higher density of points (i.e., where darker blue squares overlap with darker red squares, the RCMs agree). The trends produced using the PDD and ITM methods in all regions tend to fall in the range of the RCM results, although there are some differences. Both the PDD and ITM models produce higher maximum melt values in the North, and particularly in the Northeast, REMBO produces more accumulation than either of the RCMs. Nonetheless, these differences are minor, since accumulation values there are small. In the South, all models agree better. RACMO2/GR generally produces a much wider range of accumulation values, due to the high resolution (11 km) of topographic features (Ettema et al., 2009). The wider spread in the RCM surface mass balance also likely results from a more detailed representation of precipitation, which can vary based on regional processes, whereas precipitation in REMBO is inherently smoother. This comparison shows that for present-day conditions, both the PDD and ITM approach produce melt values that fall in the range of RCM results, and that they can also align with each other, depending on parameter choices. As mentioned before, the surface mass balance simulated by ITM is very sensitive to the parameter  $c$ . A higher value of  $c$  shifts

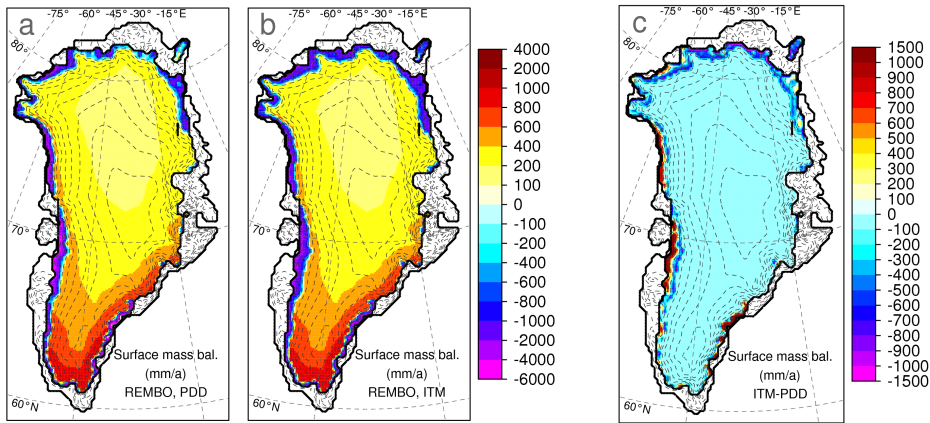


Figure 2.5: Diagnosed surface mass balance for fixed, present-day topography using REMBO with ablation determined by (a) PDD and (b) ITM. Panel (c) shows the difference between the two. Elevation contours are shown at 300 m intervals.

the snow line to higher elevations. Also, there is a gap in the near-zero negative SMB values for the ITM model. This stems from the discontinuity in surface albedo that occurs when surface melt begins (when switching from the dry snow albedo of 0.8 to the wet snow albedo of 0.6). This gap, however, has little effect on overall SMB, since it occurs only for very low melt values.

To evaluate the sensitivity of REMBO to climate change, using different melt parameterizations, we performed experiments under uniform (in space and time) warming of 1 and 3 °C with present-day insolation, and warming of 3 °C with insolation corresponding to Eemian orbital parameters. In these experiments (referred to in Table 2.3 as “equil.”), REMBO coupled to the snowpack model was run at least for 200 years, ensuring full equilibrium of the SMB was reached with the perturbed boundary conditions. When comparing two different melt schemes, it is important that they have similar present-day surface mass balance values (Table 2.2), because simulated anomalies strongly depend on the tuning of the models. Results presented in Table 2.3 show that the equilibrium response of SMB to regional temperature change is rather similar for both melt schemes. In units of sea

Table 2.3: Diagnosed equilibrium (equil.) and instantaneous (inst.) change in surface mass balance for the GIS from present day, under 1 °C and 3 °C of warming with present-day insolation and 3 °C of warming with Eemian insolation (EE). All values are in Gt/a and are relative to a present day estimate of ca. 300 Gt/a (see Table 2.2).

	+1 °C	+3 °C	+3 °C (EE)
PDD (equil.)	-90	-365	-407
ITM (equil.)	-94	-378	-696
PDD (inst)	-65	-224	--
ITM (inst)	-39	-113	--

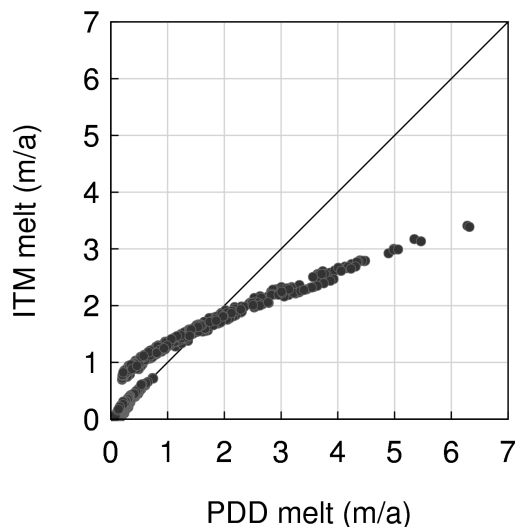


Figure 2.6: Annual melt rate calculated using the ITM approach vs. annual melt rate calculated using the PDD approach at each point on the ice sheet.

level rise, the changes in SMB for present-day conditions correspond to ca.  $0.3 \text{ mm}/(\text{a } ^\circ\text{C})$ , which is again in line with the findings of van de Wal (1996). A similar sensitivity of Greenland SMB to temperature was found by Janssens and Huybrechts (2000) who only used the annual PDD approach. However, this number is considerably higher than in simulations using output of coupled GCMs (e.g., Huybrechts et al., 2004). This makes sense because, in transient GCM experiments, simulated warming over the ablation zone is considerably lower than the average temperature change over Greenland, while the latter is used to calculate the sensitivity of SMB to regional temperature change.

Obtaining rather similar values for SMB sensitivity to warming obtained using both the PDD and ITM approaches is in apparent contradiction to Bougamont et al. (2007), who found that the PDD scheme predicts much larger changes in Greenland SMB as compared to a physically-based energy-balance model in a transient warming scenario. At least partly, this discrepancy can be explained by differences in equilibrium and transient SMB sensitivities to temperature change. The standard PDD scheme (calculated as an annual sum, as opposed to our daily scheme) does not include an evolving snowpack, which means it has no memory of previous years and, therefore, always simulates equilibrium SMB. In reality, the gradual rise of the snowline with a temperature increase will lead to slow melting of the thick snowpack at higher elevations, which will mostly refreeze and will not contribute to the mass loss of GIS. Since our simulations include a snowpack model which has memory, we can illustrate this effect via the instantaneous SMB response to the temperature rise, i.e., the change in SMB that occurs after the first year of applying the temperature anomaly (see the lower rows in Table 2.3, labeled “inst.”). For our PDD scheme, the simulated



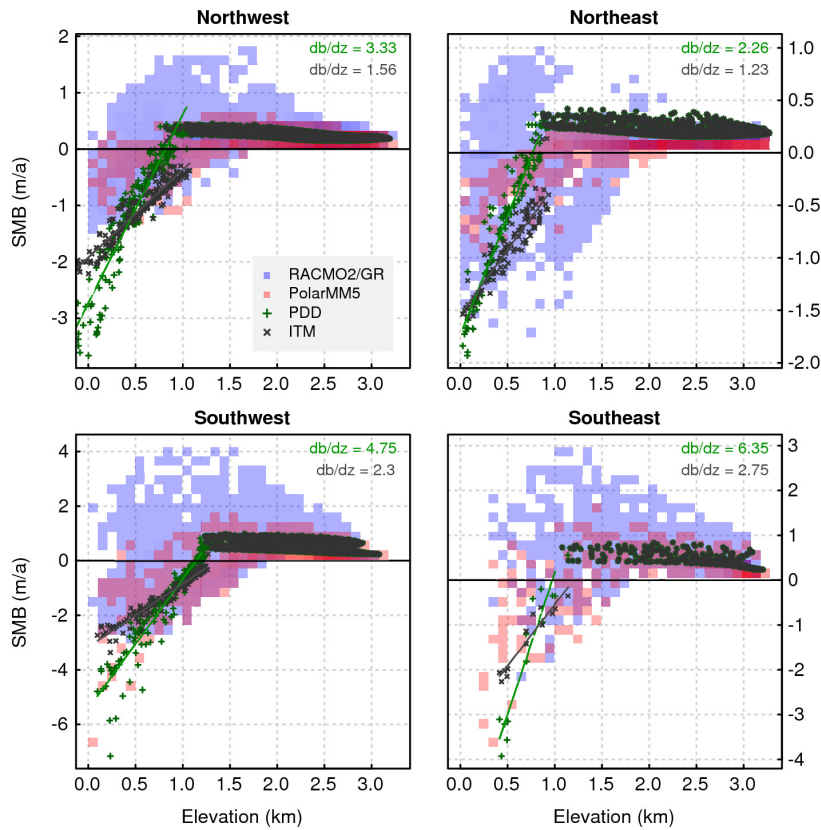


Figure 2.7: Diagnosed surface mass balance versus elevation by region for two RCMs and REMBO using the PDD and ITM approaches. The regions are defined as quadrants on Greenland with the origin near Summit ( $-39^{\circ}\text{E}$ ,  $72^{\circ}\text{N}$ ). RACMO2/GR results (Ettema et al., 2009) and PolarMM5 results (Box et al., 2006) were binned to reduce data density, with darker squares indicating a higher density of points. Trendlines and the slopes are shown for the negative points of the PDD and ITM approaches.

instantaneous response of SMB to an increase in temperature is appreciably smaller than that obtained in equilibrium. For the ITM scheme, the instantaneous response is less than half of the equilibrium response. The ITM scheme reacts more slowly initially, because it is not driven by temperature changes alone, but also by decreasing albedo as the snowpack melts. In both cases, for transient global warming scenarios, the sensitivity of SMB to an increase in temperature can be expected to lie between the instantaneous and equilibrium response and thereby should be considerably smaller than the equilibrium one. Therefore, our equilibrium results support the notion that the standard (annual) PDD approach does tend to overestimate the rate of GIS mass losses.

When considering the SMB response of these melt models to past climate change during the Eemian interglacial (including an increase in insolation), the ITM scheme shows a stronger equilibrium response. Since orbital variations occur on a multi-millennial timescale, one can expect that, in this case, the response of SMB to climate change can be considered to be in equilibrium. To mimic climate conditions during the Eemian, we



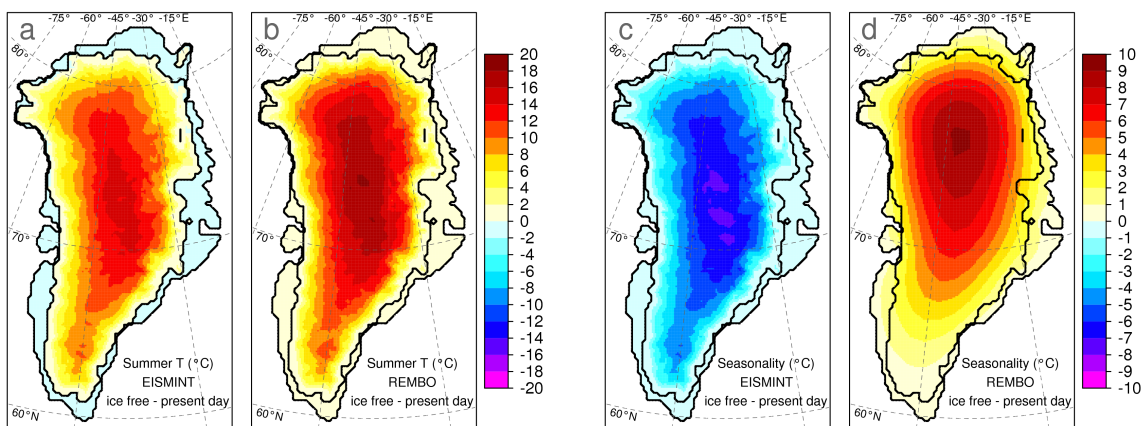


Figure 2.8: Summer (JJA) temperatures for ice-free, uplifted bedrock topography minus those of present-day, ice-covered conditions for (a) the EISMINT temperature parameterization and (b) REMBO. Difference in seasonality (June-July-August temperature minus December-January-February temperature) for the uplifted, ice-free topography compared to present-day, ice-covered conditions using (c) the EISMINT temperature parameterization and (d) REMBO.

again apply the uniform temperature anomaly of 3 °C, along with changes in insolation corresponding to Earth’s orbital parameters at 126 kaBP (kiloyears before present). While Eemian temperature anomalies likely exhibit strong seasonal variations, only summer temperatures are important for the SMB simulations and the 3 °C warming is consistent with empirical and modeling estimates of summer temperature changes around the GIS (e.g., Otto-Bliesner et al., 2006). SMB changes computed with the PDD scheme differ only slightly from the response to 3 °C warming (due to additional warming over the Greenland interior simulated by REMBO). However, the SMB change simulated with the ITM scheme increases dramatically due to the increased insolation. Thus, the Eemian change in SMB simulated by the ITM scheme is more than 50% greater than that simulated by the PDD scheme. These results indicate that changes in insolation are of comparable importance to temperature changes on orbital timescales and, therefore, the PDD scheme likely underestimates the past ice sheet response to climate warming via insolation changes considerably.

To assess the ability of REMBO to simulate the climate under boundary conditions radically different from the present, we performed simulations with a fixed topography of ice-free Greenland with corresponding uplifted bedrock (i.e., equilibrium bedrock after isostatic rebound). This test provides insight into the sensitivity of the REMBO climate to the presence of the ice sheet and can be compared with similar GCM simulations. It is also noteworthy to compare REMBO results with the EISMINT parameterization, which clearly demonstrates the advantages of a more physically-based approach.

Figure panels 2.8a and 2.8b show the difference in the mean summer (Jun-Jul-Aug) tem-

perature between the ice-free and present-day Greenland simulations, obtained with the EISMINT parameterization and with REMBO, respectively. Both modeling approaches produce qualitatively similar warming patterns associated with the lowering of elevation over currently ice-covered Greenland. However, there are significant quantitative differences. REMBO shows a surface air temperature increase of 18 °C in summer and only 10 °C in winter over the central part of Greenland. These numbers agree favorably with the results of simulations performed with GCMs for ice-free Greenland (Toniazzi et al., 2004; Lunt et al., 2004). Meanwhile, the EISMINT approach produces less warming in summer, but stronger warming in winter. As a result, REMBO shows that the magnitude of seasonal temperature variation over central Greenland increases by ca. 8 °C for ice free conditions (Fig. 2.8c), while the EISMINT parameterization shows a decrease of 6 °C (Fig. 2.8d). The increase of seasonality and stronger summer warming in the REMBO model can be attributed to the additional warming caused by a lower albedo for ice free conditions during summer, while winter albedo remains practically unaffected by the removal of the ice sheet. The result is stronger warming in the summer and, therefore, an increase in seasonality. The opposite, unrealistic effect produced by the EISMINT parameterization is explained by the higher lapse rate used in winter. As a result, the decrease in elevation leads to a reduction of the temperature difference between summer and winter and a decrease in seasonality. Due to the large increase of summer temperature, positive surface mass balance (not shown) is only diagnosed over highly elevated areas in eastern and southern Greenland. This has implications for the possible existence of two (or more) equilibrium states under current climate conditions, which will be addressed in a separate paper.

### **2.3.2 Coupled simulations of equilibrium state**

For the next step of model validation, we performed equilibrium simulations of the GIS with constant (present-day) climatological conditions at the lateral boundaries of the model domain. The REMBO model and the surface interface were coupled bi-directionally and asynchronously with SICOPOLIS, which was run for 100,000 years, ensuring all relevant characteristics reached equilibrium state. As an initial condition, we used present-day data for the GIS elevation and bedrock (Bamber et al., 2001), and the ice temperature was set to 0 °C. The geothermal heat flux was constant and set to 60 mW/m<sup>2</sup>. Since the longest time scale of GIS response is comparable with orbital time scales, an assumption about GIS equilibrium forced only by present-day conditions is not very accurate and, instead, a simulation over several glacial cycles would be a more appropriate procedure. However, because here we are primarily interested in understanding the sensitivity of the simulated GIS to the different methods for determining the surface boundary conditions, we prefer the simpler approach of using constant climatological forcing.

Given the good agreement between the surface mass balance partition estimates determined using PDD or ITM, it is not surprising that using either melt scheme produces

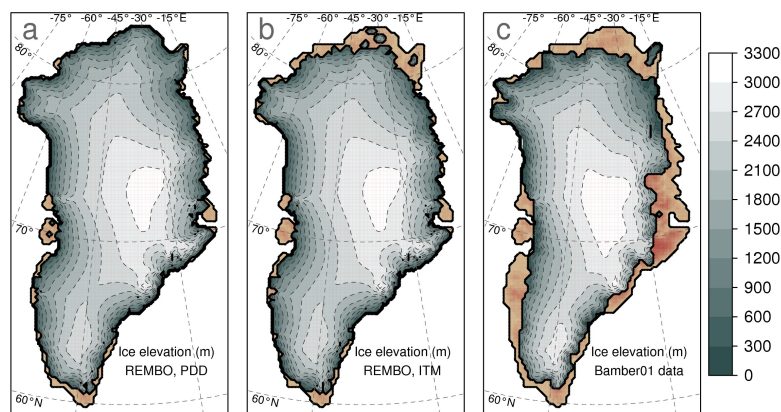


Figure 2.9: Equilibrium simulated GIS elevations using REMBO with (a) PDD ablation and (b) ITM ablation, compared with (c) the actual GIS elevation from observations

quite similar results (shown in Figs. 2.9a and 2.9b). In both cases, the simulated equilibrium ice sheet covers almost the entire area of Greenland, which also occurs in other GIS simulations using similar approaches (Letréguilly et al., 1991; Calov and Hutter, 1996; Ritz et al., 1997; Greve, 2005). The largest discrepancies with observations appears in the southwest and the Northeast, where using the REMBO climatology results in more extended ice coverage. This is mainly due to the overestimation of accumulation in those places by REMBO. Using the ITM approach does significantly improve the agreement with observations in the North, which follows from the stronger diagnosed melt in this region. In our simulations, the volume of the GIS is overestimated by ca. 10-15%. In other words, it was not possible to simulate an ice sheet, which has both the right geometry and the right surface mass balance components. This may be related, not so much to the deficiencies of the model used for simulation of the surface mass balance, but rather to an intrinsic problem of ice sheet models based on the shallow ice approximation. Since such models do not properly incorporate fast ice transport by ice streams, they require too much contact between the ice sheet and the ocean to produce a considerable amount of ice calving. In reality, the areas where the GIS is in direct contact with the ocean are rather small and yet, ice calving constitutes roughly half of the total ice loss from the GIS. Furthermore, simulating the ice sheet through past glacial cycles would likely improve the present-day representation, a topic that will be addressed in future work.

## 2.4 Conclusions

A regional energy-moisture balance model (REMBO) has been developed, which simulates temperature and precipitation over Greenland. The model is simple and very computationally efficient. Furthermore, it is physically based and includes an explicit representation of

seasonal changes in albedo – attributes that are crucial for simulation of climate conditions considerably different from present day.

Simulated temperature fields agree well with observational data and, particularly, improve the representation of the seasonal cycle as compared to the EISMINT temperature parameterization. Moreover, for ice-free conditions, REMBO and the EISMINT parameterization predict rather different changes. REMBO simulates a large summer warming and enhanced magnitude of seasonal temperature changes, while the EISMINT parameterization shows decreased seasonality. In this respect, the results from REMBO are more consistent with GCM experiments. Simulated precipitation matches observations in large-scale patterns, as well as the annual sum. However, regional deficiencies exist that cannot be eliminated unless more processes are included in the model.

Two different melt parameterizations were evaluated: the PDD approach and the ITM approach, with the latter explicitly accounting for the effects of temperature and insolation on snow and ice melt. The melt models were used to force a simple snowpack model with a daily time step. With the appropriate choice of model parameters, both methods produce similar total ablation rates for present-day conditions, but they differ in regional details. Both schemes also exhibit rather similar equilibrium SMB sensitivity to temperature changes. However the instantaneous SMB sensitivity to temperature change is different for each model and, therefore, each can be expected to produce different SMB changes in transient global warming experiments. For climate conditions that mimic the Eemian interglacial, even the equilibrium response of Greenland SMB differs considerably between the two schemes, with the ITM model simulating a more than 50% greater change in SMB.

Equilibrium simulations of the present-day GIS with REMBO coupled to the three-dimensional, polythermal ice sheet model SICOPOLIS demonstrate that both melt models allow us to simulate a reasonably realistic GIS. However for both methods, the simulated volume and spatial extent of the GIS are overestimated. Therefore, the present-day surface mass balance and GIS extent and volume do not provide sufficient criteria for a choice between PDD and ITM methods. Nonetheless, the ITM method looks preferable for transient and paleo simulations.

## **Acknowledgements**

We would like to thank the editor S. Marshall and the two anonymous reviewers for very helpful comments, which we believe improved this paper considerably. We would like to thank R. Greve for providing us with the ice sheet model SICOPOLIS. We are also very grateful to J. Ettema for providing the RACMO2/GR data and to J. Box for providing the PolarMM5 data used in this study. A. Robinson is funded by the European Commission's Marie Curie 6<sup>th</sup> Framework Programme, and is a part of the Research Training Network, Network for Ice and Climate Interactions (NICE), and R. Calov is funded by the

Deutsche Forschungsgemeinschaft RA 977/6-1. ERA-40 Reanalysis data was provided by the ECMWF, obtained from their website. GC-NET data was provided by K. Steffen via the GC-NET portal. Radiation data was obtained from the International Satellite Cloud Climate Project (ISCCP) website.



# 3. GREENLAND ICE SHEET MODEL PARAMETERS CONSTRAINED USING SIMULATIONS OF THE EEMIAN INTERGLACIAL<sup>2</sup>

## Abstract

Using a new approach to force an ice sheet model, we performed an ensemble of simulations of the Greenland Ice Sheet evolution during the last two glacial cycles, with emphasis on the Eemian Interglacial. This ensemble was generated by perturbing four key parameters in the coupled regional climate-ice sheet model and by introducing additional uncertainty in the prescribed “background” climate change. Sensitivity of the surface melt model to climate change was determined to be the dominant driver of ice sheet instability, as reflected by simulated ice sheet loss during the Eemian Interglacial period. To eliminate unrealistic parameter combinations, constraints from present-day and paleo information were applied. The constraints include (i) the diagnosed present-day surface mass balance partition between surface melting and calving, (ii) the modeled present-day elevation at GRIP; and (iii) the modeled elevation reduction at GRIP during the Eemian. Using these three constraints, a total of 270 simulations with 90 different model realizations were filtered down to 47 simulations and 20 model realizations considered valid. The paleo constraint eliminated more sensitive melt parameter values, in agreement with the surface mass balance partition assumption. The constrained simulations result in a range of Eemian ice loss of 0.4-4.1 m sea level (m.s.l.) equivalent, with a more likely value of about 4.1 m.s.l. if the GRIP  $\delta^{18}\text{O}$  isotope record can be considered an accurate proxy for the precipitation-weighted annual mean temperatures.

## 3.1 Introduction

Prediction of the future response of the Greenland Ice Sheet (GIS) to global warming is of great practical importance since the GIS can contribute up to 7 meters to global sea level rise. On short (centennial) timescales, the response of GIS is primarily controlled by changes in surface mass balance (which can now be modeled relatively accurately) and by changes in fast flow (which is still poorly understood). On millennial timescales,

---

<sup>2</sup> Robinson, A., Calov, R., and Ganopolski, A.: Greenland Ice Sheet model parameters constrained using simulations of the Eemian Interglacial, *Climate of the Past Discussions*, 6, 1551-1588, doi:10.5194/cpd-6-1551-2010, 2010, **in discussion**.

when the GIS can lose a considerable portion of its volume, the situation is additionally complicated by a number of climate-ice sheet feedbacks. Explicit simulation of all of these processes requires the use of fully-coupled, high resolution Earth system models, which is still impractical on this time scale. In addition, the information of the present-day GIS does not provide sufficiently strong constraints on its long-term evolution. Therefore, a study of past climate changes, and the response of the ice sheet to these changes, could help improve and better constrain the ice sheets models.

The Eemian Interglacial (ca. 130-115 kaBP) was characterized by high maximum summer insolation and warmer conditions in the high latitudes of both hemispheres. Paleo data suggest that sea level was higher than today by 4-6 meters (Overpeck et al., 2006), or even as much as 6-8 meters (Kopp et al., 2009). These numbers suggest a considerable contribution from both the Greenland and Antarctic ice sheets. At the same time, the presence of Eemian and older ice in several ice cores indicate that a large portion of the GIS survived the Eemian Interglacial. Moreover, the isotopic composition of Eemian ice from the Greenland summit can be interpreted to show that the height of the summit was not much lower during the Eemian compared to the present day. These data can potentially provide useful constraints for ice sheet models.

A number of attempts to simulate the response of the GIS to Eemian climate conditions have been made with different models and approaches (Cuffey and Marshall, 2000; Huybrechts, 2002; Tarasov and Peltier, 2002, 2003; Greve, 2005; Lhomme et al., 2005; Otto-Bliesner et al., 2006). These works reveals large uncertainties in the simulated contribution of the GIS to the sea level high-stand during the Eemian Interglacial, ranging from almost no contribution to over 5 m sea level (m.s.l.). The main problem with simulating the ice sheet's evolution during the Eemian Interglacial is the definition of surface boundary conditions for the ice sheet model. At a minimum, the ice sheet models require prescription of the seasonal variations of temperature and precipitation when using the standard positive degree day approach. However, not only do the Greenland ice cores lack continuous records of temperature and precipitation through the entire Eemian Interglacial, they also do not extend any further back in time. Simulation of the GIS response to Eemian climate conditions also requires data from the previous glacial cycle to properly initialize the ice sheet. In addition, even the existing record only provides information about precipitation-weighted temperatures (annual mean temperatures weighted more heavily for months with higher precipitation), while models require annual mean and, even more importantly, summer temperatures. Several attempts have been made to construct the temporal evolution of climatic forcing by combining Greenland climate reconstructions for the last glacial cycle and Antarctic ice core records for the penultimate glacial cycle (Cuffey and Marshall, 2000; Huybrechts, 2002; Tarasov and Peltier, 2003; Greve, 2005). Although the Greenland and Antarctic temperature record do bear a certain similarity, this is still a rather crude approach, since both the magnitude and temporal dynamics of temperature changes in the high latitudes of the northern and southern hemispheres differed considerably. Moreover,



the most crucial characteristic of summer temperature anomalies are not well constrained by the existing ice core records. In particular, the  $\delta^{18}\text{O}$  content of Eemian ice may have been affected by both changes in surface elevation and the seasonality of precipitation (Jouzel et al., 1997). This approach also does not explicitly account for the additional effect of insolation changes, which is of comparable importance to temperature changes on the surface melting of ice for this period (Robinson et al., 2010a). A coupled climate model (with an additional downscaling procedure) can provide all necessary climate information needed to force an ice sheet model, but running coupled GCMs through the whole glacial cycle, or even just for the interglacial period, is still computationally too expensive. Until now, only a time slice simulation has been used to force a model of the GIS in this way (Otto-Bliesner et al., 2006). However, the GIS has a multi-millennial time scale response to climate change and the climate did not remain constant during the interglacial. Such an approach also does not solve the problem with the initialization of the GIS at the onset of the Eemian Interglacial.

Earth system models of intermediate complexity (EMICs, Claussen et al., 2002) are useful tools for the study of the evolution of ice sheets on millennial to orbital timescales, since some of them (like CLIMBER-2, Petoukhov et al., 2000) are computationally efficient enough to be run through the glacial cycles (e.g., Bonelli et al., 2009; Ganopolski et al., 2010) and the only required boundary conditions are readily available information: Earth's orbital parameters and the atmospheric concentration of greenhouse gases. The problem is, however, that this type of model has a very low spatial resolution and it can neither accurately simulate the regional climate over the GIS, nor the feedbacks associated with the melting of the ice sheets. To overcome this problem, we developed a regional energy and moisture balance model (REMBO, Robinson et al., 2010a), which produces a physically-based downscaling of the climate over the GIS using a present-day climatology, and anomalies simulated by a coarse resolution climate model. Unlike most previous studies, we replace the traditionally used positive degree day (PDD) melt scheme with a surface melt scheme that explicitly accounts for changes in insolation. The latter is crucial for simulation of the Eemian Interglacial when summer insolation was much higher than at present.

The aim of this study is to investigate whether existing paleo data from the Eemian Interglacial, in conjunction with present-day data about the GIS and its mass balance, provide sufficient constraints on the choice of model parameters and the GIS contribution to the sea level high-stand during the Eemian Interglacial. To this end, we performed an ensemble of simulations of the GIS over the last two glacial cycles by varying two ice sheet model parameters, one melt scheme parameter and one regional climate model parameter (four model parameters in total). In addition, we vary the magnitude of the Eemian background warming. Present-day observations and paleoclimate data are used to select the subset of model versions that is consistent with empirical constraints.

### 3.2 Model setup and experimental design

The coupled REMBO-ITM-SICOPOLIS model used in this study is identical to that described by Robinson et al. (2010a), except for a slight modification to the surface albedo parameterization (see Appendix A). A brief description of the main components is provided below.

REMBO (Regional Energy-Moisture Balance Orographic model) produces daily climatological fields of temperature and precipitation for Greenland with 100 km resolution. Monthly ECMWF Reanalysis data (ERA-40) of 2-meter temperature and relative humidity (Uppala et al., 2005), averaged over the period 1958-2001 and linearly interpolated in time to produce daily fields, are used as boundary conditions around Greenland. In a previous analysis, Robinson et al. (2010a) show that REMBO is able to capture the present-day seasonal cycle of temperatures over Greenland and that it improves the fit with observations as compared to conventional bilinear parameterizations. While the precipitation field mismatches observations in several local areas, the large-scale field is correct and sufficient enough for long timescale simulations. This lends confidence to the idea that present-day climatic forcing is fairly accurate, and that the energy reaching the surface determined by the model would not be far from reality.

The daily temperature and precipitation output from REMBO is used to determine the surface mass balance of the ice sheet and the evolution of surface albedo via the surface mass balance model ITM (Insolation-Temperature Melt). ITM represents a computationally efficient alternative to the commonly used PDD (Positive Degree Day) approach (Braithwaite and Olesen, 1989; Reeh, 1991). Similar to PDD, the ITM model is also semi-empirical. However it has two advantages: it explicitly accounts for short-wave radiation (while PDD does implicitly, via different melt coefficients for snow and ice); and, since it incorporates a simple snowpack model, it has a memory which the standard PDD scheme does not. The ITM model is tuned to use climatological fields of temperature, precipitation and insolation at the top of the atmosphere and is driven by the elevation-corrected output of REMBO. ITM simulates surface mass balance and mean annual ice sheet surface temperature on the same grid used by the ice sheet model.

The ice sheet model used for these simulations is SICOPOLIS, version 2.9. It is a 3D thermomechanical ice sheet model based on the shallow ice approximation (SIA) and it includes a physically-based treatment of the temperate layer at the base of the ice sheets via explicit calculation of the water content of the temperate basal ice (Greve, 1997a,b). This model has been used in numerous studies of ice sheet evolution both in the past and future (e.g., Greve, 2000, 2005; Calov et al., 2002, 2005) and is comparable to other SIA models (e.g., Huybrechts et al., 1991). It is run on a 20 km resolution grid and is forced from above by the annual surface mass balance and surface temperature fields obtained from REMBO. At the base of the ice sheet, geothermal heat flux is prescribed, and the lithosphere deforms locally with a time lag of 3 ka.

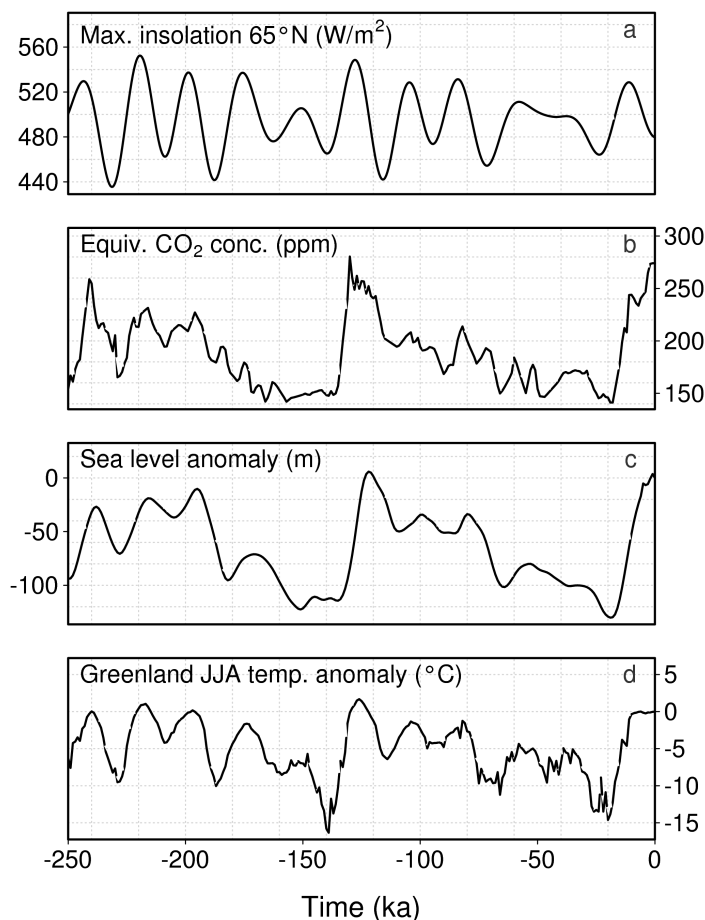


Figure 3.1: Examples of forcing used for simulations of the last two glacial cycles: (a) maximum solar insolation at 65 °N; (b) equivalent CO<sub>2</sub> concentration; (c) global sea level anomaly from SPECMAP; (d) Summer (June-July-August averaged) temperature anomaly prescribed at the boundaries of Greenland.

In this study, we use results of transient simulations of the last two glacial cycles performed with the intermediate complexity model CLIMBER-2 to drive REMBO. The model and experimental setup is identical to that described by Ganopolski et al. (2010), except that here we only apply the results from the last two glacial cycles. CLIMBER-2 (Petoukhov et al., 2000) is a coarse-resolution EMIC that has been shown to produce a realistic present-day climate, climate sensitivity (Ganopolski et al., 2001) and changes in climate over the last glacial cycle (Ganopolski et al., 2010). The CLIMBER-2 simulation was forced by variations in Earth’s orbital parameters, computed following Berger (1978), and by a prescribed time series of the equivalent atmospheric CO<sub>2</sub> concentration. The resulting global temperature anomaly time series agrees well with paleoclimate reconstructions, in that, for example, the Greenland annual temperature at the Last Glacial Maximum (LGM) is approximately 20 °C cooler than today and the Eemian Interglacial is ca. 2 °C warmer than today.

To force the transient simulations performed here, we used the same insolation at the top of the atmosphere (July insolation at 65 °N is shown in Fig. 3.1a as an illustration) and equivalent CO<sub>2</sub> concentration (Fig. 3.1b) as in the CLIMBER-2 run. The boundary temperature field of REMBO was modified by adding the spatially uniform, regional monthly temperature anomaly computed by CLIMBER-2 to the present-day climatological fields (the anomaly time series is shown in Fig. 3.1d). We assumed no changes (compared to the present day) in relative humidity at the Greenland borders. The anomalies from the CLIMBER-2 simulation provide us with self-consistent, regionally relevant time-series and enable us to avoid problems involved with relying on discontinuous oxygen isotope records.

Changes in sea level were prescribed using an appropriately scaled SPECMAP time series (Imbrie et al., 1984), shown in Fig. 3.1c. We found that while this allowed more ice to grow during the glacial periods, the inclusion of sea level changes played only a small role in the evolution of the ice sheet in warmer periods. Nonetheless, we include sea-level adjustments to the margin to allow for its effect on total volume. Note that sea level changes modeled by CLIMBER-2 agree favorably with the SPECMAP reconstruction and, in principle, could instead have been used to drive the ice sheet model without any appreciable differences.

All simulations began at 250 kaBP and were run until the present. The ice sheet model was initialized with the present-day GIS topography from Bamber et al. (2001) and the standard set of model parameters as initial conditions. Since the model was run for more than 100 ka before the Eemian Interglacial, there should be no dependence on the choice of initial conditions.

### **3.3 Modern and paleo empirical constraints**

Assuming that the climate obtained from REMBO is fairly well represented, but other processes (such as fast flow in the ice sheet model) are ignored, we believe that there are then at least two aspects of the ice sheet that are possible to model with reasonable uncertainty and that can provide information about the sensitivity of various model parameters: the diagnosed, present-day partition of GIS mass balance between surface melting and ice discharge into the ocean, and the elevation (and elevation changes) of the summit of the GIS. Arguably, both of these characteristics are less affected by the lack of fast ice streams and low resolution than the spatial extent and the volume of the GIS.

In addition, we would like to explore the possibility of using available paleoclimate information from the Eemian Interglacial to further reduce the range of possible combinations of model parameters. This leads to the three constraints used in this study, described below.

### 3.3.1 Present-day surface mass balance partition

The first constraint is the estimate of the present-day partition between GIS surface mass balance (SMB) and ice discharge into the ocean, for the fixed topography of present-day Greenland. As we do not explicitly model calving, we use the ratio of diagnosed surface mass balance to the total precipitation over the GIS, assuming the remaining mass is lost to ice discharge (calving). The benefit of using this ratio is that (1) it eliminates biases in the absolute values that result from different ice sheet surface area masks, (2) allows an analysis of the reasonable sensitivity range of the surface mass balance model without incorporating additional uncertainty from the ice sheet model or paleoclimate forcing and (3) keeps the focus on the partition between surface mass balance and calving. We believe the last consideration is especially important for properly estimating the correct sensitivity of the ice sheet to long-term climatic forcing.

For the present-day GIS, several estimates from regional climate models (RCMs) show that positive surface mass balance should account for about 50% (ranging from 48-63%) of the total incoming precipitation (Box et al., 2006; Fettweis, 2007; Ettema et al., 2009), while the remaining incoming mass is lost via calving or ice discharge into the ocean. These results do not necessarily encompass the range of all possible values, and furthermore our approach does not account for all physical processes at the surface (e.g., blowing snow or evaporation). Thus, we allow for additional uncertainty by choosing the range 40-65%.

### 3.3.2 Present-day GRIP elevation

The present-day summit elevation at GRIP (73N, 38W, 3230 m) is a robust feature of the ice sheet that provides a useful constraint for our ensemble. Because it is located in the middle of the ice sheet at essentially the thickest location, changes in this elevation reflect large-scale changes in the ice sheet surface mass balance, rather than highly dynamic changes that occur near the margins (Alley et al., 2010). Raynaud et al. (1997) indicate that even with margin position varying in the range of 100-200 km, no more than 100 m elevation difference is modeled. A similar sensitivity is also reflected in our own simulations. Although biases in simulated accumulation at the summit can affect the modeled elevation, the precipitation field obtained from REMBO agrees best with observations for the large-scale field over the interior of the ice sheet. Indeed with several combinations of model parameters, it is possible to model the summit location and elevation correctly. Thus, as a second constraint, we assume that the present-day GRIP elevation should be obtained to within +/- 100 m.

### 3.3.3 Eemian GRIP elevation

The ice core drilled at the Greenland Ice Sheet summit (GRIP, 1993) provides important information that can be used to further constrain the paleo simulations. A reliable time reference for this ice core cannot be determined for ice older than ca. 100 ka, likely due

to stratigraphic folding of the ice (Alley et al., 1995). However, the total gas content in the ice core indicates isotopically warmer conditions (Raynaud et al., 1997). Because these values are comparable to those of the Holocene, the minimum elevation of the GRIP location during the Eemian must have been no more than a few hundred meters less than that of present day (Cuffey and Marshall, 2000). It is difficult to determine an exact correspondence of the GRIP elevation to the total gas content, so we apply the somewhat conservative constraint that the elevation at GRIP was at most 400 m below present day. We also test the effect of choosing different values for this constraint, in case it plays an important role in eliminating ensemble members.

Using the three constraints outlined above, we are able to determine which model simulations are more likely to be realistic, and more important for the future stability of the ice sheet, which model parameter combinations should be considered valid.

### 3.3.4 Additional possible paleoclimate constraints

It could also be possible to further constrain the ensemble using information from other ice core locations, such as Camp Century (77N, 61W, 1890 m) or DYE-3 (65N, 43W, 2490 m). However, our model's resolution, lack of fast processes and spatially-constant boundary temperature anomaly means we have less confidence in our ability to accurately capture the behavior of the ice sheet in these locations. This is complicated by the fact that little is known with certainty about regions closer to the margin. For example, DYE-3 may or may not have remained ice-covered during the Eemian Interglacial (Jansen et al., 2007; Alley et al., 2010). Eemian ice layers do exist at the base, however older ice has not been found. Meanwhile,  $\delta^{18}\text{O}$  anomalies indicate an elevation difference of perhaps 500 m (Johnsen et al., 2001; NGRIP, 2004), and DNA evidence from the silty layers beneath the ice sheet indicate that plant growth only occurred much earlier, perhaps during MIS11 (Willerslev et al., 2007). The latter does not rule out the possibility of ice-free, permafrost conditions at this location, as opposed to only a reduced-thickness ice sheet. In light of the existing controversy and our model's poor representation of these locations, we do not consider data from them as hard constraints. Nonetheless, we will comment on the results from different model versions for these locations.

## 3.4 Perturbed model parameters

Four of the most influential parameters in REMBO, ITM and SICOPOLIS were considered as likely to contribute significant uncertainty to modeling the evolution of the GIS through the glacial cycles: (1) the geothermal heat flux field at the base of the ice sheet, (2) the basal sliding coefficient, (3) a free parameter in the melt equation, and (4) the moisture diffusion constant in REMBO (that affects the strength of large-scale precipitation). In addition we considered possible uncertainties in temperature anomalies simulated by CLIMBER-2. Namely, we changed the magnitude of warming around Greenland during the Eemian

Table 3.1: All parameter values used to generate the ensemble of model versions.

Parameter	Units	Values	Description
$Q_{geo}$	mW/m <sup>2</sup>	50, 60, 70	Geothermal heat flux
$\gamma_s$	m/(a Pa)	10, 15, 20	Sliding law coefficient
$c$	W/m <sup>2</sup>	-45, -50, -55, -60, -65	ITM constant
$\kappa_Q$	kg/s	8.4e5, 9.8e5	Moisture diffusion constant
$f_p$	- -	1.0, 1.5, 2.0	Paleo anomaly factor

Interglacial. These areas of uncertainty are discussed in detail below, and Table 3.1 provides a list of the parameters and the values used in this study.

### 3.4.1 Geothermal heat flux

The geothermal heat flux (the lower boundary condition of the ice sheet model in the bedrock) was set to a constant value everywhere. Little is known about the exact values underneath the ice sheet, but the large-scale field is likely to be fairly uniform and recent estimates put the value near 50 mW/m<sup>2</sup>, with some variation around the margins (Shapiro and Ritzwoller, 2004; Vinther et al., 2009). It cannot be ruled out, however, that this value is significantly larger in some localized areas below the GIS. To account for the uncertainty in the broad sense, we chose geothermal heat flux values of 50, 60 and 70 mW/m<sup>2</sup>. The geothermal heat flux is one factor that determines how much of the ice sheet base is temperate (at the pressure melting point) and thus is sliding at the base. In this way, it can be used as a way to tune the shape and size of the ice sheet in general.

### 3.4.2 Sliding coefficient

The sliding law used in this study,

$$v_s = \gamma_s \rho g H |\nabla h|^2 \nabla h, \quad (3.1)$$

is a Weertman-type equation with a third-order dependence on the gradient of elevation, where  $v_s$  is the ice sliding velocity,  $H$  is the ice thickness,  $\rho$  is the density of ice,  $g$  is the gravitational force and  $h$  is the surface elevation. For our purposes, the constant  $\gamma_s$  was chosen as the uncertain parameter varied in this study. Increasing this parameter has the effect of increasing the ice velocity at the base of regions of temperate ice. Mostly this should occur around the margins and it acts to adjust the slope of the ice sheet. Higher values of sliding also generally decrease the total volume of ice.

### 3.4.3 Melt model parameter, $c$

Surface melt of snow and ice is calculated in ITM from a simple energy balance equation (van den Berg et al., 2008),

$$M_s = \frac{\Delta t}{\rho_w L_m} [\tau_a (1 - \alpha_s) S + c + \lambda T], \quad (3.2)$$

where the potential melt rate,  $M_s$ , is assumed to largely derive from two main contributions. In the first term, representing incoming short-wave radiation at the surface,  $S$  is the incoming solar radiation at the top of the atmosphere,  $\tau_a$  is the transmissivity of the atmosphere and  $\alpha_s$  is the surface albedo. The transmissivity is assumed to be a linear function of elevation (Robinson et al., 2010a) and the surface albedo is calculated following the method described in the Appendix. The second term  $c + \lambda T$  is a linear parameterization of the long-wave radiation and turbulent heat flux, where  $T$  is the daily mean temperature and  $\lambda$  and  $c$  are constants. The choice of  $\lambda$  derives from the empirical value of long-wave radiation absorbed by snow and ice, which corresponds to a melt rate of 3 mm w.e. per degree (analogous to the choice of degree day factor in the PDD approach, see Reeh, 1991). The remaining term,  $c$ , is then assumed to be a free constant parameter, the value of which can vary widely depending on the domain in question (van den Berg et al., 2008) and the albedo parameterization used.

Robinson et al. (2010a) determined that for modeling present-day conditions over Greenland,  $c = -55 \text{ W/m}^2$  gives the best partition of surface mass balance components. When performing equilibrium simulations fully coupled to an ice sheet model, however, it was found that several values of  $c$  could still produce a reasonable present-day ice sheet. Therefore, in this study we chose to incorporate melt model uncertainty into the ensemble via the parameter  $c$ , allowing a range of  $-45$  to  $-65 \text{ W/m}^2$ .

We further considered that the parameterization of surface albedo (as described by Robinson et al., 2010a) is also imperfect and is likely the source of large uncertainty. However, several simulations combining various values of the melt parameter  $c$  with changes to the surface albedo scheme show that the first order changes to surface albedo can be captured simply by changing the value of  $c$ .

#### 3.4.4 Atmospheric moisture diffusion coefficient

Uncertainty in the climatic forcing likely plays the key role in determining both the past and future stability range of the GIS. The parameters used in REMBO to determine temperature are tuned to match present-day observations, with both annual mean temperatures and the seasonal cycle well reproduced (Robinson et al., 2010a). Therefore, no uncertainty was considered in the temperature equation itself; rather, uncertainty in the temperature forcing is represented via the paleo factor (see below). To introduce uncertainty in the representation of precipitation by REMBO, we chose to vary the strength of the overall precipitation field. This was achieved via the moisture diffusion constant. By decreasing this value, less moisture at the boundaries is able to diffuse inward, decreasing the total amount of precipitation. Although this does not improve the local deficiencies of the model, it does allow adjustment of the large-scale field (especially over the interior of the ice sheet), which plays a role in determining the total volume and the maximum elevation of the ice sheet.



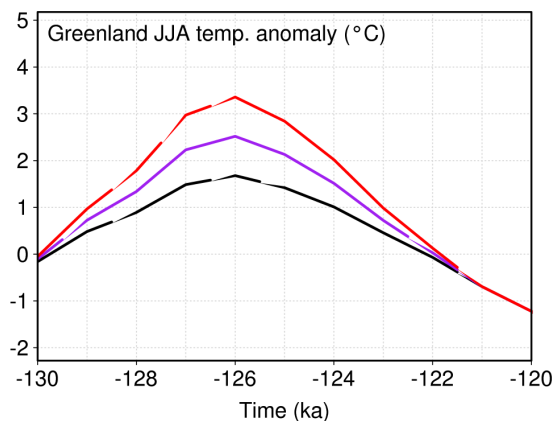


Figure 3.2: Summer temperature anomalies during the Eemian for the applied paleo modification factors of 1 (black), 1.5 (purple) and 2 (red).

### 3.4.5 Paleo climate forcing

When performing paleo simulations using an anomaly approach, large uncertainty can exist depending on the choice of anomaly forcing. In REMBO, changes in precipitation are controlled by changes in temperature and elevation, while relative humidity is prescribed. This means that aside from the prescribed variations in  $\text{CO}_2$  equivalent radiative forcing, the only anomaly forcing needed as input is for the temperature field. We chose to prescribe a spatially-uniform monthly temperature anomaly to the boundaries of Greenland. The anomaly temperatures were determined in the glacial cycle simulations of CLIMBER-2 by Ganopolski et al. (2010). We obtained temperatures by averaging values from the two CLIMBER-2 grid cells that encompass Greenland for each month and interpolating these into daily values for input to REMBO.

Our approach does not account for possible regional differences in temperature changes around Greenland, which would introduce additional uncertainties into the analysis. GCM simulations of the Eemian disagree about both the pattern and magnitude of warming. In the absence of more information, and to be consistent with previous modeling studies, we therefore apply a spatially constant anomaly to the boundary temperature field.

The maximum Eemian summer temperature anomaly in the “Greenland” grid cells simulated in CLIMBER-2 is just under  $2^\circ\text{C}$  (Fig. 3.1d). Due to its coarse spatial resolution, it is likely that CLIMBER-2 underestimates the amount of local warming over the GIS at that time. The CAPE project (CAPE, 2006) compiled a map of Eemian summer temperature anomalies obtained from marine sediment cores for several locations in the Arctic region. Most data show that warming was anywhere from  $2\text{-}5^\circ\text{C}$  compared to pre-industrial values. Several coupled GCMs used to performed Eemian climate simulations give the range of  $2.5\text{-}5^\circ\text{C}$  for summer temperature anomalies over the GIS as well (Masson-Delmotte et al., 2010). To account for potentially higher Eemian warming than simulated

by CLIMBER-2, we choose to apply a scaling factor to the positive temperature anomalies. Negative anomalies were not modified in any way, since the negative temperature anomalies during glacial periods are well simulated and also much less important. This approach is intended to provide a reasonable adjustment to the climate anomalies to account for uncertainty. As shown by Cuffey and Marshall (2000), it is not so much the duration of the warm period that determines the mass loss during the Eemian, but rather the maximum temperature anomaly. Therefore, we apply factor values of 1, 1.5 and 2, resulting in maximum prescribed Eemian summer warming around Greenland of 1.7, 2.5 and 3.4 °C, respectively. The resulting Eemian temperature anomaly time series for summer are shown in Fig. 3.2.

### 3.5 Transient simulations of the GIS

Permuting the above five parameters using the values in Table 3.1 produced 270 simulations, which correspond to 90 independent model versions (since the paleo factor only modifies the boundary forcing and, thus, does not produce additional model versions). Figure 3.3 shows the temporal evolution of ice volume and area computed in the ensemble of model simulations over the last two glacial cycles. During glacial periods, different model versions produce rather similar results, which is not surprising since under cold climate conditions, the GIS occupies the whole land area and surface melt is essentially absent. However, it appears that any reasonable combination of parameter values (based on present-day tuning) can result in dramatically different evolution histories for the GIS. With some model versions, the GIS melts entirely during the Eemian and with others, minimal changes occur for the same period (see Fig. 3.4). Similarly, simulated precipitation-weighted mean annual temperatures over the summit remain very close in all model versions over the glacial period, but during the Eemian, they differ by up to 15 °C which is much larger than the differences imposed by using different temperature anomalies around Greenland (i.e., different paleoclimate factors). This large range in simulated temperatures is explained by both changes in surface elevation and changes in surface albedo (in the model versions where a substantial portion of GIS melts away during the Eemian).

In Fig. 3.4, the simulated present-day distribution of ice (**a-e**) and the Eemian minimum extent (**f-j**) is shown for each value of the melt parameter  $c$  (maintaining  $\gamma_s = 15$ ,  $f_p = 1.5$  and  $Q_{geo} = 50 \text{ mW/m}^2$ ). For the present day, all simulations have a similar distribution of ice, covering almost the entire land area. The total present-day volume is simulated to be 2% smaller than present to up to 35% larger, mainly due to the additional ice at the margin. The interior distribution of ice in all simulations reflects the present day reasonably well, in terms of elevation and surface slope. By contrast, the minimum volume simulated for the Eemian Interglacial differs drastically between the five model versions. Depending on the melt parameter  $c$ , the GIS can experience minimal changes or melt almost completely. The age at which the minimum volume is reached is related to the total amount of ice

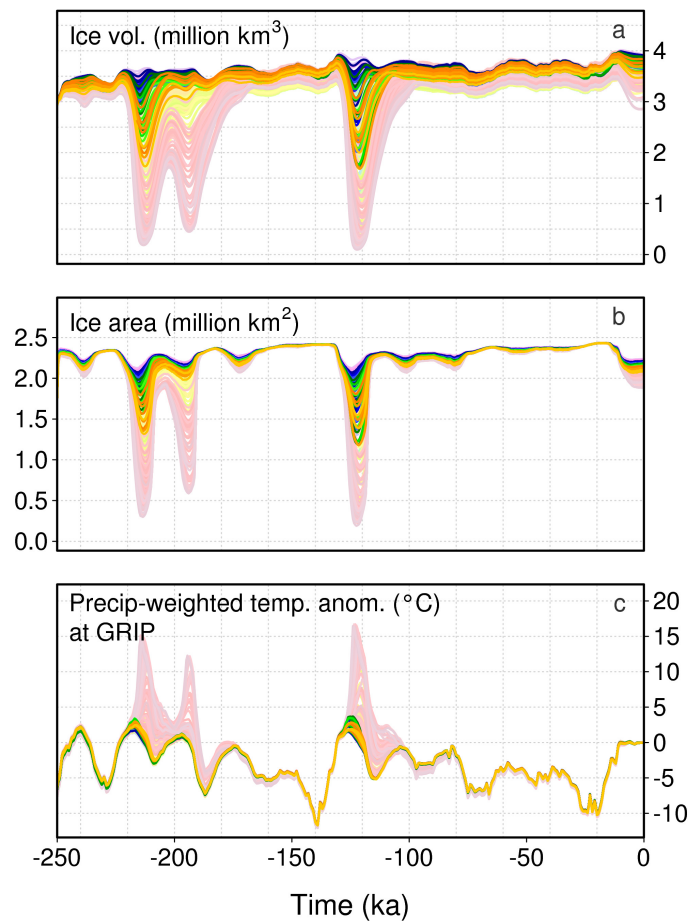


Figure 3.3: Temporal evolution of (a) the volume and (b) the surface area of the GIS, as well as (c) the precipitation-weighted annual temperature anomaly at GRIP, as simulated by the ensemble of model versions. Lighter lines correspond to “invalid” simulations. Each color band is determined by the melt parameter  $c$ , as explained in the caption of Fig. 3.6.

melted and can vary between 123 kaBP and 121 kaBP. When more volume is lost, this state is maintained longer and the minimum is reached later in time.

Figure 3.5 shows the precipitation-weighted annual temperature distribution for the same simulations at the Eemian minimum extent. Over the ocean, the temperature anomaly is prescribed, however the inland distribution is largely affected by the distribution of ice. In the cases where a large portion of ice disappeared, anomalies of up to 18 °C can persist long after the boundary warming has decreased. This is partly due to elevation changes, but the explicit representation of surface albedo also reinforces this warming.

It is interesting that model versions which produce more realistic present-day GIS distributions (less ice volume and area, e.g.,  $c = -45 \text{ W/m}^2$ ) simulate an almost complete disappearance of the GIS during the Eemian, even under very modest warming anomalies

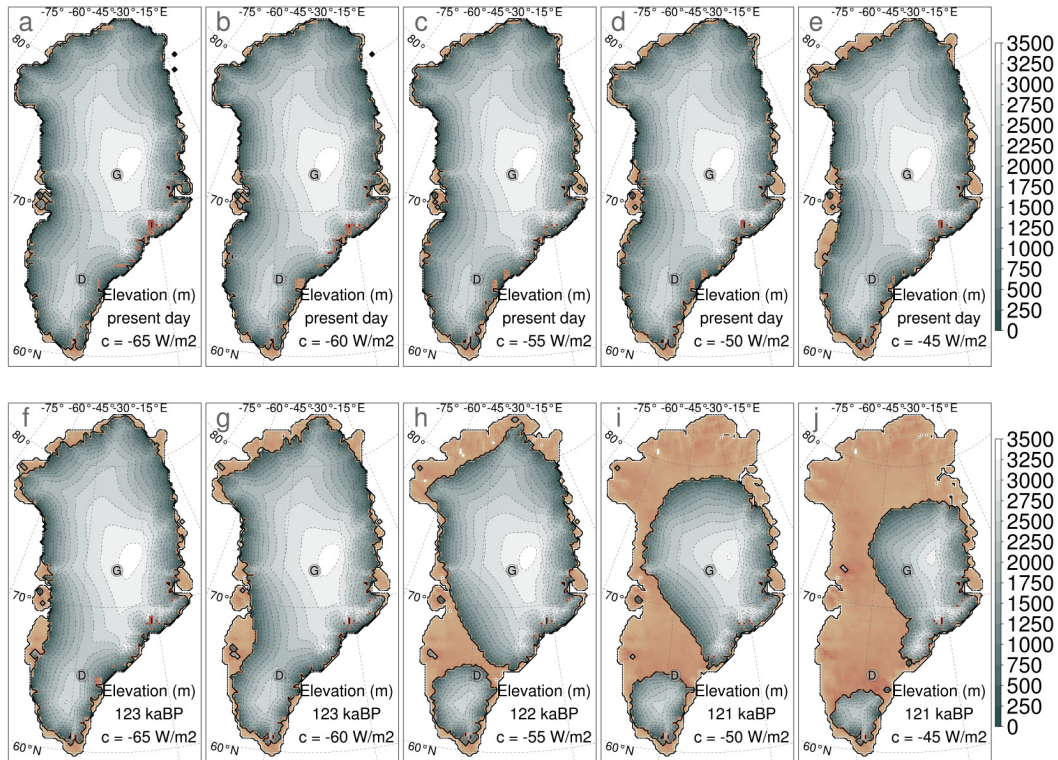


Figure 3.4: GIS distribution for different values of the melt parameter  $c$ , as simulated for (a-e) the present and (f-j) the Eemian minimum volume. The locations of GRIP (G) and DYE-3 (D) are plotted as shaded circles.

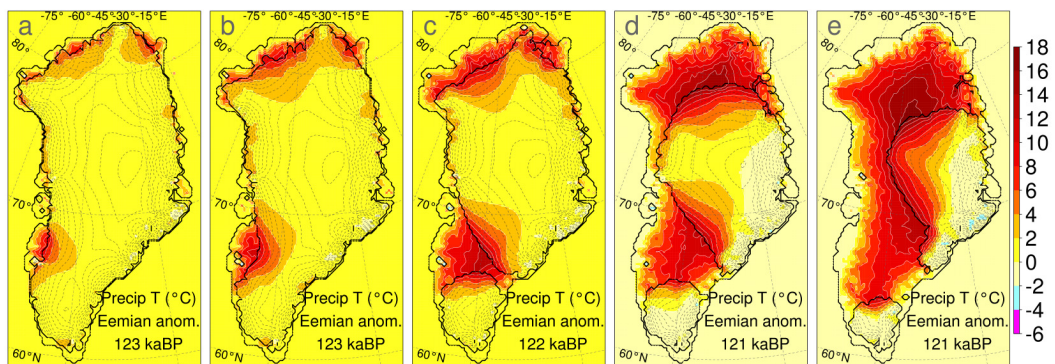


Figure 3.5: Precipitation-weighted annual temperature anomaly at the Eemian minimum extent for each of the five simulations (f-j) in Fig. 3.4.

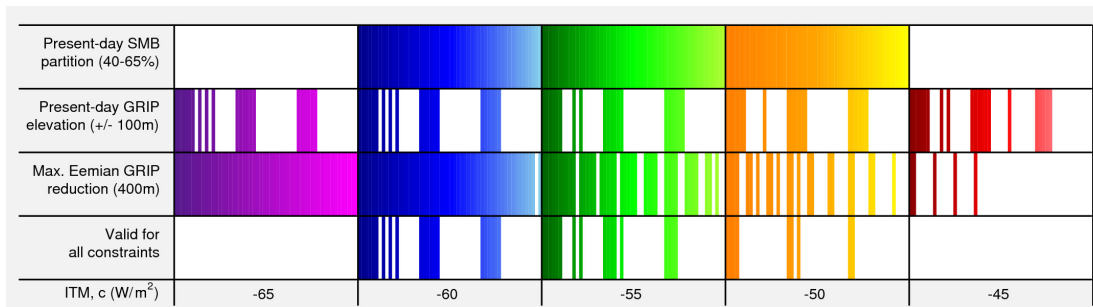


Figure 3.6: Schematic table of constraints applied to the paleo simulations of the Greenland Ice Sheet. Each color band contains 54 simulations, corresponding to the choice of melt parameter  $c$ , where lighter shades correspond to more sensitive secondary parameter combinations for added distinction (this color scheme is used for all plots). Each row corresponds to a specific constraint – so if a simulation is consistent with the constraint, it is plotted in that row (otherwise, white regions indicates rejected simulations). The last row shows the simulations that were consistent with all constraints and thus are considered valid.

( $f_p = 1$ ). This is unrealistic, but in line with arguments presented by Robinson et al. (2010a). Due to the lack of fast processes and/or model resolution, too much surface melt is required to model the GIS extent close to the observed one. This violates the observed partition between surface melt and calving, and shifts the model much closer to an unstable threshold than it should be in reality. Therefore the “realistic” (in the traditional meaning of this term) simulations of the modern GIS provide no constraints on the magnitude of Eemian melting. However, as we discuss below, other constraints indeed help to narrow the range of valid model parameters.

### 3.6 Constraining the model parameters

Figure 3.6 is a schematic representation of the constraints as they apply to all simulations in the ensemble. Using this plot, we are able to identify which constraints are responsible for rejecting different simulations. For example, the present-day surface mass balance partition serves to eliminate the most and least sensitive melt parameter values ( $-45$  and  $-65$  W/m<sup>2</sup>), whereas the Eemian summit constraint generally only eliminates the more sensitive melt parameter values. This is discussed in more detail below.

It is important to distinguish between the set of simulations and the set of different models in the ensemble. This distinction arises because each model version produced three simulations, corresponding to the modified Eemian climate (via the paleo factor,  $f_p$ ). Thus, a simulation is considered valid if it does not violate any constraints. A model version is considered valid if at least one of its simulations has been considered valid.

Figure 3.7a shows that the dependence of the modern surface mass balance partition on the melt parameter  $c$  is essentially linear. In our ensemble, only the moisture diffusion constant,  $\kappa_Q$ , and the melt parameter  $c$  can affect the diagnosed SMB partition, since it



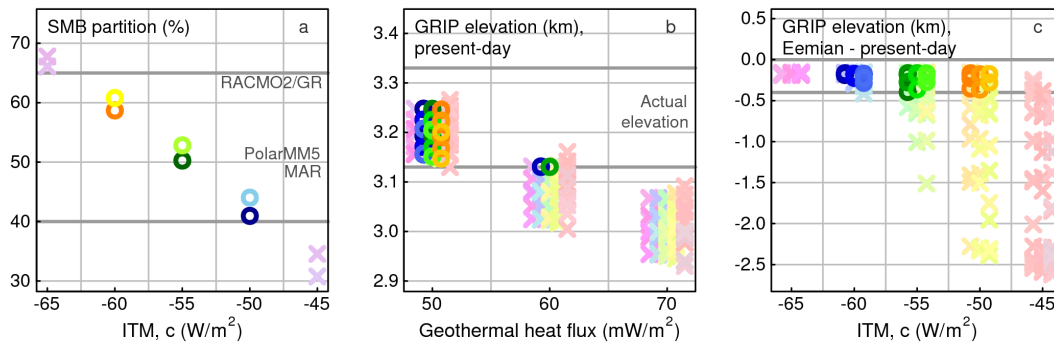


Figure 3.7: Ensemble results for the three constraints versus the most influential parameter in each case: (a) diagnosed SMB partition for the present-day GIS, compared to results from regional climate models (PolarMM5: Box et al., 2006; MAR: Fettweis et al., 2007; RACMO2/GR: Ettema et al., 2009); (b) simulated present-day GRIP elevation versus the prescribed geothermal heat flux at the base of the ice sheet; (c) maximum reduction in the modeled GRIP elevation for the Eemian Interglacial relative to the modeled present-day elevation. Darker circles and lighter crosses correspond to “valid” and “invalid” simulations, respectively, and the grey lines show the outer limits used for each constraint.

is determined for a fixed ice sheet topography. For each value of  $c$ , two points are present – one for each modeled value of  $\kappa_Q$ . Changing the latter parameter modulates the total precipitation in a minor way relative to the effect of changing  $c$ . It is also clear that the more extreme values of  $c$  produce either too much or too little melt, and thus do not reflect the present-day mass balance partition. With an acceptable partition range of 40-65%, the remaining valid  $c$  values for our model setup fall between  $-50$  and  $-60$   $\text{W}/\text{m}^2$ . As shown in the first row of Fig. 3.6, the partition constraint essentially sets an upper and lower bound on the sensitivity of the surface mass balance model by eliminating the most extreme values.

Figure 3.7b shows the present-day GRIP elevation versus geothermal heat flux ( $Q_{geo}$ ). Of the five parameters varied, the geothermal heat flux plays the largest role in determining the elevation at GRIP. In fact, with a value of  $60$   $\text{mW}/\text{m}^2$ , already only one simulation is able to obtain a present-day GRIP elevation greater than  $3200$  m. The more likely valid choice for  $Q_{geo}$  would thus be  $50$   $\text{mW}/\text{m}^2$ , which conforms to recent estimates (e.g., Shapiro and Ritzwoller, 2004; Vinther et al., 2009). NGRIP ( $75\text{N}$ ,  $42\text{W}$ ,  $2920$  m), which lies only a few hundred kilometers away along the ice divide, shows a similar relationship to geothermal heat flux, although some more simulations using  $60$   $\text{mW}/\text{m}^2$  are able to produce the right elevation. For comparison, we also looked at the present-day elevations at Camp Century and DYE-3, however for reasonable simulations, no systematic relationship between  $Q_{geo}$  and elevation can be found. The second row in Fig. 3.6 shows that this constraint filters out simulations with high values of geothermal heat flux.

Figure 3.7c shows the difference between the modeled minimum Eemian and present-

day elevation at GRIP. The melt model sensitivity is the strongest factor that determines the Eemian GRIP elevation reduction, followed by the sliding coefficient. For many simulations, all ice is lost at GRIP and these are clearly too sensitive. In fact, none of the model versions with  $c = -45 \text{ W/m}^2$  and only a few with  $c = -50 \text{ W/m}^2$  satisfy this constraint. Therefore, we are able to exclude essentially the same subset of the most sensitive model versions as excluded by the constraint on the present-day SMB partition. It does not affect models with a small response of the GIS to Eemian warming. Data from  $\delta^{18}\text{O}$  records indicate that the annual mean temperature at GRIP (or, more precisely, the precipitation-weighted mean annual temperature) was 4-6 °C warmer than at present (Johnsen et al., 2001). Using this information would additionally reduce the number of valid simulations (primarily by only permitting runs with high paleoclimate forcing and excluding model versions with a low sensitivity to Eemian warming). It is very encouraging that both paleoclimate constraints and the modern constraint on the SMB partition are consistent in the simulations that are eliminated. However, even for the reduced range of valid model runs, a wide range of possible GIS responses to Eemian warming remains.

### 3.7 Discussion

From 270 simulations, the above three constraints reduce the ensemble to just 47 valid simulations and 20 valid combinations of model parameters. In Fig. 3.4, showing the transient evolution of the GIS, the lighter colored lines indicate “invalid” simulations. From the color bands, it can be seen that the melt parameter  $c$  dominantly determines the sensitivity of the ice sheet to the climate. Furthermore, the applied constraints are able to eliminate the most sensitive cases and reduce the valid range of Eemian melt. Figure 3.8 shows the fraction of the ice sheet that melted during the Eemian versus the maximum warming experienced at GRIP for the same period (invalid results are shown by the much lighter crosses). For the ensemble of valid simulations, the range of ice lost during the Eemian is 5-55% (or 0.4-4.1 m.s.l.), relative to the present-day modeled values.

If we consider an additional constraint on the Eemian temperature anomaly at the boundaries, the number of “realistic” simulations and valid parameter combinations can be further reduced. This is because the range of Eemian ice loss has an important dependence on the assumed warming at the boundaries. In Fig. 3.8, the cluster of valid points can be separated into 3 lines going from minimum to maximum ice loss. Each of these lines corresponds to a different choice of the paleo factor used to increase the Eemian temperature anomaly at the boundaries. As the paleo factor,  $f_p$ , increases from 1.0 to 2.0, the maximum ice loss increases from about 45% to 55%, and the minimum estimate increases from 5% to 25%. Thus, if it is true that the annual boundary warming during the Eemian reached temperatures of up to 4 °C, this would imply a range of ice loss of 25-55% (or 1.9-4.1 m.s.l.). Furthermore, the ice core record at GRIP implies that annual temperatures reached an anomaly of 5 °C (Johnsen et al., 2001). Even assuming relatively

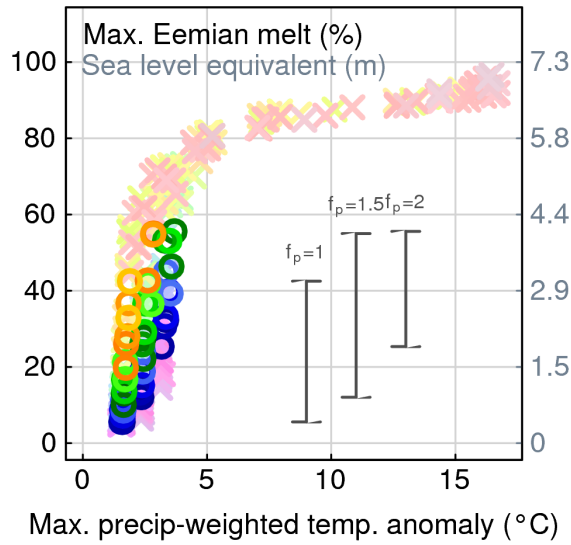


Figure 3.8: Maximum percent of Eemian ice loss versus the maximum precipitation-weighted temperature anomaly experienced at GRIP during the Eemian. The percent loss is also converted into sea-level equivalent, assuming 100% corresponds to the present-day volume of the GIS. Darker circles and lighter crosses correspond to “valid” and “invalid” simulations, respectively. The valid range corresponding to each choice of the paleo factor,  $f_p$ , is indicated by the dark lines.

high boundary warming, the only simulations that present an anomaly at GRIP close to 5 °C are those that have a lower GRIP elevation and lost more volume. Therefore, it becomes more likely that the volume lost during the Eemian was closer to 55% (or 4.1 m.s.l.). This reinforces earlier results (see Jansen et al., 2007) in a robust way.

We also checked the effect of using different values for the paleo constraint, by limiting the Eemian elevation loss at GRIP to 300 m and 500 m. Using 300 m or the original value of 400 m for the limit results in a similar maximum amount of ice loss during the Eemian (53% and 55%, respectively), whereas using 500 m allows cases with 5% more ice loss (corresponding to an additional 0.4 m.s.l.). This difference is rather small compared to the overall range of uncertainty.

Previous estimates of ice loss from Greenland during the Eemian are generally consistent with the results presented here, even though other mass balance schemes were applied. In at least three cases, the annual PDD approach was applied and a wide range of climatic forcing was tested: Cuffey and Marshall (2000) provide a plausible range of 4.0-5.5 m.s.l. and Huybrechts (2002) provided a similar maximum contribution. Tarasov and Peltier (2003) estimate a range of 2.7-4.5 m.s.l. using a similar approach to that of Cuffey and Marshall (2000), but they include additional constraints based on  $\delta^{18}\text{O}$  tracers at the ice core locations. In a more recent study, using an ice sheet model and climate time slices from a Global Circulation Model, Otto-Bliesner et al. (2006) estimate a range of 2.0-3.5 m.s.l. All estimates fall within a similar range, and highlight the fact that without more



information, it may be difficult to provide a narrower estimate.

In terms of other locations on the ice sheet, the constrained model ensemble produces various results. Most simulations considered valid by our three chosen constraints maintain ice at DYE-3 throughout the Eemian Interglacial. The range of elevation loss is quite large, however, ranging from almost no change to a 1500 m decrease for the most extreme cases (or total loss of DYE-3 ice in 3 cases). If the DYE-3 elevation did decrease by 1500 m and, correspondingly, the GRIP elevation decreased by the maximum allowed amount of 400 m, the relative elevation change between the two locations would be over 1000 m. This would imply an additional 6 °C of Eemian warming at DYE-3, which would not be consistent with  $\delta^{18}\text{O}$  record here. Nonetheless, it is worth mentioning that in our model it is possible to melt a significant portion of the GIS while maintaining reduced-thickness ice at DYE-3.

### 3.8 Conclusions

Simulations of the evolution of the Greenland Ice Sheet have been performed for the last 250 kaBP using a coupled regional climate-ice sheet model that is physically-based and applicable for a wide range of climatic and topographic change scenarios. Several key model parameters were perturbed to produce an ensemble of model versions, which were then constrained using information about the ice sheet for the Eemian Interglacial and the present day.

The stability of the GIS is predominantly determined by the surface mass balance, and particularly, by the sensitivity of the melt equation to external climatic changes. Other parameters, such as the geothermal heat flux and sliding coefficient, play appreciable but less significant roles in determining the past evolution and present geometry of the simulated GIS (as found by others, e.g., Ritz et al., 1997).

Combined information about the present day and the Eemian helps to reduce the range of valid parameter combinations and model simulations considerably. The modern and paleo constraints produce consistent and, in some respects, mutually complimentary, limitations of the model parameters. Using both modern and paleo constraints together reduces the number of valid model versions to 22% of the initial subset (20 out of 90). Without the use of additional information about the range of Eemian temperature changes, the estimate of the contribution of the GIS to Eemian sea level rise is rather uncertain. From our study, an acceptable range of Eemian melt is 5-55% mass loss (0.4-4.1 m.s.l.). However, when additional constraints on the boundary warming are considered, the likely range narrows to 25-55% mass loss (1.9-4.1 m.s.l.). The highest value in this range is the most likely, given the estimate of up to 5 °C warming at GRIP. These numbers are, of course, only rough estimates, given the poor representation of the ice sheet at the margins. But assuming that the Eemian high stand was 6-8 m above present, this estimate for Greenland melt still requires a considerable contribution to sea level rise from the Antarctic Ice Sheet.

None of our model versions produce a sufficiently realistic present-day GIS in terms of volume and spatial extent to choose a best set of parameter values. The most “realistic” simulations of the modern GIS (less volume and surface area) were obtained in the experiments that produced completely unrealistic simulations of the Eemian GIS (almost complete melting). At the same time, many model versions that satisfy the Eemian paleo constraint are also consistent with the modern constraint on the GIS mass balance partition. This would support the idea that in view of the imperfectness of existing ice sheet models, the latter constraint (criterion) is more appropriate for the selection of model parameters for past and future simulations of the GIS – at least, on the millennial time scale.

Finally, in spite of limitations of the model used and remaining uncertainties, our work indicates that using past and present constraints together, it is possible to rule out both too sensitive and too insensitive model versions, which enhances the credibility of modeling the stability of the GIS under global warming scenarios.

## 3.9 Appendix A

### 3.9.1 Surface albedo parameterization

Surface albedo is parameterized, following van den Berg et al. (2008), as

$$\alpha_s = \min \left( \alpha_g + \frac{d}{d_{crit}} (\alpha_{s,max} - \alpha_g), \alpha_{s,max} \right), \quad (3.3)$$

where  $\alpha_{s,max}$  is the maximum snow albedo (0.8 for dry snow; 0.6 for wet snow),  $\alpha_g$  is the ground albedo (0.4 for ice; 0.2 for bare ground), and  $d$  is the snow depth. If no snow is present, the surface albedo equals the ground albedo, while up to a critical snow depth,  $d_{crit}$ , albedo increases linearly until the maximum albedo is reached. This parameterization produces the right range of albedo values for the given surface types, however, using the original formulation, it was found to prolong the melt season. Because the surface albedo of ice-free grid points was that of land, melt tended to be overestimated and snow was prevented from growing until much colder conditions were reached. In reality, the transition to snow cover is not smooth, and in one snow storm, the albedo of the region can change dramatically. To allow the model to develop snow-covered regions in a more realistic way, we first assume that the minimum ground albedo is that of ice (since if there is no snow or ice present, there is nothing to melt anyway). After melt is calculated, using this albedo in the ITM equation, and a new snow depth determined, the albedo is calculated as in the original formulation to provide an estimate for the planetary albedo used in the energy-moisture balance equations of REMBO (since the albedo of land would play a role here).

Furthermore, we modified the critical snow depth in Eq. (3.3) to depend on the type of vegetation that would be present. To do so, we calculate the available positive degree days based on temperature and convert this to a land type.

We tested the effect of changing the albedo parameterization via the critical snow depth and the minimum ground albedo, along with variations to the ITM parameter  $c$ . These three parameters are interrelated and changing one can offset the effects of the other. However, to simulate realistic glacial cycles (in that the ice sheet regrows completely during cold periods), it was necessary to increase the minimum ground albedo (as described above) to that of an ice-covered surface (0.4). In the annual average, the model produces comparable results to those presented by Robinson et al. (2010a).

## Acknowledgements

We would like to thank R. Greve for providing us with the ice sheet model SICOPOLIS. A. Robinson is funded by the European Commission's Marie Curie 6<sup>th</sup> Framework Programme in the Research Training Network, Network for Ice and Climate Interactions (NICE), and R. Calov is funded by the Deutsche Forschungsgemeinschaft RA 977/6-1.



## 4. MULTISTABILITY AND CRITICAL THRESHOLDS OF THE GREENLAND ICE SHEET<sup>3</sup>

Many recent studies have focused on the contribution of the Greenland Ice Sheet (GIS) to sea-level rise on the centennial timescale, yet little is known about the long-term stability of the ice sheet. While the existence of multiple equilibria for the ice sheet was proposed decades ago, the temperature threshold leading to a complete collapse of the GIS is not accurately known. The accepted estimate of this threshold, 1.9-4.6 °C above the preindustrial climate (Meehl et al., 2007), is based on the modelled surface mass balance of the ice sheet turning negative given the present-day topography. Here, using a regional energy-moisture balance model bi-directionally coupled to an ice sheet model, we show that the GIS does possess hysteresis behaviour and is likely to be significantly more sensitive to long-term climate change than previously thought. We estimate that the threshold in global temperature anomaly leading to a monostable, essentially ice-free state is in the range of 1.3-2.3 °C. The time needed to melt the GIS completely strongly depends on how much the temperature anomaly exceeds the threshold value. Furthermore, by testing the ability of the GIS to regrow after partial mass loss, we found that an intermediate equilibrium state is possible, and that for sufficiently high initial temperature anomalies, total loss of the ice sheet becomes irreversible.

Like many components of the climate system, ice sheets are believed to exhibit hysteresis behaviour (Oerlemans and Van Den Dool, 1978; Letréguilly et al., 1991; Crowley and Baum, 1995). The theoretical foundation for the possibility of bifurcations between different states rests on the existence of the strongly positive elevation and albedo feedbacks. As an ice sheet begins to melt around the margin, the local elevation decreases and temperatures warm. A decrease in area of the ice sheet additionally contributes to warming through a reduction in surface and planetary albedo. This results in further melting inward and further warming until a new equilibrium is reached. The level of warming needed to melt the ice sheet completely is considered to be a critical threshold, or tipping point (Lenton et al., 2008). Although precise knowledge of this threshold may not aid in centennial timescale predictions of sea level rise, it is important for assessing the probability of irreversible changes to the cryosphere given the extremely long life-time of anthropogenic CO<sub>2</sub> in the

---

<sup>3</sup> Robinson, A., Calov, R., and Ganopolski, A.: Multistability and critical thresholds of the Greenland Ice Sheet, **submitted**.

atmosphere (Archer et al., 2009).

Coupled climate-ice sheet models have been used in paleo simulations to show that the Antarctic Ice Sheet exhibits hysteresis behaviour for varying levels of the atmospheric CO<sub>2</sub> concentration (DeConto and Pollard, 2003) and that multiple stable states exist for the continental Northern Hemisphere ice sheets under different levels of orbital forcing (Calov and Ganopolski, 2005). For the GIS, it has been shown that irreversible melt back is likely beyond a certain temperature threshold (Toniazzo et al., 2004; Charbit et al., 2008). Using a three-dimensional ice sheet model coupled to an AOGCM, Ridley et al. (2005) showed that under high CO<sub>2</sub>-induced warming, the GIS would melt away completely, with strong regional effects on the climate. In another study (Ridley et al., 2009), the authors conclude that not only is Greenland bi-stable for present-day temperatures, but there may be other intermediate equilibrium states resulting from climate-ice sheet interactions.

Thus, previous studies support the idea of multi-stable behaviour of the GIS, but the critical temperature leading to the transition to an ice-free Greenland remains highly uncertain. For example, the last IPCC report gives the range 1.9-4.6 °C for the global mean temperature change leading to total loss of the GIS (Meehl et al., 2007). These estimates are determined using the modelled surface mass balance of the modern GIS (with a fixed topography – i.e., no ice sheet model), assuming that a transition to a negative surface mass balance implies a loss of stability (Gregory and Huybrechts, 2006). Although this criterion is indeed reasonable as a sufficient condition for melting the GIS, it has never been demonstrated that it is also a necessary condition. Moreover, in previous studies, a relatively simple, semi-empirical approach has been used to determine the melt rate. This method allows simulation of the present-day GIS with a sufficient degree of accuracy, but it remains unclear how appropriate it is for the simulation of the GIS under very different climate conditions (Bougamont et al., 2007). To study the long-term response of the GIS to rising temperatures, we used an intermediate complexity, regional climate model (Robinson et al., 2010a) coupled to an ice sheet model (Greve, 1997a – see Methods). As a first step, we evaluated the sensitivity of the model to a wide range of model parameter combinations through simulations of the GIS for present-day and last interglacial conditions (Robinson et al., 2010b). Unrealistic parameter combinations were eliminated by observational and paleo data constraints. The state of the simulated ice sheet proved to be especially sensitive to a free parameter in the surface mass balance scheme (see Supplementary Information). Thus, for this study we selected three values of this parameter, which represent cases of high, medium and low sensitivity of the GIS to temperature changes. All three chosen model versions are consistent with observational and paleoclimate constraints. With this approach, we cannot claim that we span the whole possible range of valid parameter combinations. We rather demonstrate that even such a relatively narrow range of uncertainty in the surface mass balance scheme leads to significant differences in the response of the GIS to climate change and its critical temperature thresholds. To trace the stability of the GIS relative to temperature changes, we used the technique routinely used to analyse the

stability of the Atlantic meridional overturning circulation (Rahmstorf, 1995) – namely, we applied a temperature anomaly changing very slowly in time (i.e., at a rate, much slower than the response time of the ice sheet), so as to maintain a quasi-equilibrium state at all times. We used the present-day GIS obtained from paleo simulations (Robinson et al., 2010b) to initialize the ice sheet. We applied the slowly-increasing temperature anomaly until complete deglaciation was achieved; the anomaly was then decreased slowly until regrowth completed, thus tracing both branches of the stability diagram. Each simulation was run for at least 1 million years to ensure that the GIS was always close to equilibrium. For the sake of simplicity, the applied temperature anomaly was spatially and seasonally uniform outside of Greenland (the temperature over Greenland is computed by the regional climate model). In a set of additional experiments (not shown here), we found that the GIS response to temperature change is dominated by the summer temperature changes. Climate models suggest that the summer temperature response over Greenland is less than the local annual mean and more close to the global mean (Christensen et al., 2007). Therefore, to the first approximation, the applied regional temperature anomaly can be considered as the global mean temperature anomaly, although this is likely to be conservative estimate. Furthermore, data suggest that the mean summer temperature around Greenland for the period 1958-2001 (used for the boundary conditions of the regional climate model) was not considerably higher than preindustrial (most of the warming in this region took place in the last decade, Box et al., 2009), so the temperature anomalies used in this study can be considered as relative to preindustrial temperatures rather than present day.

The results from these experiments can be seen in Fig. 4.1a, which shows three separate stability curves, corresponding to the high, medium and low sensitivity cases for varying levels of the temperature anomaly. The temperature threshold leading to a collapse in each case is between 1.3-2.3 °C. Hysteresis behaviour is apparent in all cases, in that the ice sheet will only regrow for a temperature approximately 1.3 °C colder than needed to melt it. For the medium sensitivity case, the ice sheet is stable until an anomaly of 1.8 °C, above which it transitions to an essentially ice-free state (ca. 10% of the modern GIS volume). Our results indicate that the GIS is already rather close to this threshold and could cross it within the next several decades, highlighting the importance of understanding both the timescale and irreversibility of the meltback.

We address the question of irreversibility by mapping the basins of attraction towards the stable branches of the hysteresis diagram (for the central case). Following a methodology from previous work (Ridley et al., 2009), we produced a set of reduced-volume ice sheet configurations from a transient experiment, by applying a constant temperature anomaly just above the deglaciation threshold. Using a reduced-volume configuration as initial conditions, we then applied a different constant temperature anomaly and ran the model until equilibrium was reached. When a temperature anomaly outside of the multi-stable region is applied for any initial conditions, the GIS inevitably evolves towards one of the two hysteresis branches shown in Fig. 4.1b; namely, for temperatures above the deglaciation

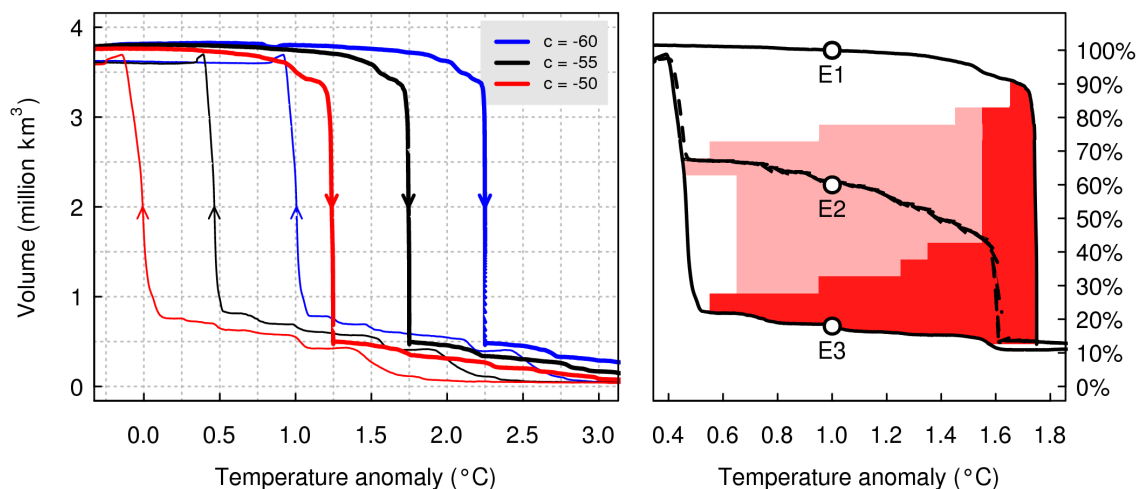


**Figure 4.1: Stability analysis.** **a**, Stability diagrams of the GIS for the low (blue), medium (black) and high (red) sensitivity cases. The thicker lines show the GIS quasi-equilibrium volume when the temperature anomaly was increasing, starting from the complete ice sheet; thinner lines show the volume when the temperature anomaly was decreasing, starting from ice-free conditions. **b**, Stability diagram of the medium sensitivity case, also showing the modelled “basins of attraction” within the multi-stable region. Simulations that start with a given volume for a temperature anomaly in the red region inevitably approach the lower branch of the diagram in equilibrium. Simulations that start in the pink region eventually reach an intermediate equilibrium volume, and those that start in the white region fully regrow to reach the upper branch of the diagram. The dashed line corresponds to the intermediate equilibrium branch. The open circles labelled E1, E2 and E3 correspond to the equilibrium states shown in Fig. 4.2.

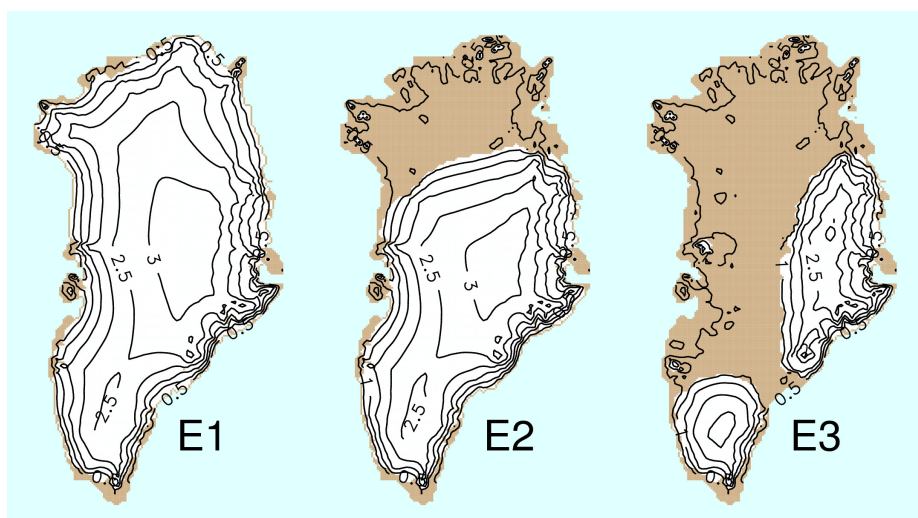


**Figure 4.2: Equilibrium states of the GIS.** Three equilibrium states of the GIS obtained for the medium sensitivity model version and a temperature anomaly of 1 °C. These states correspond to those denoted by the open circles in Fig. 4.1b.



threshold, the GIS melts completely (e.g., state E3 in Fig. 4.1b and Fig. 4.2) and for temperatures below the deglaciation threshold, the GIS approaches its full size (e.g., state E1 in Fig. 4.1b and Fig. 4.2). For temperatures inside the multi-stable range, the equilibrium state of the GIS is strongly dependent on the initial conditions. A reduced-volume ice sheet that initially lies within the dark red area for a given temperature anomaly (Fig. 1b) will eventually approach the lower branch of the diagram (i.e., almost complete deglaciation). Ice sheet configurations that are initially located within the pink region evolve towards intermediate equilibrium states (e.g., state E2 in Fig. 4.1b and Fig. 4.2). Therefore, as long as the GIS volume remains in the attraction domain of the lower branch of the stability diagram, it will continue to melt irreversibly, even if the temperature anomaly gradually decreases.

Crossing the deglaciation threshold, however, does not imply a rapid collapse of the ice sheet. In fact, the closer temperatures are to the threshold, the slower the response time of the GIS is, as shown in Fig. 4.3a. The time needed to melt a significant portion of the GIS is strongly dependent on the level of warming. For 2.0 °C, which is just above the deglaciation threshold for the central case, complete melting of GIS takes about 50,000 years. In contrast, with warming of 4.0 °C, the ice sheet needs ca. 8000 years to melt completely, and for warming of 8.0 °C, 20% of the ice sheet melts in just 500 years and the entire ice sheet melts within ca. 2000 years.

The temperature threshold for deglaciation of the GIS found here (1.3-2.3 °C above preindustrial) indicates a much stronger sensitivity of the ice sheet to climate change than previously thought. This discrepancy can at least partly be explained by differences with the criterion of reaching zero surface mass balance used to determine the previous estimate (Gregory and Huybrechts, 2006). Figure 4.3b shows the transient evolution of the surface mass balance (SMB) for temperature anomalies of 0.0-6.0 °C. Simulations that exhibit negative SMB within the first few centuries (purple) certainly lead to a disappearance of the GIS, indeed making this criterion sufficient to confirm that the threshold temperature has been crossed. However, several other simulations (red lines) also result in strong GIS decline, yet they do not exhibit negative mass balance throughout the first millennia. Therefore, consistent with previous findings, we find that a zero surface mass balance of the GIS will be achieved for 3-4 °C global warming, but the actual threshold temperatures leading to a collapse of the ice sheet are significantly closer to the preindustrial climate state. Our study shows that the global temperature already lies near to the critical threshold for melting the GIS. Of course, crossing the critical threshold does not imply “instantaneous” melting of the GIS and its long-term future depends strongly on the magnitude and the duration of the temperature overshoot above the critical threshold. For a sufficiently large temperature anomaly, a significant portion of the ice sheet may be lost within several centuries, and the GIS will continue to melt even if temperatures later drop below the threshold value. Therefore, if anthropogenic CO<sub>2</sub> emissions in the coming century drive the temperature considerably above the deglaciation threshold, irreversible total loss of the

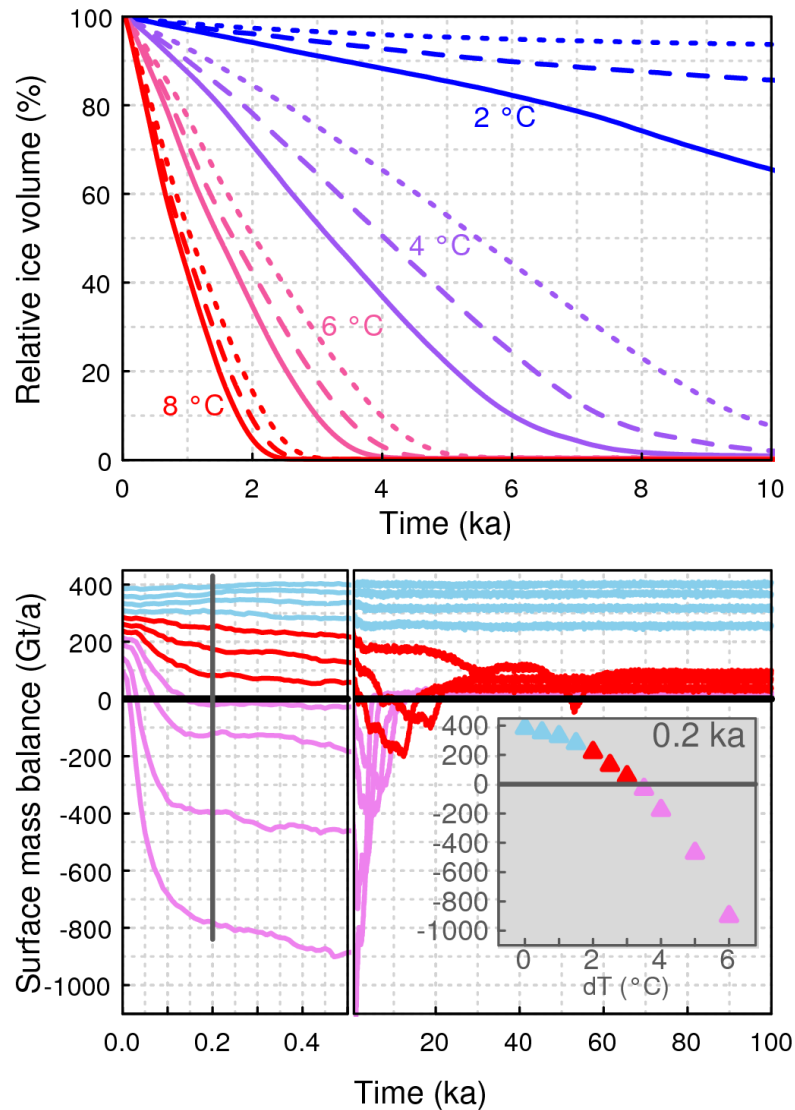


*Figure 4.3: Transient GIS evolution.* **a**, Relative GIS volume change in transient simulations over the next 10,000 years. Each line corresponds to either the low (dotted lines), medium (dashed lines) or high (solid lines) sensitivity case with an applied constant temperature anomaly (blue: 2 °C, purple: 4 °C, pink: 6 °C, red: 8 °C). **b**, The modelled transient GIS surface mass balance (SMB) for the medium sensitivity case with an applied constant temperature anomaly ranging from 0.0-6.0 C. Simulations are separated into those that melt the ice sheet completely and exhibit negative SMB within the first 200 years (purple), those that melt completely but do not exhibit negative SMB in the first 200 years (red) and those that do not melt substantially (blue). The grey inset shows a time slice of the surface mass balance after 200 years versus the applied temperature anomaly in each case. Two hundred years was chosen because it corresponds to the equilibration time of the snowpack model, but to minimal changes in the ice sheet topography.

---

GIS would be difficult to avoid, ensuring continued substantial sea level rise for millennia.

## 4.1 Methods

The regional energy-moisture balance model REMBO (Robinson et al., 2010a) simulates daily temperature and precipitation fields over Greenland. It is coupled bi-directionally to the three-dimensional, polythermal ice sheet model SICOPOLIS (Greve, 1997a), via a surface interface used to determine the surface mass balance of the ice sheet. As the boundary condition for the regional climate model, we use ERA-40 reanalysis climatological temperature outside of the Greenland. The model variables, including surface mass balance, snowpack thickness and surface temperature, are calculated daily in order to track changes in surface albedo. In transient simulations, the climate and surface mass balance fields are updated every 10 years to provide surface forcing to the ice sheet, while in the quasi-equilibrium simulations, the climate is updated every 100 years. This model compares well to state of the art results from regional climate models and, most importantly, explicitly captures elevation and albedo feedbacks in the climate-ice sheet system at relatively high resolution (20 km).

## Acknowledgements

We would like to thank R. Greve for providing us with the ice sheet model SICOPOLIS. A. Robinson is funded by the European Commission's Marie Curie 6<sup>th</sup> Framework Programme in the Research Training Network, Network for Ice and Climate Interactions (NICE), and R. Calov is funded by the Deutsche Forschungsgemeinschaft RA 977/6-1.

## 4.2 Supplementary Information

### 4.2.1 Insolation-temperature melt

The equation used in this study to determine the potential melt rate at the surface (van den Berg et al., 2008),  $M_s$ , is

$$M_s = \frac{\Delta t}{\rho_w L_m} [\tau_a (1 - \alpha_s) S + c + \lambda T], \quad (4.1)$$

where  $\Delta t$  is the conversion factor for the time-step (seconds per day),  $\rho_w$  is the density of water and  $L_m$  is the latent heat of melting. The short-wave radiation reaching the surface is calculated from  $S$ , the insolation at the top of the atmosphere, and  $\alpha_s$  and  $\tau_a$ , the surface albedo and atmospheric transmissivity, respectively. Surface albedo is obtained via a simple parameterization based on the type of ground surface present and the snow-thickness (Robinson et al., 2010b). Transmissivity is a linear function of elevation, but the average value of  $\tau_a$  is around 0.5 near the margins (Robinson et al., 2010a). The long-wave radiation is calculated from the near surface air temperature,  $T$ , and the empirical factor  $\lambda$ , leaving  $c$  as a tuneable constant parameter.

### 4.2.2 Simulations of the basins of attraction

The approach originally presented by Ridley et al. (2009) was used as the basis for our simulations of Greenland Ice Sheet (GIS) regrowth after partial loss of volume and area. The question addressed here is: when a portion of the GIS has melted away and the boundary temperature is returned to a lower value (e.g., by eventually reducing the atmospheric CO<sub>2</sub> concentration), will the ice sheet regrow, find a new equilibrium or continue to decline irreversibly? These simulations were performed for the medium sensitivity version of our model ( $c = -55 \text{ W/m}^2$ ). The climate and surface mass balance fields were updated every 10 years to account for feedbacks and changes in the ice sheet topography. To obtain the initial reduced-volume ice sheet configurations, the present-day GIS resulting from a paleo simulation (Robinson et al., 2010b) was prescribed as the initial ice sheet, and an instantaneous, constant temperature anomaly of 2 °C was applied. As the ice sheet lost volume, the simulated ice sheet state was saved at intervals of 5% of volume loss (several states are shown in Fig. 4.4a-f). In this way, 17 different ice sheet configurations were produced, which were then used as initial conditions to determine the domains of attractions of different equilibrium branches of the hysteresis curve.

The fractional states ranging from 15-95% were used to test how applying a temperature anomaly (much lower than the deglaciation threshold) to a reduced-volume ice sheet would affect the final equilibrium state. Ridley et al. (2009) tested one case, with the temperature anomaly equal to 0.0 °C (preindustrial conditions). We extended this experiment by testing several temperatures in and near the multi-stable region of the stability diagram (at intervals of 0.1 °C). Every simulation was allowed to run for at least 200 ka to ensure

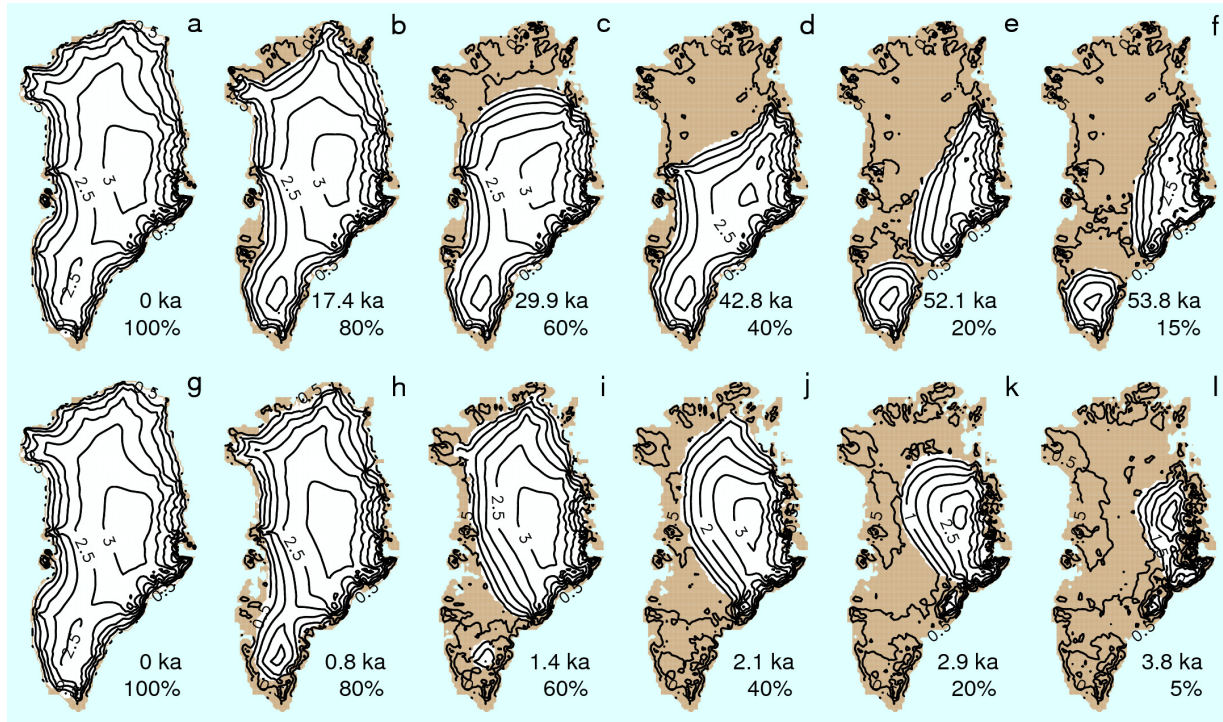


Figure 4.4: Snapshots of GIS corresponding to different volumes obtained in transient experiments with applied constant temperature anomalies of 2 °C (a-f) and 6 °C (g-l).

equilibrium was reached. This is especially important for temperatures near a bifurcation point, where the timescale for changes is extremely slow (Calov et al., 2009).

Figure 4.5 shows the transient volume evolution for several cases, with each panel corresponding to a different temperature anomaly. Outside of the multi-stable region, the simulations produce the expected results – for temperature anomalies below the threshold for regrowth (panel a), all simulations regrew to the “full volume” state and for temperature anomalies above the threshold for decay, all simulations result in almost complete melting of the ice sheet (i.e., less than 20% remaining, panel f). Between these two limits, intermediate equilibrium states can exist, and these depend on the temperature anomaly applied (panels b-e). Our simulations corroborate previous results (Ridley et al., 2009) rather well, although new and systematic responses are also revealed from testing multiple temperature anomalies. We find an intermediate equilibrium branch (with ca. 40-60% of the present-day ice volume) that can be traced in much the same way as the upper and lower branches. For lower temperature anomalies, e.g. 1 °C, the intermediate equilibrium state has about 60% of the present-day ice volume. As the temperature increases, this state reduces in volume until about 45% at 1.5 °C, after which this state also collapses to the ice-free equilibrium state.

Figure 4.6 provides additional information to Fig. 4.1b. Here the final equilibrium states of all reduced-volume runs are also plotted as crosses. Grey crosses show simulations that reached to within 10% of one of the branches of the stability diagram, otherwise the crosses

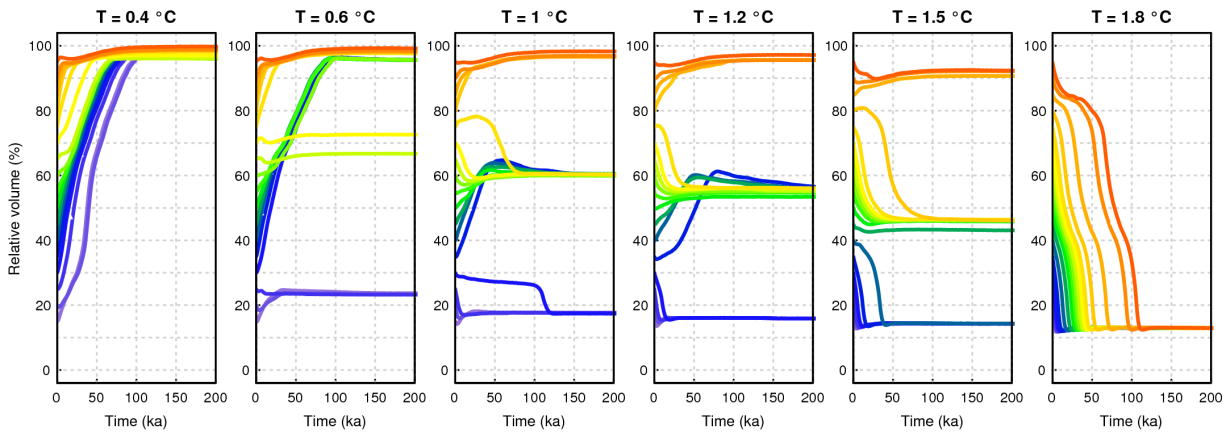


Figure 4.5: Temporal evolution of ice sheet volume for different temperature anomalies (shown at the top of the panels) and different initial volumes. Each color corresponds to a different initial volume (relative to the present-day state), from 95% (red) to 15% (purple), and a gradually varying colour spectrum between.

are green (indicating simulations that equilibrated to intermediate states). The choice of this cut-off percentage is somewhat arbitrary, since several states denoted by grey crosses did not reach the upper branch of the diagram. These minor differences between several equilibrium states and continuous quasi-equilibrium solution are explained by a relatively coarse spatial resolution of the model. Simulations that start with a large volume fraction for low temperature anomalies (white region of Fig. 4.6) equilibrate to the upper branch of the stability diagram. Figure 4.2 shows an example of this equilibrium state for 1 °C (labelled E1), which is representative of the state of the present-day ice sheet (i.e., fully ice-covered Greenland).

Conversely, simulations that start with a very low volume for a low temperature anomaly eventually equilibrate to the lower branch of the stability diagram at around 20% volume fraction, as found by others (Ridley et al., 2009). Depending on the temperature anomaly, the lower branch varies between volumes of 15-20%, yet we would still consider these cases as representing one equilibrium state, because the distribution of ice is quite similar in each case. As a representative example of this state, Fig. 2 shows the equilibrium ice distribution for the case that started with 15% volume for an applied anomaly of 1 °C (labelled E3). It consists of ice limited to the high elevation mountainous regions in the Southeast, and a small ice cap in the South.

An intermediate state is also found, with a volume of approximately 40-50% of the present-day volume (Fig. 2, labelled E2). This state exists for temperature anomalies in the range of 0.5-1.5 °C. In this case, the ice is distributed into one ice sheet occupying the southern half of Greenland, and the northern regions remain ice free. This occurs because after melting large portions in the North, lower albedo and low precipitation prevents regrowth of ice in these areas. As the temperature anomaly increases to 1.5 °C,

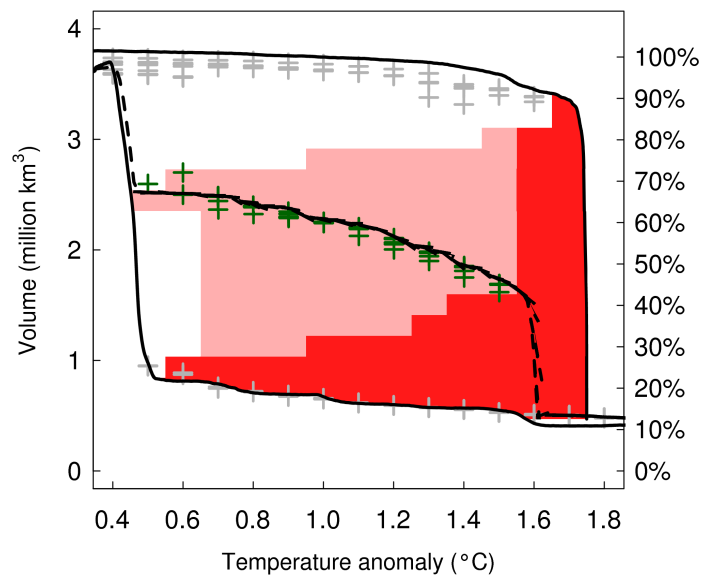


Figure 4.6: Basins of attraction for the medium sensitivity model (the same as Fig. 4.1b), along with the locations of equilibrium states (grey and green crosses) obtained by long-term simulations for different temperature anomalies and different initial conditions. Grey crosses correspond to equilibrium states that are close to the main branches obtained by continuous tracing of the stability diagram. Green crosses correspond to the intermediate equilibrium states and the dashed line shows the intermediate branch of the stability diagram.

the intermediate ice sheet reaches an unsustainable condition and collapses to the lower branch of the stability diagram.

The three equilibrium states found in this study do not necessarily reflect all possible equilibria. For example, although the intermediate state (E2) is qualitatively rather similar to that found in a previous study (Ridley et al., 2009), it is not identical. Nonetheless, this study demonstrates that for the underlying complex Greenland topography, intermediate states are possible within a certain range of temperature anomalies. Moreover, our stability analysis show that for higher temperature anomalies, less of the ice sheet needs to be melted before the decline becomes irreversible (e.g., for a boundary temperature anomaly of 1 °C, the decline is irreversible after 70% of the ice sheet melts, whereas for a boundary anomaly of 1.6 °C, the decline is irreversible after only 20% of the ice sheet melts).

We also repeated the above experiments using intermediate states as initial conditions that were obtained by melting the ice sheet with a much higher temperature anomaly of 6 °C (assuming a climate sensitivity of 3 °C per doubling of CO<sub>2</sub>, this corresponds to four times the preindustrial concentration), which was also used by Ridley et al. (2009). For the same volume, these initial states differ considerably from those obtained in the 2 °C experiment (Fig 4.4). In spite of these differences, simulated domains of attraction were rather similar, which support robustness of the results shown in Fig. 4.1b.





## 5. DISCUSSION

In this thesis, a new intermediate complexity modeling approach for simulating the GIS response to climate change has been presented. A discussion of each of the main questions addressed with this research, in the context of the broader scientific implications, is presented below.

### **Can the surface conditions of the GIS and its regional climate be accurately captured by a simple, yet physically-based approach?**

In the new setup developed here, a regional climate and surface mass balance model provides surface boundary conditions to an ice sheet model. This intermediate complexity model, REMBO, has been validated against present-day climate and surface mass balance observations and other modeling approaches. The simulated seasonal cycles of temperature and precipitation over the ice sheet compare favorably to observations. In addition, cumulative quantities, such as precipitation, snowfall, melt and refreezing summed over the area of the GIS, agree well with estimates from regional climate models. The dependence of melt on elevation as determined by more detailed energy balance models is, to a first order approximation, produced by REMBO.

The good performance of REMBO can partly be attributed to the accuracy of the prescribed ERA-40 boundary data (Uppala et al., 2005). The energy diffusion equation determines the temperature over Greenland, but the boundary data provides temperatures over the surrounding ocean. This means the model has less freedom to evolve near the coasts. For present-day conditions, this is where most melt occurs and, thus, the boundary temperature is a critical parameter. The approach used by REMBO has only become feasible in recent years, as global data reanalysis products have become available. As data for various climatic scenarios from regional climate models becomes available in the future, it should be possible to account for more complex changes taking place at the boundaries (e.g., due to shifting storm tracks).

We found that the modeled surface mass balance depends most on a proper representation of the temperature forcing. The surface mass balance is highly sensitive to the amount and distribution of surface melt, which strongly depends on insolation, surface albedo and air temperature. Insolation can be calculated with a high degree of accuracy (Berger, 1978) and the albedo parameterization used here agrees well with satellite data. Air temperature, the final and most influential prerequisite for an accurate SMB, is also properly simulated by REMBO, matching observations quite well. In fact, the fundamental assumption – that the temperature at sea level can be obtained via atmospheric diffusion and then adjusted

for elevation changes using the free atmospheric lapse rate – proved to be valid over this domain. Indeed, this successful proof of concept was crucial for the remaining work.

Detailed modeling of the precipitation generally played a less critical role in achieving a realistic representation of the surface mass balance. Still, it is important to correctly produce the large-scale precipitation pattern – after all, this is the positive term in the surface mass balance. Consistent with the available observations, REMBO produces precipitation rates below 500 mm/a for over 80% of the GIS area. Over the coastal mountain ranges of the southeast, REMBO's precipitation rates are less accurate, reaching a maximum of roughly 1100 mm/a, while regional modeling shows that highly localized precipitation rates can reach over 4000 mm/a (Ettema et al., 2009). Nevertheless, REMBO is able to reproduce the large-scale distribution of precipitation well, which is the most important aspect for ice sheet model forcing, since the ice flow acts to smooth out any local variations over time.

In addition to the present-day representation of climatic and surface variables, their sensitivity to changes in GIS topography or climate forcing was found to be similar to that of more complex approaches. Over an ice-free Greenland, for example, precipitation patterns are largely similar to present-day patterns, but the amount of snowfall is greatly reduced due to warmer temperatures. Only the mountainous regions in the south maintain a positive surface mass balance. Furthermore, for such conditions, changes in summer temperatures are higher than changes in winter temperatures, since a lower summer albedo tends to increase temperatures even more. These results agree well with the few advanced GCM studies available for comparison (Toniazzi et al., 2004; Lunt et al., 2004). The ability to realistically model drastically different conditions on Greenland provides strong support to the notion that REMBO can be used for long timescale simulations through the glacial cycles and into the future.

Another fundamental result of this work is that a more advanced melt model can have a strong impact on the results. For comparison, we performed simulations using both the newer ITM equation and the more conventional PDD melt equation (see Chapter Two). The ITM approach showed an over 50% stronger response than the PDD approach, when forced with conditions similar to those of the Eemian Interglacial. The warm temperature anomalies during the Eemian mainly resulted from increased solar insolation compared to today. The PDD approach is a function of temperature only, and only considers albedo implicitly, while the ITM approach accounts for changes in the solar insolation and albedo explicitly. This can explain the discrepancy between the two models, and it highlights the practical advantage of using the ITM approach for simulating the GIS on orbital timescales. This does not exclude the possibility of using the PDD approach for this type of study, but it does imply that it is more difficult to ensure it provides realistic forcing under strongly different climatic conditions.

---

## Can model parameters be constrained and uncertainties reduced using available present-day and paleo data? What was the contribution of the Greenland Ice Sheet to the sea level high-stand during the Eemian Interglacial?

Although REMBO realistically simulates the surface conditions of the ice sheet, large uncertainty still existed in the choice of model parameters. For this reason, an ensemble approach was used to systematically evaluate the sensitivity of the model to various parameters and to determine a realistic range of their values. Performing ensemble simulations has become prevalent in global climate modeling as a means of understanding and reducing uncertainty (e.g., Meehl et al., 2007), however such a systematic analysis is more difficult to achieve on the long timescale necessary for ice sheet modeling. The superior computational performance of REMBO enables a rigorous sensitivity analysis of several parameters in the coupled climate-ice sheet model to be performed.

From testing and previous experience, we found four model parameters to be particularly influential: the geothermal heat flux at the base of the ice sheet, the magnitude of basal sliding for temperate ice, the strength of the large-scale precipitation field and a free parameter in the ITM surface mass balance scheme. In addition to these four parameters, we varied the amount of anomaly warming prescribed for the Eemian Interglacial, as this is both influential and not well defined. Several influential model parameters were modified to make an ensemble of 270 simulations in total. Thus, an ensemble of 270 simulations were performed using the fully coupled climate-ice sheet model, running over the last two glacial cycles (250,000 years).

An additional innovation applied here was to force the model with anomaly fields of temperature, CO<sub>2</sub> and insolation obtained from a global modeling study over several glacial cycles (Ganopolski et al., 2010). These fields can be considered fully self-consistent, in contrast with the anomalies applied in previous studies based on  $\delta^{18}\text{O}$  records from Greenland and Antarctica. In practical terms, the boundary forcing from the model is not that much different, but it does extend over the entire time period of the simulations and is relevant to the region in question. As global glacial cycle simulations become more detailed and produce more metrics for comparison to available data, using their output to force regional simulations will become more prevalent.

The results of the ensemble of simulations were compared both to present-day data and to paleo data available for the Eemian Interglacial (130-115 ka before present), when global temperatures were warmer by several degrees and sea level perhaps rose 6-8 m higher than today (Kopp et al., 2009). Uncertainty in the surface mass balance model parameter affected the sensitivity of the GIS to climate change most, while other parameters such as the geothermal heat flux and the basal sliding factor had only secondary effects.

In contrast to most previous studies, we did not use accurate modeling of the present-day volume and area of the GIS as a constraint for realistic model performance. Using the shallow-ice approximation ice sheet model at 20 km resolution, it was not possible to accurately simulate the ice sheet margins and apply realistic surface boundary conditions.

The new constraint applied in this study, based on the present-day ratio of positive surface mass balance to precipitation, proved powerful in limiting the acceptable range of melt model sensitivity to climate change. Combining this constraint with information about the summit of the ice sheet, we were able to eliminate most model versions (80%) as unrealistic. Furthermore, many of the same model versions were eliminated by each of the different constraints, which is an encouraging indicator that these constraints are consistent with each other. By combining present-day and paleo climate constraints, it was possible to significantly reduce the range of valid model parameter combinations and, thus, to reduce the uncertainty obtained for future model predictions.

The sensitivity of the ice sheet to climate change is reflected by the modeled mass loss during the Eemian. According to our simulations, the GIS contribution to the Eemian sea-level high-stand falls within the range of 0.5-4.1 m. By additionally considering paleo data about the temperature anomaly at the summit to be robust, then a value approaching the upper boundary becomes most likely. This corresponds to a little over half of the current mass of the ice sheet. This confirms previous estimates of the possible range of the GIS contribution to sea level during the Eemian from a different perspective. Most previous estimates were based on simulations that used the semi-empirical PDD and bilinear temperature approach to obtain surface forcing. Here we achieved realistic model performance based more directly on physical principles. It is not surprising, however, that we were unable to reduce the range of uncertainty in this estimate. Very little additional information about this time period is available that can be used to constrain model performance. Furthermore, our ensemble approach explored a wide range of uncertainty in the model parameters, including melt model uncertainty that had not been accounted for previously. Our results indicate that by addressing the uncertainty in the melt model, significant reductions in the uncertainty of estimates for the past and predictions for the future of the GIS could be achieved.

Climatic conditions of the Eemian are not analogous to the expected future climate, however the behavior of the GIS during this warm period can provide insight into its general sensitivity to warming. Summer insolation was higher during the Eemian, but the average summer temperature around Greenland was likely not more than a few degrees higher than today. In our simulations, the maximum summer temperature anomaly applied to the simulations over the glacial cycles was 3.4 °C relative to preindustrial temperatures. Even in simulations with warming of only 1.7 °C, the GIS lost significant mass. In fact, had the Eemian warm period lasted longer, the GIS would have continued losing mass, which indicates that the ice sheet had likely already crossed a threshold. In a broader sense, this study confirms that it is possible to melt substantial portions of the GIS under relatively modest warming.

---

**What is the long-term sensitivity of the GIS to future climate change? What is the temperature threshold that would lead to complete melting of the GIS? At what point would such a disappearance become irreversible?**

The constrained ensemble of model versions obtained from the paleo simulations was used to investigate the stability of the GIS under potential anthropogenic climate change. A key aim of this study was to determine the temperature forcing that would cause the GIS to melt completely. This is a highly relevant and important question for society, but in general, very little is known about what thresholds exist for the ice sheet (both for growth and decline), and whether the ice sheet is bi-stable or multi-stable. In previous studies, it was proposed that the GIS may exhibit hysteresis behavior, in that if the ice sheet melts completely for a given temperature, much lower temperatures are needed to regrow it (Letréguilly et al., 1991). Given such hysteresis, another important question concerns the possibility of irreversibility in the system: how much ice sheet melt is needed for the decline to become irreversible?

To answer these questions, the constrained model versions were forced with slowly increasing temperature anomalies until the GIS melted completely. In the paleo simulations, we found that the melt model parameter (the free parameter  $c$ , see Chapter Two) largely dictates the sensitivity of the overall ice sheet to climate change. Here we chose three values of this parameter to represent low, medium and high sensitivity model versions and we found that the threshold leading to the decline of the GIS is 1.3, 1.8 and 2.3 °C above preindustrial levels, respectively. The previous estimate of this threshold had a range of 1.9-4.6 °C (Gregory and Huybrechts, 2006). Thus, our results indicate that the GIS is more sensitive to warming in the long-term than currently assumed.

The simulations performed for this study also show that the cumulative SMB does not provide an accurate estimate of the threshold for GIS decline in the long-term response. The cumulative SMB of the GIS simulated using REMBO turns negative for temperatures within a range of about 3-4 °C, which is consistent with previous estimates (Gregory and Huybrechts, 2006). However, several simulations maintained a positive SMB of the GIS for several thousand years, even though the volume of the ice sheet declined substantially. This can be attributed to the relatively high precipitation rates in the Southeast and Greenland's unique topography. When the SMB is calculated cumulatively (summed over the whole ice sheet), these high precipitation rates can offset significant melt occurring over the majority of the ice sheet. In addition, a significant portion of the mass gain in the mountainous regions continues to discharge into the ocean. Meanwhile, the strongly positive albedo and elevation feedbacks ensure that a large part of the ice sheet melts away.

We also confirm that the shift in equilibrium states from ice-covered to ice-free (and vice-versa) is "abrupt" in the temperature-forcing phase space, in the sense that the ice sheet approximately maintains its full present-day volume until reaching the threshold temperature. A shift of the temperature less than a tenth of a degree warmer than this threshold starts the decline of the ice sheet towards the essentially ice-free equilibrium

state. These results confirm that the GIS is indeed a tipping element in the Earth system, and furthermore, that the threshold leading to its decline is relatively near to present-day conditions.

We should note that while the shift in equilibrium is abrupt in terms of the temperature forcing applied, it is certainly not abrupt in time. The timescale of complete decline can vary from hundreds of thousands of years, when the temperature is near the bifurcation point, to just several hundred years, when the temperature overshoots the threshold by several degrees. Therefore, if temperatures continue to rise, a shorter time to melt the ice sheet will be needed.

From a more theoretical perspective, the existence of such a threshold confirms the expected equilibrium response of a land-based ice sheet to increased temperatures. Using our approach, we were also able to perform the opposite experiment – namely, starting from ice-free conditions, we determined the temperature threshold that would lead to regrowth of the ice sheet. For each model version, hysteresis behavior was confirmed. The ice sheet needed boundary temperatures at least 1.3 °C lower than the threshold, in order for regrowth of the GIS to occur. Regrowth occurs on a slower timescale than melting, however it is still abrupt in terms of the temperature forcing – only a small shift to lower temperatures triggers regrowth. This abruptness results from the albedo and elevation feedbacks working in reverse. Once the ice sheet begins to grow, the albedo and elevation increase, both leading to cooler temperatures and less melt, thus promoting further growth. According to our results, only the most sensitive model version predicts that the GIS is bi-stable for pre-industrial temperatures.

Given the abrupt nature of the GIS response to temperature forcing and the bifurcation in equilibrium states, a natural question arose: is complete melting of the GIS irreversible? Using a coupled climate-ice sheet model for Greenland, Ridley et al. (2009) found at least one intermediate state, and in some cases, the complete melting of the ice sheet was irreversible. They tested the case when temperatures were reverted to preindustrial levels. In this thesis, a systematic analysis of the irreversibility of the system was performed. The ice sheet was partially melted under a temperature anomaly of its critical threshold. Then a cooler temperature was applied to determine if the reduced-volume ice sheet would continue to decline, or regrow to its full size. This method was applied to a range of partially melted ice sheets (in 5% intervals) and to every temperature anomaly inside of the hysteresis loop (at 0.1 °C intervals). This methodology allowed us to roughly map the basins of attraction of the bifurcation diagram for the first time.

Depending on the amount of ice loss that was permitted to occur and the subsequent equilibrium temperature anomaly applied, both irreversibility in the system and the existence of an intermediate equilibrium state of the GIS were confirmed. The intermediate state can exist with approximately 50% of the current ice volume, and is largely a result of the complex bedrock topography of Greenland. The high elevation mountains ensure that some small regions of Greenland maintain positive mass balance, and for different levels of

---

mass loss, there are corresponding levels of bedrock uplift (see the Appendix for details). The result is that a partially melted GIS can find equilibrium with the southern portion of the ice sheet largely intact, and the northern portion of the ice sheet missing.

For higher temperature anomalies, the decline of the ice sheet became irreversible. In cases where more than 20% of the ice sheet has melted and the equilibrium temperature is less than 0.2 °C below the temperature threshold, the GIS melts irreversibly (see Fig. 4.1). The limit of irreversibility (i.e., the basin of attraction) rapidly declines with lower temperatures, allowing ice sheet configurations that have lost up to 60% of the original volume to regrow. However, in any case, the ice sheet should maintain at least 70-80% of its original volume to allow regrowth to a fully ice-covered state. When the volume drops below this threshold, the attraction domain leads either to the intermediate or ice-free equilibrium state.

Examining the irreversibility of the climate-ice sheet system improves our understanding of the sensitivity of the ice sheet to climate change. The stability diagram produced from this work is a two-dimensional simplification of several complex, interacting systems. However, it provides insight into the balance between competing mechanisms. Indeed, whether as a result of increased insolation in the past or from anthropogenic forcing now, temperature forcing at the surface is the most important factor influencing the long-term behavior of the ice sheet. Fundamentally, this work provides further confirmation that the actions of humanity in the coming years may have significant consequences on the future evolution of the Earth System for millennia to come.





## 6. CONCLUSIONS AND OUTLOOK

In this thesis, a new model, REMBO, was developed to study the GIS under different climatic conditions in the past and future. It fills a gap between semi-empirical approaches and more advanced (but computationally intensive) regional climate models. The most significant advantage of the approach is that it is both computationally efficient and physically-based, incorporating key climate-ice sheet feedbacks that affect the evolution of the ice sheet. Three complementary studies have been presented that provide new insight into questions of the long-term stability of the GIS.

The first study served as a proof of concept that such a modeling approach is possible and, additionally, provides several advantages over previous methods. REMBO uses a set of energy-moisture balance equations to produce the daily distribution of temperature and precipitation over Greenland. The daily timestep allows the model to account for seasonal changes in surface albedo, melt rates, refreezing and the snowpack thickness, which play a role in the evolution of the climate. In comparison with simpler approaches for present-day conditions, REMBO improves the representation of the climate and the surface mass balance. Crucially, realistic changes to these variables are also simulated when conditions are different, for example, in warmer climates or for an ice-free Greenland.

In the second study, REMBO coupled to the ice sheet model SICOPOLIS was used to simulate the evolution of the GIS over the last two glacial cycles. An ensemble of simulations with varied model parameters was performed and information about the GIS during the Eemian Interglacial and today was used to constrain the parameter values to realistic ranges. The systematic sensitivity analysis revealed that uncertainty in the melt model most strongly affected the evolution of the ice sheet. This, combined with uncertainty in the boundary temperature anomaly, added uncertainty to the estimate of the GIS contribution to the high sea level during the Eemian. The range of 0.5-4.1 m estimated here is consistent with the general consensus. In addition, the applied constraints served to limit the model parameter uncertainty, providing realistic model versions for simulations into the future.

In the third study, the constrained ensemble of model versions was applied to investigate the future stability of the GIS under potential anthropogenic climate change. A temperature threshold leading to complete disappearance of the GIS was found, confirming the hypothesis that the GIS is a tipping element in the Earth system. For low, medium and high sensitivity model versions, the threshold leading to complete meltback was determined to be 1.3, 1.8 and 2.3 °C above preindustrial levels, respectively. In addition, the

GIS exhibits hysteresis: when starting from ice-free conditions, a temperature 1.3 °C lower than the threshold is needed for the GIS to regrow. Depending on the amount of ice loss that occurs and the equilibrium temperature anomaly applied, an intermediate equilibrium state of the GIS can also exist with approximately 50% of the current ice volume.

This thesis is the first study to identify the critical thresholds of the GIS using a fully coupled regional climate-ice sheet model of intermediate complexity, and to assess an associated uncertainty range. Most importantly, it shows that the critical threshold in global temperature for melting the GIS likely lies closer to the preindustrial temperature than was previously reported. It was also shown that the timescale of GIS melt is roughly inversely proportional to the overshoot of the critical temperature threshold. Although this timescale is rather long, in view of the long lifetime of CO<sub>2</sub> in the atmosphere, the probability of irreversible collapse of the GIS will depend strongly on the anthropogenic CO<sub>2</sub> emissions in the next century.

The ability to perform reliable long timescale simulations of the GIS will provide an opportunity to investigate several additional scientific questions related to the stability of the ice sheet in the future. For example, the temperature threshold identified in this study showed an uncertainty range of 1 °C. By examining the physical characteristics of the surface mass balance response to climate change in scenarios that cause the GIS to decline, it may be possible to identify a more accurate indicator of GIS stability that can be measured in the real world (e.g., changes to the equilibrium line altitude or cumulative melt area – both of which can be monitored by satellite). In addition, by including inter-annual variability in the climatic forcing of the model, it would be possible to analyze how climatic changes besides a simple increase in the mean temperature affect the ice sheet. It is possible that climatic variability will increase with global warming, which has a non-linear effect on the cryosphere (i.e., warm years melt more ice than can be regained in cold years). This could increase the sensitivity of the GIS to climate change and reduce the mean temperature threshold leading to its decline. To answer these questions, it is necessary to have a model such as REMBO that includes natural variability and can perform a large number of simulations reliably, under a wide range of physical situations and on long timescales.

While the current version of REMBO simulates the climatic forcing over Greenland well compared to conventional approaches, further improvements to the model could also aid in reducing uncertainty. The surface mass balance interface currently includes a simple one-layer snowpack model and the melt equation does not explicitly include radiative terms. To include these in the model would imply changes to the governing atmospheric equations as well, and thus, an increase in the computational cost of running the model. In the concrete implementation, a balance between computational efficiency and model complexity must be maintained. With this in mind, it should be possible to include several additional processes (radiative forcing, more complex snowpack, sublimation, etc.) and improve the model's capabilities. Moreover, this would allow a more detailed comparison of this approach to

more advanced regional climate models, leading to a further reduction in model uncertainty.

Overall, it will be important to continue to use all data resources available for model validation and to recognize the advantages of the intermediate complexity approach. Although observations are sparse, data sets produced by regional climate modeling provide a rich source of validated quantities for comparison. Furthermore, satellite data is continuously increasing and new algorithms are developed to translate the information into usable data. As REMBO is refined and validated against other approaches, it facilitates understanding of the GIS on different timescales. REMBO is a tool that can provide a link between near-term, diagnostic information and the long-term evolution of the ice sheet.



## 7. APPENDIX

### 7.1 Ice sheet model field equations

An ice sheet can be considered to evolve as a continuum under the principles of creeping flow – namely, that viscous forces are large relative to inertial forces. Neglecting the upper boundary snow and firn layers that compress over time, the ice sheet can also be assumed to be incompressible. The equations used to determine the fully coupled velocity and temperature distributions of the ice are obtained using the laws of conservation of energy, momentum and mass. Gravity is the only body force present, which balances with stress acting on the ice. Given the above assumptions, the momentum balance can be expressed as (Greve and Blatter, 2009):

$$\nabla \boldsymbol{\tau} + \mathbf{f} = 0, \quad (7.1)$$

where  $\boldsymbol{\tau}$  is the stress tensor and  $\mathbf{f}$  represents the body forces. The horizontal components  $f_x = f_y = 0$ , while  $f_z = \rho g$ , where  $\rho$  is the density of ice (910 kg/m<sup>3</sup>) and  $g$  is acceleration due to gravity (9.81 m/s<sup>2</sup>). Although Eq. (7.1) represents a much simplified form of the full Navier-Stokes equation, it is still demanding to solve numerically.

At this point, SIA can be applied to eliminate some stress terms by assuming a small aspect ratio of the ice sheet geometry. Combined with the hydrostatic approximation, the result is that the horizontal shear stress ( $\tau_{xz}$ ,  $\tau_{yz}$ ) simply equals the product of the overlying hydrostatic pressure and the surface gradient:

$$\begin{aligned} \tau_{xz} &= -\rho g(h - z) \frac{\partial h}{\partial x}, \\ \tau_{yz} &= -\rho g(h - z) \frac{\partial h}{\partial y}, \end{aligned} \quad (7.2)$$

where  $h$  is the surface elevation. The longitudinal and vertical stress components are eliminated and, in this way, the maximum stress (and flow direction) is always aligned with the steepest surface slope (Greve and Blatter, 2009).

To determine velocities from the stress terms, a relation between stress and strain is needed. Most ice sheet models use a relation following the form of the empirically-derived ‘‘Glen’s flow law’’ (Glen, 1955), which reads

$$\dot{\boldsymbol{\epsilon}} = EA(T') \tau_e^{n-1} \boldsymbol{\tau}', \quad (7.3)$$

where  $\dot{\boldsymbol{\epsilon}}$  is the strain rate tensor,  $\tau_e = \rho g(h - z) |\nabla h|$  is the effective stress and  $\boldsymbol{\tau}'$  is the deviatoric Cauchy stress tensor. The exponent of the flow law  $n$  is typically taken as 3 for

ice, although other values are possible (Paterson, 1994).  $E$  is the flow-enhancement factor, which can be considered to account for softening of the ice from impurities or anisotropy (Greve and Blatter, 2009). For northern hemispheric ice sheets such as the GIS,  $E = 3$ , however its value can be considered as a source of uncertainty (Ritz et al., 1997).  $A(T')$  is the rate factor, which is usually considered to only depend on the homologous temperature  $T'$  – this is the temperature of the ice corrected for the change in melting point due to pressure – via the Arrhenius relation. In SICOPOLIS, special treatment of the ice is also considered when the homologous temperature is at the melting point. In this case, the rate factor is instead dependent on the water content of the ice (Greve, 1997a).

The horizontal components of the velocity field follow from the above assumptions and can be written as,

$$\begin{aligned} v_x &= v_{b,x} - 2(\rho g)^n |\nabla h|^{n-1} \frac{\partial h}{\partial x} \int_b^z A(T')(h - \bar{z})^n d\bar{z} \\ v_y &= v_{b,y} - 2(\rho g)^n |\nabla h|^{n-1} \frac{\partial h}{\partial y} \int_b^z A(T')(h - \bar{z})^n d\bar{z} \end{aligned} \quad (7.4)$$

and by vertically integrating the continuity equation ( $\nabla \cdot \mathbf{v} = 0$ ), the vertical component can be obtained,

$$v_z = v_{b,z} - \int_b^z \left( \frac{\partial v_x}{\partial x} + \frac{\partial v_y}{\partial y} \right) d\bar{z} \quad (7.5)$$

Thus, the horizontal velocity depends on the surface elevation gradient, the overlying hydrostatic pressure, the ice temperature (via the flow rate factor  $A(T')$ ) and the velocity at the base. The vertical velocity component is a function of the horizontal flux, a direct result of applying the continuity equation. The time-dependent evolution of ice thickness can be obtained from the continuity equation ( $\nabla \cdot \mathbf{v} = 0$ ) and kinematic boundary conditions, such that

$$\frac{\partial H}{\partial t} = -\nabla \cdot \mathbf{Q} + B - S, \quad (7.6)$$

where  $H$  is the ice thickness,  $\mathbf{Q}$  is the vertically-integrated mass flux of the ice,  $B$  is the surface mass balance (accumulation minus ablation) and  $S$  is the basal melt rate. Thus, the change in ice thickness at a given location depends only on the horizontal ice flux ( $Q_x, Q_y$ ), the addition or removal of mass at the surface and any melting that occurs at the base. Equation (7.6) generally holds for ice sheet modeling and is not specific to SIA models.

The surface height evolution additionally depends on changes to the bedrock elevation ( $\frac{\partial h}{\partial t} = \frac{\partial H}{\partial t} + \frac{\partial b}{\partial t}$ ). The underlying bedrock elevation,  $b$ , should evolve under the weight of the ice sheet – a process that occurs on a similar timescale to that of the ice sheet's evolution. Therefore, it is important to include isostatic adjustment. Various approaches of differing complexity exist, but the simplest representation is achieved via a locally deforming, elastic lithosphere resting on a viscous asthenosphere (Greve and Blatter, 2009), such that

$$\frac{\partial b}{\partial t} = -\frac{b - \left( b_0 - \frac{\rho}{\rho_a} H \right)}{\tau_a}. \quad (7.7)$$

$b$  is the bedrock elevation,  $b_0$  is the unweighted bedrock elevation,  $\rho_a$  is the density of the asthenosphere ( $3300 \text{ kg/m}^3$ ) and  $\tau_a$  is the assumed time lag of the asthenospheric response (e.g., 3000 years).

Temperature in the ice is obtained from conservation of energy. The use of the shallow ice approximation allows the assumption that horizontal thermal diffusion is small compared to the vertical component. The time-dependent temperature evolution in the ice is thus a function of vertical diffusion, advection via ice flow and strain dissipation heating, described as

$$\frac{\partial T}{\partial t} = \kappa \frac{\partial^2 T}{\partial z^2} - \mathbf{v} \cdot \nabla T + \frac{1}{\rho c_p} \text{tr}(\boldsymbol{\tau} \dot{\boldsymbol{\epsilon}}), \quad (7.8)$$

where  $\kappa$  is the thermal diffusivity and  $c_p$  is the specific heat capacity of the ice (Greve and Blatter, 2009). The velocity  $\mathbf{v}$  appears in the temperature equation, while temperature is also needed to determine  $\mathbf{v}$  and  $\dot{\boldsymbol{\epsilon}}$  (via Eq. (7.3)). Thus, the temperature and velocity equations must be solved simultaneously.

## 7.2 Boundary conditions

The ice sheet model requires boundary conditions at the base (bedrock elevation, basal temperature, basal velocity) and at the surface (surface mass balance, surface temperature).

The topography of the GIS is well mapped, both from numerous local expeditions and from remote sensing (Bamber et al., 2001), which can provide a reasonable representation of the initial bedrock elevation for present day (Fig. 1.1 and 1.2). The bedrock elevation can then be allowed to evolve under the weight of the ice sheet (e.g., via Eq. (7.7)).

At the base of the ice sheet, it is assumed that generally the ice is frozen to the bedrock and a no-slip condition applies ( $v_{b,x} = v_{b,y} = 0$ ). However, when the temperature of the ice is at the pressure melting point, the ice sheet is permitted to slide and a basal velocity must be calculated. The magnitude of the basal sliding velocity depends on the material present (e.g., deformable sediments or smooth bedrock, etc.), however it is practically impossible to obtain reliable observations of this aspect of the ice sheet. To overcome this problem, empirical studies have shown that a sliding law can be formulated that relates the basal velocity, basal shear stress and water pressure (Paterson, 1994). Weertman (1957) proposed two mechanisms for ice flow at the base of the ice sheet over bumps, namely *regelation* (transfer of heat upstream due to pressure and temperature differences) and *enhanced plastic flow* (increase in the rate of flow due to additional stress). Several forms of sliding equations are derived from these principles. In SICOPOLIS, the following Weertman-type equation is applied to determine the basal sliding velocity for regions where the basal ice is at the melting point (Greve, 1997a):

$$\mathbf{v}_b = \gamma_s \rho g H |\nabla h|^2 \nabla h. \quad (7.9)$$

which shows a third-order dependence on the gradient of elevation and a first-order dependence on the ice thickness.  $\gamma_s$  is the sliding coefficient, which can be considered as a free

parameter.

The temperature of the ice at the base is computed by balancing the energy flux through the ice-bedrock interface with the frictional heating at that interface, such that

$$k \frac{\partial T}{\partial z} \Big|_{z=b} = k_R \frac{\partial T_R}{\partial z} \Big|_{z=b} + \boldsymbol{\tau}_b \cdot \mathbf{v}_b, \quad (7.10)$$

where  $T_R$  is the temperature in a thick bedrock layer (e.g., 5 km thickness is used SICOPOLIS) and  $k$  and  $k_R$  are the thermal conductivities of ice and rock, respectively. The temperature in the bedrock is determined via a heat equation in the bedrock layer and the lower boundary condition of this layer is given by the geothermal heat flux. This means that the temperature at the base of the ice sheet can be calculated via a coupled ice-bedrock temperature model, but the geothermal heat flux is needed as an input value (Huybrechts et al., 1991; Greve and Blatter, 2009). Greve (2005) approached the problem using an inverse method. Because the temperature at the base of the ice sheet was known in locations where ice cores had been drilled, it could be used as a constraint to limit the geothermal heat flux. In a different approach, a global harmonic model has been used to make estimates consistent with observations of the large-scale geothermal heat flux (Shapiro and Ritzwoller, 2004). Although the estimates are consistent with observations, very few observations at the base of the GIS actually exist (only those obtained from ice core drilling efforts) and there could be localized variations that are important, yet unknown.

At the surface, the annual surface temperature and the surface mass balance (SMB) are needed as boundary conditions. Unlike the base of the ice sheet, the temperature at the surface of the ice can be determined directly from the near surface air temperature. Observations have shown that beneath the firn layer, the surface temperature of the ice can be approximated as a function of the mean annual air temperature,  $\bar{T}_a$  and the amount of refreezing in the firn,  $h_{i,sup}$  (Reeh, 1991),

$$T_i = \min(\bar{T}_a, 0) + 29.2h_{i,sup}. \quad (7.11)$$

The remaining boundary condition, annual surface mass balance, has been discussed at length within the thesis.



## BIBLIOGRAPHY

- Abdalati, W. and Steffen, K.: Greenland ice sheet melt extent: 1979-1999, *J. Geophys. Res.*, 106, 33 983–33 988, 2001.
- Alley, R. B., Gow, A. J., Johnsen, S. J., Kipfstuhl, J., Meese, D. A., and Thorsteinsson, T.: Comparison of deep ice cores, *Nature*, 373, 393–393, 1995.
- Alley, R. B., Andrews, J., Brigham-Grette, J., Clarke, G., Cuffey, K., Fitzpatrick, J., Funder, S., Marshall, S., Miller, G., Mitrovica, J., Muhs, D., Otto-Bliesner, B., Polyak, L., and White, J.: History of the Greenland Ice Sheet: paleoclimatic insights, *Quaternary Science Reviews*, 29, 1728–1756, 2010.
- Archer, D., Eby, M., Brovkin, V., Ridgwell, A., Cao, L., Mikolajewicz, U., Caldeira, K., Matsumoto, K., Munhoven, G., Montenegro, A., and Tokos, K.: Atmospheric Lifetime of Fossil Fuel Carbon Dioxide, *Annual Review of Earth and Planetary Sciences*, 37, 117–134, doi:10.1146/annurev.earth.031208.100206, 2009.
- Bales, R. C., Guo, Q., Shen, D., McConnell, J. R., Du, G., Burkhart, J. F., Spikes, V. B., Hanna, E., and Cappelen, J.: Annual accumulation for Greenland updated using ice core data developed during 2000-2006 and analysis of daily coastal meteorological data, *J. Geophys. Res.*, 114, D06 116, 2009.
- Bamber, J. L., Ekholm, S., and Krabill, W. B.: A new, high-resolution digital elevation model of Greenland fully validated with airborne laser altimeter data, *J. Geophys. Res.*, 106, 6733–6745, 2001.
- Berger, A. L.: Long-Term Variations of Daily Insolation and Quaternary Climatic Changes, *Journal of the Atmospheric Sciences*, 35, 2362–2367, 1978.
- Bhattacharya, I., Jezek, K. C., Wang, L., and Liu, H.: Surface melt area variability of the Greenland ice sheet: 1979–2008, *Geophys. Res. Lett.*, 36, L20 502, doi:10.1029/2009GL039798, 2009.
- Bintanja, R., van de Wal, R. S. W., and Oerlemans, J.: Global ice volume variations through the last glacial cycle simulated by a 3-D ice-dynamical model, *Quaternary International*, 95-96, 11–23, 2002.

- Bonelli, S., Charbit, S., Kageyama, M., Woillez, M.-N., Ramstein, G., Dumas, C., and Quiquet, A.: Investigating the evolution of major Northern Hemisphere ice sheets during the last glacial-interglacial cycle, *Clim. Past*, 5, 329–345, 2009.
- Bougamont, M., Bamber, J. L., Ridley, J. K., Gladstone, R. M., Greuell, W., Hanna, E., Payne, A. J., and Rutt, I.: Impact of model physics on estimating the surface mass balance of the Greenland ice sheet, *Geophys. Res. Lett.*, 34, L17 501, 2007.
- Box, J. E., Bromwich, D. H., Veenhuis, B. A., Bai, L.-S., Stroeve, J. C., Rogers, J. C., Steffen, K., Haran, T., and Wang, S.-H.: Greenland Ice Sheet Surface Mass Balance Variability (1988–2004) from Calibrated Polar MM5 Output, *Journal of Climate*, 19, 2783–2800, doi:10.1175/JCLI3738.1, 2006.
- Box, J. E., Yang, L., Bromwich, D. H., and Bai, L.-S.: Greenland Ice Sheet Surface Air Temperature Variability: 1840–2007, *Journal of Climate*, 22, 4029–4049, doi:10.1175/2009JCLI2816.1, 2009.
- Braithwaite, R.: Regional modelling of ablation in West Greenland, *Groenlands geologiske undersogelse*, 98, 1–20, 1980.
- Braithwaite, R. J. and Olesen, O. B.: Glacier fluctuations and climatic change, chap. Calculation of glacier ablation from air temperature, West Greenland, pp. 219–233, Kluwer Academic Publishers, Dordrecht, 1989.
- Budyko, M. I.: The effect of solar radiation variations on the climate of the Earth, *Tellus*, 21, 611–619, 1969.
- Bueler, E. and Brown, J.: Shallow shelf approximation as a 'sliding law' in a thermo-mechanically coupled ice sheet model, *J. Geophys. Res.*, 114, F03 008, doi:10.1029/2008JF001179, 2009.
- Calanca, P., Gilgen, H., Ekholm, S., and Ohmura, A.: Gridded temperature and accumulation distributions for Greenland for use in cryospheric models, *Annals of Glaciology*, 31, 118–120, doi:10.3189/172756400781820345, 2000.
- Calov, R. and Ganopolski, A.: Multistability and hysteresis in the climate-cryosphere system under orbital forcing, *Geophys. Res. Lett.*, 32, L21 717, 2005.
- Calov, R. and Greve, R.: A semi-analytical solution for the positive degree-day model with stochastic temperature variations, *Journal of Glaciology*, 51, 173–175, 2005.
- Calov, R. and Hutter, K.: The thermomechanical response of the Greenland Ice Sheet to various climate scenarios, *Climate Dynamics*, 12, 243–260, 1996.

- Calov, R., Ganopolski, A., Petoukhov, V., Claussen, M., and Greve, R.: Large-scale instabilities of the Laurentide ice sheet simulated in a fully coupled climate-system model, *Geophys. Res. Lett.*, 29, 2216–2220, doi:10.1029/2002GL016078, 2002.
- Calov, R., Ganopolski, A., Claussen, M., Petoukhov, V., and Greve, R.: Transient simulation of the last glacial inception. Part I: glacial inception as a bifurcation in the climate system, *Climate Dynamics*, 24, 545–561, doi:10.1007/s00382-005-0007-6, 2005.
- Calov, R., Ganopolski, A., Kubatzki, C., and Claussen, M.: Mechanisms and time scales of glacial inception simulated with an Earth system model of intermediate complexity, *Climate of the Past*, 5, 245–258, doi:10.5194/cp-5-245-2009, 2009.
- CAPE, L. I. P. m.: Last Interglacial Arctic warmth confirms polar amplification of climate change, *Quaternary Science Reviews*, 25, 1383–1400, doi:10.1016/j.quascirev.2006.01.033, 2006.
- Cappelen, J., Jrgensen, B. V., Laursen, E. V., Stannius, L. S., and Thomsen, R. S.: The observed climate of Greenland, 1958-99 – with Climatological Standard Normals, 1961-1990, Technical Report 00-18, Danish Meteorological Institute, Copenhagen, 2001.
- Charbit, S., Paillard, D., and Ramstein, G.: Amount of CO<sub>2</sub> emissions irreversibly leading to the total melting of Greenland, *Geophys. Res. Lett.*, 35, L12 503, 2008.
- Christensen, J., Hewitson, B., Busuioc, A., Chen, A., Gao, X., Held, I., Jones, R., Kolli, R. K., Kwon, W.-T., Laprise, R., Magaa Rueda, V., Mearns, L., Menndez, C. G., Risnen, J., Rinke, A., Sarr, A., and Whetton, P.: Climate Change 2007: The Physical Science Basis. Contribution of Working Group I to the Fourth Assessment Report of the Intergovernmental Panel on Climate Change, chap. Regional Climate Projections, pp. 847–940, Cambridge University Press, Cambridge, UK, 2007.
- Claussen, Mysak, Weaver, Crucifix, Fichfet, Loutre, Weber, Alcamo, Alexeev, Berger, Calov, Ganopolski, Goosse, Lohmann, Lunkeit, Mokhov, Petoukhov, Stone, and Wang: Earth system models of intermediate complexity: closing the gap in the spectrum of climate system models, *Climate Dynamics*, 18, 579–586, 2002.
- Crowley, T. J. and Baum, S. K.: Is the Greenland Ice Sheet Bistable?, *Paleoceanography*, 10, 357–363, 1995.
- Cuffey, K. M. and Marshall, S. J.: Substantial contribution to sea-level rise during the last interglacial from the Greenland ice sheet, *Nature*, 404, 591–594, 2000.
- Deblonde, G., Peltier, W. R., and Hyde, W. T.: Simulations of continental ice sheet growth over the last glacial-interglacial cycle: experiments with a one level seasonal energy balance model including seasonal ice albedo feedback, *Palaeogeography, Palaeoclimatology, Palaeoecology*, 98, 37–55, 1992.

- DeConto, R. M. and Pollard, D.: Rapid Cenozoic glaciation of Antarctica induced by declining atmospheric CO<sub>2</sub>, *Nature*, 421, 245–249, 2003.
- Esch, M. B. and Herterich, K.: A two-dimensional coupled atmosphere-ice-sheet-continent model designed for paleoclimatic simulations, *Annals of Glaciology*, 14, 55–57, 1990.
- Ettema, J., van den Broeke, M. R., van Meijgaard, E., van de Berg, W. J., Bamber, J. L., Box, J. E., and Bales, R. C.: Higher surface mass balance of the Greenland ice sheet revealed by high-resolution climate modeling, *Geophys. Res. Lett.*, 36, L12 501, 2009.
- Fanning, A. F. and Weaver, A. J.: An atmospheric energy-moisture balance model: climatology, interpentadal climate change, and coupling to an ocean general circulation model, *J. Geophys. Res.*, 101, 15 111–15 128, 1996.
- Fettweis, X.: Reconstruction of the 1979–2006 Greenland ice sheet surface mass balance using the regional climate model MAR, *The Cryosphere*, 1, 21–40, 2007.
- Ganopolski, A., Petoukhov, V., Rahmstorf, S., Brovkin, V., Claussen, M., Eliseev, A., and Kubatzki, C.: CLIMBER-2: a climate system model of intermediate complexity. Part II: model sensitivity, *Climate Dynamics*, 17, 735–751, 2001.
- Ganopolski, A., Calov, R., and Claussen, M.: Simulation of the last glacial cycle with a coupled climate ice-sheet model of intermediate complexity, *Clim. Past*, 6, 229–244, 2010.
- Glen, J. W.: The creep of polycrystalline ice, *Proceedings of the Royal Society of London. Series A, Mathematical and Physical Sciences*, 228, 519–538, 1955.
- Gregory, J. and Huybrechts, P.: Ice-sheet contributions to future sea-level change, *Philosophical Transactions of the Royal Society A: Mathematical, Physical and Engineering Sciences*, 364, 1709–1732, doi:10.1098/rsta.2006.1796, 2006.
- Greve, R.: A continuum–mechanical formulation for shallow polythermal ice sheets, *Philosophical Transactions of the Royal Society of London. Series A:Mathematical, Physical and Engineering Sciences*, 355, 921–974, 1997a.
- Greve, R.: Application of a Polythermal Three-Dimensional Ice Sheet Model to the Greenland Ice Sheet: Response to Steady-State and Transient Climate Scenarios, *Journal of Climate*, 10, 901–918, 1997b.
- Greve, R.: On the Response of the Greenland Ice Sheet to Greenhouse Climate Change, *Climatic Change*, 46, 289–303, 2000.
- Greve, R.: Relation of measured basal temperatures and the spatial distribution of the geothermal heat flux for the Greenland ice sheet, *Annals of Glaciology*, 42, 424–432, doi:10.3189/172756405781812510, 2005.

- Greve, R. and Blatter, H.: Dynamics of Ice Sheets and Glaciers, Springer-Verlag, Berlin, 2009.
- GRIP, G. I. C. P. M.: Climate instability during the last interglacial period recorded in the GRIP ice core, *Nature*, 364, 203–207, 1993.
- Hanna, E. and Valdes, P.: Validation of ECMWF (re)analysis surface climate data, 1979–1998, for Greenland and implications for mass balance modelling of the ice sheet, *Int. J. Climatol.*, 21, 171–195, 2001.
- Hanna, E., Huybrechts, P., Janssens, I., Cappelen, J., Steffen, K., and Stephens, A.: Runoff and mass balance of the Greenland ice sheet: 1958–2003, *J. Geophys. Res.*, 110, D13 108, 2005.
- Hanna, E., Huybrechts, P., Steffen, K., Cappelen, J., Huff, R., Shuman, C., Irvine-Fynn, T., Wise, S., and Griffiths, M.: Increased Runoff from Melt from the Greenland Ice Sheet: A Response to Global Warming, *Journal of Climate*, 21, 331–341, doi:10.1175/2007JCLI1964.1, 2008.
- Hebeler, F., Purves, R. S., and Jamieson, S. S.: The impact of parametric uncertainty and topographic error in ice-sheet modelling, *Journal of Glaciology*, 54, 899–919, doi:10.3189/002214308787779852, 2008.
- Hubbard, A., Bradwell, T., Golledge, N., Hall, A., Patton, H., Sugden, D., Cooper, R., and Stoker, M.: Dynamic cycles, ice streams and their impact on the extent, chronology and deglaciation of the British-Irish ice sheet, *Quaternary Science Reviews*, 28, 758–776, 2009.
- Hutter, K.: *Theoretical Glaciology: Material Science of Ice and the Mechanics of Glaciers and Ice Sheets*, D. Reidel, Norwell, Mass., 1983.
- Huybrechts, P.: Report of the Third EISMINT Workshop on Model Intercomparison, Tech. rep., European Science Foundation, Strasbourg, 1998.
- Huybrechts, P.: Sea-level changes at the LGM from ice-dynamic reconstructions of the Greenland and Antarctic ice sheets during the glacial cycles, *Quaternary Science Reviews*, 21, 203–231, doi:10.1016/S0277-3791(01)00082-8, 2002.
- Huybrechts, P. and de Wolde, J.: The Dynamic Response of the Greenland and Antarctic Ice Sheets to Multiple-Century Climatic Warming, *Journal of Climate*, 12, 2169–2188, 1999.
- Huybrechts, P., Letréguilly, A., and Reeh, N.: The Greenland ice sheet and greenhouse warming, *Global and Planetary Change*, 3, 399–412, 1991.

- Huybrechts, P., Gregory, J., Janssens, I., and Wild, M.: Modelling Antarctic and Greenland volume changes during the 20th and 21st centuries forced by GCM time slice integrations, *Global and Planetary Change*, 42, 83–105, 2004.
- Imbrie, J., Hays, J. D., Martinson, D. G., McIntyre, A., Mix, A. C., Morley, J. J., Pisias, N. G., Prell, W. L., and Shackleton, N. J.: *Milankovitch and Climate, Part I*, chap. The orbital theory of Pleistocene climate: Support from a revised chronology of the marine  $\delta^{18}\text{O}$  record, pp. 269–305, Reidel, Dordrecht, 1984.
- Jansen, E., Overpeck, J., Briffa, K. R., Duplessy, J. C., Joos, F., Masson-Delmotte, V., Olago, D., Otto-Bliesner, B., Peltier, W. R., Rahmstorf, S., Ramesh, R., Raynaud, D., Rind, D., Solomina, O., Villalba, R., and Zhang, D.: *Climate Change 2007: The Physical Science Basis*, chap. Palaeoclimate, pp. 434–498, Cambridge University Press, Cambridge, UK, 2007.
- Janssens, I. and Huybrechts, P.: The treatment of meltwater retention in mass-balance parameterizations of the Greenland ice sheet, *Annals of Glaciology*, 31, 133–140, doi:10.3189/172756400781819941, 2000.
- Jenssen, D.: A three-dimensional polar ice sheet model, *Journal of Glaciology*, 18, 373–389, 1977.
- Johnsen, S. J., Dahl-Jensen, D., Gundestrup, N., Steffensen, J. P., Clausen, H. B., Miller, H., Masson-Delmotte, V., Sveinbjrnsdottir, A. E., and White, J.: Oxygen isotope and palaeotemperature records from six Greenland ice-core stations: Camp Century, Dye-3, GRIP, GISP2, Renland and NorthGRIP, *J. Quaternary Sci.*, 16, 299–307, doi:10.1002/jqs.622, 2001.
- Jouzel, J., Alley, R. B., Cuffey, K. M., Dansgaard, W., Grootes, P., Hoffmann, G., Johnsen, S. J., Koster, R. D., Peel, D., Shuman, C. A., Stievenard, M., Stuiver, M., and White, J.: Validity of the temperature reconstruction from water isotopes in ice cores, *J. Geophys. Res.*, 102, 26 471–26 487, doi:10.1029/97JC01283, 1997.
- Konzelmann, T., van de Wal, R. S., Greuell, W., Bintanja, R., Henneken, E. A., and Abe-Ouchi, A.: Parameterization of global and longwave incoming radiation for the Greenland Ice Sheet, *Global and Planetary Change*, 9, 143–164, 1994.
- Kopp, R. E., Simons, F. J., Mitrovica, J. X., Maloof, A. C., and Oppenheimer, M.: Probabilistic assessment of sea level during the last interglacial stage, *Nature*, 462, 863–867, doi:10.1038/nature08686, 2009.
- Lemke, P., Ren, J., Alley, R., Allison, I., Carrasco, J., Flato, G., Fujii, Y., Kaser, G., Mote, P., Thomas, R., and Zhang, T.: *Climate change 2007 : The Physical Science*

- Basis, chap. Observations: Changes in Snow, Ice and Frozen Ground, pp. 337–383, Cambridge University Press, Cambridge, UK, 2007.
- Lenton, T. M., Held, H., Kriegler, E., Hall, J. W., Lucht, W., Rahmstorf, S., and Schellnhuber, H. J.: Tipping elements in the Earth’s climate system, *Proceedings of the National Academy of Sciences*, 105, 1786–1793, 2008.
- Letréguilly, A., Huybrechts, P., and Reeh, N.: Steady-state characteristics of the Greenland ice sheet under different climates, *Journal of Glaciology*, 37, 149–157, 1991.
- Lhomme, N., Clarke, G. K., and Marshall, S. J.: Tracer transport in the Greenland Ice Sheet: constraints on ice cores and glacial history, *Quaternary Science Reviews*, 24, 173–194, doi:10.1016/j.quascirev.2004.08.020, 2005.
- Lunt, D. J., de Noblet-Ducoudr, N., and Charbit, S.: Effects of a melted greenland ice sheet on climate, vegetation, and the cryosphere, *Climate Dynamics*, 23, 679–694, 2004.
- Lunt, D. J., Foster, G. L., Haywood, A. M., and Stone, E. J.: Late Pliocene Greenland glaciation controlled by a decline in atmospheric CO<sub>2</sub> levels, *Nature*, 454, 1102–1105, 2008.
- Masson-Delmotte, V., Stenni, B., Pol, K., Braconnot, P., Cattani, O., Falourd, S., Kageyama, M., Jouzel, J., Landais, A., Minster, B., Barnola, J., Chappellaz, J., Krinner, G., Johnsen, S., Rthlisberger, R., Hansen, J., Mikolajewicz, U., and Otto-Bliesner, B.: EPICA Dome C record of glacial and interglacial intensities, *Quaternary Science Reviews*, 29, 113–128, doi:10.1016/j.quascirev.2009.09.030, 2010.
- Meehl, G., Stocker, T., Collins, W., P., F., Gaye, A., Gregory, J., Kitoh, A., Knutti, R., Murphy, J., Noda, A., Raper, S., Watterson, I., Weaver, A., and Zhao, Z.-C.: *Climate Change 2007: The Physical Science Basis. Contribution of Working Group I to the Fourth Assessment Report of the Intergovernmental Panel on Climate Change*, chap. Global Climate Projections, Cambridge University Press, Cambridge, UK, 2007.
- Mikolajewicz, U., Sein, D. V., Jacob, D., Knigk, T., Podzun, R., and Semmler, T.: Simulating Arctic sea ice variability with a coupled regional atmosphere-ocean-sea ice model, *Meteorologische Zeitschrift*, 14, 793–800, doi:10.1127/0941-2948/2005/0083, 2005.
- Mikolajewicz, U., Vizcano, M., Jungclaus, J., and Schurgers, G.: Effect of ice sheet interactions in anthropogenic climate change simulations, *Geophys. Res. Lett.*, 34, L18 706, 2007.
- Mote, T. L.: Greenland surface melt trends 1973–2007: Evidence of a large increase in 2007, *Geophys. Res. Lett.*, 34, L22 507, doi:10.1029/2007GL031976, 2007.

- NGRIP, N. G. I. C. P. m.: High-resolution record of Northern Hemisphere climate extending into the last interglacial period, *Nature*, 431, 147–151, doi:10.1038/nature02805, 2004.
- Nick, F. M., Vieli, A., Howat, I. M., and Joughin, I.: Large-scale changes in Greenland outlet glacier dynamics triggered at the terminus, *Nature Geosci*, 2, 110–114, doi:10.1038/ngeo394, 2009.
- North, G. R., Cahalan, R. F., and Coakley, James A., J.: Energy balance climate models, *Rev. Geophys.*, 19, 91–121, 1981.
- Oerlemans, J.: The mass balance of the Greenland ice sheet: sensitivity to climate change as revealed by energy-balance modelling, *The Holocene*, 1, 40–48, 1991.
- Oerlemans, J. and Van Den Dool, H. M.: Energy Balance Climate Models: Stability Experiments with a Refined Albedo and Updated Coefficients for Infrared Emission, *Journal of the Atmospheric Sciences*, 35, 371–381, 1978.
- Otto-Bliesner, B. L., Marshall, S. J., Overpeck, J. T., Miller, G. H., Hu, A., and CAPE, L. I. P. m.: Simulating Arctic Climate Warmth and Icefield Retreat in the Last Interglaciation, *Science*, 311, 1751–1753, 2006.
- Overpeck, J. T., Otto-Bliesner, B. L., Miller, G. H., Muhs, D. R., Alley, R. B., and Kiehl, J. T.: Paleoclimatic Evidence for Future Ice-Sheet Instability and Rapid Sea-Level Rise, *Science*, 311, 1747–1750, doi:10.1126/science.1115159, 2006.
- Parizek, B. R. and Alley, R. B.: Implications of increased Greenland surface melt under global-warming scenarios: ice-sheet simulations, *Quaternary Science Reviews*, 23, 1013–1027, 2004.
- Paterson, W. S. B.: *The physics of glaciers*, Pergamon, Oxford, UK, Tarrytown, NY, 3 edn., 1994.
- Pattyn, F.: A new three-dimensional higher-order thermomechanical ice sheet model: Basic sensitivity, ice stream development, and ice flow across subglacial lakes, *J. Geophys. Res.*, 108, 2382, doi:10.1029/2002JB002329, 2003.
- Pellicciotti, F., Brock, B., Strasser, U., Burlando, P., Funk, M., and Corripio, J.: An enhanced temperature-index glacier melt model including the shortwave radiation balance: development and testing for Haut Glacier d’Arolla, Switzerland, *Journal of Glaciology*, 51, 573–587, doi:10.3189/172756505781829124, 2005.
- Peltier, W. R. and Marshall, S.: Coupled energy-balance/ice-sheet model simulations of the glacial cycle: A possible connection between terminations and terrigenous dust, *J. Geophys. Res.*, 100, 14 269–14 289, 1995.



- Petoukhov, V., Ganopolski, A., Brovkin, V., Claussen, M., Eliseev, A., Kubatzki, C., and Rahmstorf, S.: CLIMBER-2: a climate system model of intermediate complexity. Part I: model description and performance for present climate, *Climate Dynamics*, 16, 1–17, doi:10.1007/PL00007919, 2000.
- Pollard, D.: A simple parameterization for ice sheet ablation rate, *Tellus*, 32, 384–388, doi:10.1111/j.2153-3490.1980.tb00965.x, 1980.
- Pollard, D. and Deconto, R. M.: A Coupled Ice-Sheet/Ice-Shelf/Sediment Model Applied to a Marine-Margin Flowline: Forced and Unforced Variations, Blackwell Publishing Ltd., doi:10.1002/9781444304435.ch4, 2009.
- Rahmstorf, S.: Bifurcations of the Atlantic thermohaline circulation in response to changes in the hydrological cycle, *Nature*, 378, 145–149, 1995.
- Ramillien, G., Lombard, A., Cazenave, A., Ivins, E., Llubes, M., Remy, F., and Biancale, R.: Interannual variations of the mass balance of the Antarctica and Greenland ice sheets from GRACE, *Global and Planetary Change*, 53, 198–208, 2006.
- Raynaud, D., Chappellaz, J., Ritz, C., and Martinerie, P.: Air content along the Greenland Ice Core Project core: A record of surface climatic parameters and elevation in central Greenland, *J. Geophys. Res.*, 102, 26 607–26 613, doi:10.1029/97JC01908, 1997.
- Reeh, N.: Parameterization of melt rate and surface temperature on the Greenland ice sheet, *Polarforschung*, 59, 113–128, 1991.
- Ridley, J., Gregory, J., Huybrechts, P., and Lowe, J.: Thresholds for irreversible decline of the Greenland ice sheet, *Climate Dynamics*, online, 1–9, doi:10.1007/s00382-009-0646-0, 2009.
- Ridley, J. K., Huybrechts, P., Gregory, J. M., and Lowe, J. A.: Elimination of the Greenland Ice Sheet in a High CO<sub>2</sub> Climate, *Journal of Climate*, 18, 3409–3427, doi:10.1175/JCLI3482.1, 2005.
- Rignot, E. and Kanagaratnam, P.: Changes in the Velocity Structure of the Greenland Ice Sheet, *Science*, 311, 986–990, 2006.
- Rignot, E., Box, J. E., Burgess, E., and Hanna, E.: Mass balance of the Greenland ice sheet from 1958 to 2007, *Geophys. Res. Lett.*, 35, L20 502, 2008.
- Ritz, C., Fabre, A., and Letrguilly, A.: Sensitivity of a Greenland ice sheet model to ice flow and ablation parameters: consequences for the evolution through the last climatic cycle, *Climate Dynamics*, 13, 11–23, doi:10.1007/s003820050149, 1997.

- Robinson, A., Calov, R., and Ganopolski, A.: An efficient regional energy-moisture balance model for simulation of the Greenland Ice Sheet response to climate change, *The Cryosphere*, 4, 129–144, doi:10.5194/tc-4-129-2010, 2010a.
- Robinson, A., Calov, R., and Ganopolski, A.: Greenland Ice Sheet model parameters constrained using simulations of the Eemian Interglacial, *Climate of the Past Discussions*, 6, 1551–1588, doi:10.5194/cpd-6-1551-2010, 2010b.
- Sellers, W. D.: A Global Climatic Model Based on the Energy Balance of the Earth-Atmosphere System., *Journal of Applied Meteorology*, 8, 392–400, 1969.
- Shapiro, N. M. and Ritzwoller, M. H.: Inferring surface heat flux distributions guided by a global seismic model: particular application to Antarctica, *Earth and Planetary Science Letters*, 223, 213–224, doi:10.1016/j.epsl.2004.04.011, 2004.
- Smith, W. H. F. and Sandwell, D. T.: Global Sea Floor Topography from Satellite Altimetry and Ship Depth Soundings, *Science*, 277, 1956–1962, doi:10.1126/science.277.5334.1956, 1997.
- Steffen, K., Box, J. E., and Abdalati, W.: Greenland Climate Network: GC-Net, CRREL monograph 96-27, CRREL, 1996.
- Tarasov, L. and Peltier, W. R.: Impact of thermomechanical ice sheet coupling on a model of the 100 kyr ice age cycle, *J. Geophys. Res.*, 104, 9517–9545, doi:10.1029/1998JD200120, 1999.
- Tarasov, L. and Peltier, W. R.: Greenland glacial history and local geodynamic consequences, *Geophysical Journal International*, 150, 198–229, doi:10.1046/j.1365-246X.2002.01702.x, 2002.
- Tarasov, L. and Peltier, W. R.: Greenland glacial history, borehole constraints, and Eemian extent, *J. Geophys. Res.*, 108, 2143–2163, doi:10.1029/2001JB001731, 2003.
- Toniazzo, T., Gregory, J. M., and Huybrechts, P.: Climatic Impact of a Greenland Deglaciation and Its Possible Irreversibility, *Journal of Climate*, 17, 21–33, 2004.
- Uppala, S. M., Kllberg, P. W., Simmons, A. J., Andrae, U., Bechtold, V. D. C., Fiorino, M., Gibson, J. K., Haseler, J., Hernandez, A., Kelly, G. A., Li, X., Onogi, K., Saarinen, S., Sokka, N., Allan, R. P., Andersson, E., Arpe, K., Balmaseda, M. A., Beljaars, A. C. M., Berg, L. V. D., Bidlot, J., Bormann, N., Caires, S., Chevallier, F., Dethof, A., Dragosavac, M., Fisher, M., Fuentes, M., Hagemann, S., Hlm, E., Hoskins, B. J., Isaksen, L., Janssen, P. A. E. M., Jenne, R., McNally, A. P., Mahfouf, J.-F., Morcrette, J.-J., Rayner, N. A., Saunders, R. W., Simon, P., Sterl, A., Trenberth, K. E., Untch, A., Vasiljevic, D., Viterbo, P., and Woollen, J.: The ERA-40 re-analysis, *Q.J.R. Meteorol. Soc.*, 131, 2961–3012, 2005.

- van de Wal, R. S. W.: Mass balance modelling of the Greenland ice sheet: A comparison of energy balance and degree-day models, *Annals of Glaciology*, 23, 36–45, 1996.
- van de Wal, R. S. W. and Oerlemans, J.: An energy balance model for the Greenland ice sheet, *Global and Planetary Change*, 9, 115–131, 1994.
- van den Berg, J., van de Wal, R., and Oerlemans, H.: A mass balance model for the Eurasian Ice Sheet for the last 120,000 years, *Global and Planetary Change*, 61, 194–208, 2008.
- van den Broeke, M., Bamber, J., Ettema, J., Rignot, E., Schrama, E., van de Berg, W. J., van Meijgaard, E., Velicogna, I., and Wouters, B.: Partitioning Recent Greenland Mass Loss, *Science*, 326, 984–986, doi:10.1126/science.1178176, 2009.
- van der Veen, C.: Polar ice sheets and global sea level: how well can we predict the future?, *Global and Planetary Change*, 32, 165–194, doi:10.1016/S0921-8181(01)00140-0, 2002.
- Velicogna, I.: Increasing rates of ice mass loss from the Greenland and Antarctic ice sheets revealed by GRACE, *Geophys. Res. Lett.*, 36, L19 503, 2009.
- Velicogna, I. and Wahr, J.: Greenland mass balance from GRACE, *Geophys. Res. Lett.*, 32, L18 505, 2005.
- Vinther, B. M., Buchardt, S. L., Clausen, H. B., Dahl-Jensen, D., Johnsen, S. J., Fisher, D. A., Koerner, R. M., Raynaud, D., Lipenkov, V., Andersen, K. K., Blunier, T., Rasmussen, S. O., Steffensen, J. P., and Svensson, A. M.: Holocene thinning of the Greenland ice sheet, *Nature*, 461, 385–388, doi:10.1038/nature08355, 2009.
- Vizcano, M., Mikolajewicz, U., Grger, M., Maier-Reimer, E., Schurgers, G., and Winguth, A.: Long-term ice sheet–climate interactions under anthropogenic greenhouse forcing simulated with a complex Earth System Model, *Climate Dynamics*, 31, 665–690, 2008.
- Weertman, J.: On the sliding of glaciers, *Journal of Glaciology*, 3, 33–38, 1957.
- Willerslev, E., Cappellini, E., Boomsma, W., Nielsen, R., Hebsgaard, M. B., Brand, T. B., Hofreiter, M., Bunce, M., Poinar, H. N., Dahl-Jensen, D., Johnsen, S., Steffensen, J. P., Bennike, O., Schwenninger, J.-L., Nathan, R., Armitage, S., de Hoog, C.-J., Alfimov, V., Christl, M., Beer, J., Muscheler, R., Barker, J., Sharp, M., Penkman, K. E. H., Haile, J., Taberlet, P., Gilbert, M. T. P., Casoli, A., Campani, E., and Collins, M. J.: Ancient Biomolecules from Deep Ice Cores Reveal a Forested Southern Greenland, *Science*, 317, 111–114, doi:10.1126/science.1141758, 2007.
- Wouters, B., Chambers, D., and Schrama, E. J. O.: GRACE observes small-scale mass loss in Greenland, *Geophys. Res. Lett.*, 35, L20 501, 2008.

Zhang, Y., Rossow, W. B., Lacis, A. A., Oinas, V., and Mishchenko, M. I.: Calculation of radiative fluxes from the surface to top of atmosphere based on ISCCP and other global data sets: Refinements of the radiative transfer model and the input data, *J. Geophys. Res.*, 109, D19 105, 2004.